
THE UNIVERSITY OF QUEENSLAND

AUSTRALIA

# Improving the Performance of Air-Cooled Condensers by Using Metal Foams

Ampon Chumpia
M.Sc, M.Eng

*A thesis submitted for the degree of Doctor of Philosophy at*
*The University of Queensland in 2015*
School of Mechanical and Mining Engineering

**Abstract**

This research investigates the implementation of porous metals particularly aluminum foam as an enhanced surface to improve heat transfer on the air side of air-cooled, tubular heat exchangers. The target application for these heat exchangers is the condensers for geothermal power plants in remote locations of Australia where water for wet cooling is scarce. Traditional practices for liquid-to-air or vapor-to-air heat exchangers rely predominantly on finned surfaces to enhance heat transfer rate. Heat transfer enhancement in these designs is achieved via an increased surface area of simple geometries. Recent advancement in manufacturing and availability of porous materials make them possible to be utilized in thermal exchange equipment to improve efficiency and compactness.

This work describes heat exchanger tubes based on circular cylinders with aluminum foam covering on the outer surface. Thermo-hydraulic performances are evaluated experimentally in a cross-flow using low-speed wind tunnel. The tests are performed on single cylinders, single row arrays, and multi-row tube bundles in both aligned and staggered configurations subjected to airflow of 0.5 to 5.0 m/s. This range of air velocities is chosen as it encompasses vertical flow regimes occur inside typical cooling towers. The effects of foam layer thickness, transversal and longitudinal tube pitches, foam-to-tube bonding methods, and tube bank patterns, are collectively investigated. The results are compared to baseline data obtained from conventional, annular finned tubes and tube bundles tested under the same conditions.

The overall conclusions are drawn on heat transfer and pressure drop as two main comparison parameters. Experimental results on these parameters confirm the trend of numerical findings of a previous in-house study, although with varying degrees of differences on their magnitude. In all finned- versus foam-surface comparisons, under the same testing conditions and using specimens of similar dimensions, the latter shows convincing benefits on heat transfer/pressure drop ratios over the full range of chosen airflows. Within this range, the maximum relative advantage of the foam-covered heat exchangers over the finned type is observed at the midrange of airflow between 2.0 and 2.5 m/s. This result is both desirable and opportune because these designated airflows coincide with the top end velocity found inside most natural-draft cooling towers. Beyond this range of airflow up to 5.0 m/s, a typical range at the lower end of induced- or forced-draft cooling towers, the relative merit of heat transfer/pressure drop is rapidly degraded. However, in a situation where the increased heat transfer is under demand and compactness is not a critical factor, the pressure drop can be reduced satisfactorily by choosing a suitable transversal pitch within the tube bundle. Under this reduced blockage condition, metal foam heat exchanger bundles tend to behave as a group of an individual tube; therefore, retain higher relative benefit in terms of the sum of heat transfer/pressure drop ratio over their finned-surface counterpart.

## Declaration by author

This thesis is composed of my original work, and contains no material previously published or written by another person except where due reference has been made in the text. I have clearly stated the contribution by others to jointly-authored works that I have included in my thesis.

I have clearly stated the contribution of others to my thesis as a whole, including statistical assistance, survey design, data analysis, significant technical procedures, professional editorial advice, and any other original research work used or reported in my thesis. The content of my thesis is the result of work I have carried out since the commencement of my research higher degree candidature and does not include a substantial part of work that has been submitted to qualify for the award of any other degree or diploma in any university or other tertiary institution. I have clearly stated which parts of my thesis, if any, have been submitted to qualify for another award.

I acknowledge that an electronic copy of my thesis must be lodged with the University Library and, subject to the policy and procedures of The University of Queensland, the thesis be made available for research and study in accordance with the Copyright Act 1968 unless a period of embargo has been approved by the Dean of the Graduate School.

I acknowledge that copyright of all material contained in my thesis resides with the copyright holder(s) of that material. Where appropriate I have obtained copyright permission from the copyright holder to reproduce material in this thesis.

## Publications during candidature

- A.Chumpia and K. Hooman *Performance Evaluation of Tubular Aluminum Foam Heat Exchangers in Single Row Arrays.* Journal of Applied Thermal Engineering **83**, 121 – 130 (2015)
- A. Chumpia and K. Hooman *Performance Evaluation of Single Tubular Aluminum Foam Heat Exchangers.* Journal of Applied Thermal Engineering **66**, 266 – 273 (2014)
- A. Chumpia and K. Hooman *Quantification of Contact Resistance of Metal Foam Heat Exchangers for Improved, Air-cooled Condensers in Geothermal Power Application.* In *18$^{th}$ Australasia Fluid Mechanics Conference* (Australasia Fluid Mechanics Society, AMC-UTAS, Launceston, Tasmania, Australia, 2012)

## Publications included in this thesis

1. A.Chumpia and K. Hooman *Performance Evaluation of Tubular Aluminum Foam Heat Exchangers in Single Row Arrays.* Journal of Applied Thermal Engineering **83**, 121 – 130 (2015)

   – reformatted, removed repetitive texts of literature reviews and part of experimental setup, and incorporated as Chapter 4.

| Contributor | Statement of contribution |
|---|---|
| Ampon Chumpia | Designed experiments (90%)<br>Wrote the paper (75%) |
| Kamel Hooman | Designed experiments (10%)<br>Edited and suggested changes to manuscript (20%)<br>Advised on the preparation of reviewers' rebuttal (5%) |

2. A. Chumpia and K. Hooman *Performance Evaluation of Single Tubular Aluminum Foam Heat Exchangers.* Journal of Applied Thermal Engineering **66**, 266 – 273 (2014)

   – reformatted, removed repetitive texts of literature reviews and part of experimental setup, and incorporated as Chapter 3.

| Contributor | Statement of contribution |
|---|---|
| Ampon Chumpia | Designed experiments (90%)<br>Wrote the paper (70%) |
| Kamel Hooman | Designed experiments (10%)<br>Analyzed preliminary data, constructed two correlations, and advised on the preparation of reviewers' rebuttal (10%)<br>Edited and suggested changes to manuscript (20%) |

## Contributions by others to the thesis

No contributions by others.

## Statement of parts of the thesis submitted to qualify for the award of another degree

None.

**Acknowledgements**

In the order of importance, I am grateful to: (i) Queensland Geothermal Energy Centre of Excellence (QGECE) via Professor Hal Gurgenci for providing financial support to this study; (ii) Dr Kamel Hooman, my principal advisor for his unconditional help throughout my candidature, particularly during the time I faced tight deadlines. Thanks Kamel for always putting up with the promise I failed to upkeep repeatedly; (iii) Professor Thomas Rösgen, Institut Für Fluiddynamik, ETH-Zurich for his work in setting up the PIV suite in our lab and for running an in-house tutorial session for this incredibly expensive tool. I am also highly indebted to Professor Rösgen for adopting me into his labs and provided me with top class facilities to pursue the related part of my research under the UQ-GSITA visit. I'll always remember trekking the freezing Zurich behind his back and scouting for the missing parts for the wind tunnel when anyone else would stay home for a nice Christmas in that week of 2013.

In no particular order, I also express my sincere gratitude to the following organizations/individuals: Advanced Water Management Centre (AWMC) via its former Director, Professor Jürg Keller, for giving me a fractional contract to do technical works within the centre. This extra income benefited me, sustained my family, and helped us make the ends meet; A gentle man, Paul Cochrane, who I don't personally know but who shared his version of a very nice LaTeX style file for the UQ thesis format plus a ready-to-go structured folder allowing anyone with a rudimentary LaTeX skill like myself to start typesetting. Paul definitely saves me weeks of headache; Mostafa Odabaee for his hard work in ordering and importing test specimens, as well as setting up a basic version of the test platform for undergraduate heat transfer pracs –from where I could comfortably build more suitable add-ons for my own work; Dr Morteza Khashehchi, QGECE, who helped run and process PIV data for velocity check which proved that our control hardware worked the way it was intended; EAIT Instrumentation Workshop, Joy Wang and Peter Bleakley for helping with LabVIEW data logging; Dejan Subaric for making sure that all thermocouples and RTDs are well calibrated and that data logging is always noise-free; Douglas Malcolm for helping with wind tunnel operation and air velocity PID control program; Berto Di Pasquale, EAIT Mechanical Workshop for general fabrication of in-house parts and accessories; John Farmer, my lifelong teacher – one of the finest instructors at SQ-TAFE College, for telling me I'm not going into his new, personal workshop and the lathe machine until I submitted this thesis, unfortunately Lyn Farmer tended to agree; Dr Badri Basnet, a senior GIS lecturer at the University of Southern Queensland (USQ) for lending me some technical books borrowed from the USQ library so I could evade competition of high demand references at the UQ library.

I thank the Milestone committee members, Dr Bo Feng, Professor David Mee, Professor Hal Gurgenci for keeping me in check through out the three milestones; Dr Peter Jacobs for introducing me to QGECE; The great team of secretariat and graduate co-ordinators in particulars Glenda Heyde, Katie Gollschewski, Marilyn Barton, Brianne Mackinnon, Kristin Greer, Jessica Shelley who helped tirelessly with general house-keeping and to keep the Graduate School happy; graduate colleagues Jason Czapla, Raj Singh, Carlos Ventura, Hugh

Russell, who were always around the labs and kept me awake; Jackson Richards who brought an industry project to the lab which I found very interesting.

I thank The Bützers of Zug, David, Tobias, Simone, Patrick and Silvia for offering me a warm bed during my second visit to IFD, keeping me well-fed, and spending lots of their private times to show me Zürich; The Castles of New Farm, Jessica, Angela, Helen Ma, and Peter for letting me take the refuge in their home in Mount Ommaney during the week for the first two years of my program and their generosity saved me a lot of driving. Last and the most important, my own extended family and countless members for their understanding, patience, and support throughout the continuous ups and downs of my study.

## Keywords

air-cooled condenser, dry cooling tower, geothermal, heat exchanger, heat transfer enhancement, aluminum metal foam, pressure drop

## Australian and New Zealand Standard Research Classification (ANZSRC)

ANZRC code: 091505, Heat and Mass Transfer Operations, 50%
ANZRC code: 091504, Fluid Mechanics, 40%
ANZRC code: 090608, Renewable Energy (excl. Solar Cells), 10%

## Fields of Research (FoR) Classification

FoR code: 0913, Mechanical Engineering, 80%
FoR code: 0915, Interdisciplinary Engineering, 20%

# Contents

# List of Figures

# List of Tables

# List of Symbols

## Latin

$A$ ..... area, [m$^2$]

$\bar{c}_p$ ..... specific heat capacity at constant pressure, [J/kg·K]

$d_f$ ..... strut diameter, [m]

$d_i$ ..... internal diameter of the core tube, [m]

$d_o$ ..... external diameter of the core tube, [m]

$Da$ ..... Darcy number = $K/H^2$, [–]

$D_i$ ..... foam or fin annulas internal diameter = $d_o$, [m]

$D_o$ ..... foam or fin annulas external diameter, [m]

$Dr$ ..... diameter ratio = $D_o/d_o$, [–]

$f$ ..... friction factor = $\Delta P/(\rho{\cdot}\vec{u}^2)$, [–]

$G$ ..... mass flux relative to minimum free flow area, [kg/s·m$^2$]

$H$ ..... height, [m]

$h$ ..... convective heat transfer coefficient, [W/m$^2$·K]

$K$ ..... permeability of porous media, [m$^2$]

$Kp$ ..... pressure loss coefficient = $\Delta P/(\frac{1}{2}\rho{\cdot}\vec{u}^2)$, [–]

$k$ ..... thermal conductivity, [W/m·K]

$L$ ..... length, [m]

$\dot{m}$ ..... mass flow rate, [kg/s]

$Nu$ ..... Nusselt number, [–]

$P$ ..... pressure, [Pa]

$Pr$ ..... Prandtl number, [–]

$\dot{Q}$ ..... total heat transfer, [W]

$R$ ..... thermal resistance, [K/W]

$R_c$ ..... thermal contact resistance, [K/W]

$\hat{R}$ ..... dimensionless thermal resistance, [–]

$Re$ ..... Reynolds number, [–]

$S$ ..... sum of residual square, [–]

$S$ ..... centre-to-centre distance in tube arrays or bundles, [m]

$t$ ..... foam thickness or fin height $= D_o - D_i$, [m]

$t_f$ ..... fin thickness, [m]

$t_p$ ..... fin pitch, [m]

$t_w$ ..... wall thickness of the tube, [–]

$T$ ..... temperature, [k]

$U, \vec{u}$ ..... air velocity, [m/s]

$U$ ..... universal heat transfer coefficient, [W/m$^2$·K]

$W$ ..... width, [m]

$\hat{X}$ ..... ratio of tube pitch and tube diameter $= S/Di$, [–]

## Greek

$\alpha, \beta, \psi$ ..... empirical constants, [–]

$\Gamma$ ..... porous media shape factor, [–]

$\Delta$ ..... differential of, [as per variables]

$\varepsilon$ ..... heat exchanger effectiveness, [–]

$\eta$ ..... air side surface efficiency, [–]

$\nu$ ..... kinematic viscosity, [$m^2/s$]

$\mu$ ..... dynamic viscosity, [Pa·s]

$\rho$ ..... density, [$kg/m^3$]

$\phi$ ..... porosity, [–]

$\Omega^*$ ..... surface effectiveness of foam, [–]

## Subscripts

$a$ ..... of the air side

$c$ ..... cold stream

$f$ ..... effective value

$h$ ..... hot stream

$i$ ..... of inside surface

$k$ ..... conductive heat transfer through tube wall

$L$ ..... in longitudinal/spanwise/along-the-flow direction

$liq$ ..... of the liquid

$max$ ..... maximum, bigger of the two

$min$ ..... minimum, smaller of the two

$o$ ..... of outside surface

$s$ ..... of a surface

$T$ ..... in transversal direction

$t$ ..... overall, total

$w$ ..... of the tube wall

$\infty$ ..... of the bulk air stream

## Abbreviations

FS ..... full scale

HTC ..... heat transfer coefficient, [W/m$^2$·K]

ISA ..... interfacial surface area, [m$^2$]

LMTD ..... log-mean temperature difference [K, °C]

LSM ..... least square method

NTU ..... number of transfer unit

PID ..... proportional – integral – derivative feedback control

PIV ..... particle image velocimetry

PPI ..... pores per inch

QGECE .... Queensland Geothermal Energy Excellence Centre

RTD ..... resistance temperature detector

TC ..... thermocouple

TCR ..... thermal contact resistance, [K/W]

# 1 Introduction

## 1.1 Scope of the Study

This study focuses on evaluating thermo-hydraulic performance of metal foam heat exchangers with a view to practical usage in low-temperature processes. The main target application is the condensing unit of typical turbine cycles in geothermal power plants. The project is largely experimental and influenced by an M.Phil numerical study initially carried out on a foam-covered single cylinder. Numerical results from this study showed the foam-covered cylinder to have a significantly superior performance over conventional finned-surface design. The principal objective of the proposed lab works, in one part, seeks to further verify these numerical results using an improved configuration of the test section, refined instruments, and attentive measuring techniques. In another part, it is to initiate an action plan for detailed design and testing of multi-tube single arrays and multi-row tube bundles.

Four major tasks of thermo-hydraulic evaluation are performed on the heat exchangers in: (i) single tube, (ii) single vertical row, (iii) dual vertical rows, and (iv) triple vertical rows. In setting up the test plan, each task group has the first level sub-tasks consist of:

1. single tube
    - assessing thermal contact resistance of aluminum foam samples having thermal glue as bonding agent between the foam and the cylinder
2. single vertical row
    - assessing the effect of transversal pitch
    - assessing the effect of foam layer thickness
3. multiple vertical rows
    - assessing the effect of transversal pitch
    - assessing the effect of longitudinal pitch
    - assessing the effect of foam layer thickness

Each sub-task under (1) to (3), in turn, fans out to second level sub-tasks such as checking the goodness of reference data being logged against those of established previous works which are available openly. This is to ensure the 'fit-for-purpose' of the test rig and the methodology employed during data collection. A simple smooth cylinder is used to generate a baseline data set for single tube comparisons while finned tubes of suitable number are used for the other two. Details of other second level sub-tasks associated with tube banks (one, two, or three-row) are reported in subsequent respective chapters.

## 1.2 Context and Rationale

Geoscience Australia and Australian Bureau of Agricultural and Resource Economics, (2010) [1] (http://www.ga.gov.au/energy/geothermal-energy-resources.html) published an estimate based on 2004-2005 figures that 1% of the geothermal energy shallower than five kilometres and hotter than 150°C could supply Australia's total energy requirements for 26,000 years. There are three broad categories of geothermal resource; volcanic systems, hot sedimentary aquifers (HSA), and hot fractured rocks (HFR) – but only the latter two are found in Australia. Compared to other forms of renewable energy sources such as wind, solar, and ocean tidal, geothermal energy is more expensive to develop but it is the only renewable energy source which can provide a long-term, base load power generation. HSA describes deep layer underground hot water trapped by non- or semi-permeable rocks such as sandstone or limestone. Well known sources are the Otway and Gippsland basins in Victoria and the Great Artesian Basin in Queensland and South Australia. HFR provides geothermal energy from a large mass of homogeneous and less permeable hot rock, usually granites, with some degrees of natural fracture. Most often, tapping the energy from HFR involves further modification of these fractures or creating man-made reservoirs to allow sufficient flow rate

of working fluid through the rock mass. The result is called Engineered Geothermal Systems or EGS (Atrens, (2011)[2]). EGS active sites in Australia have been explored in the Cooper basin in the vicinity of the Queensland and South Australia border.

One prohibitive factor facing the operation of power plants in such places is the lack of easily accessible surface water to operate wet cooling towers for heat rejection. Because of this constraint, it is apparent that the dry cooling towers utilizing air-cooled heat exchanger elements are the only option for that purpose. Due to their relatively low efficiency, geothermal power plants generate much higher waste heat per kWe output compared to coal-fired power plants operating at higher temperatures. Based on a cycle efficiency of 15%, a 50MWe power plant needs to sink 283MW heat and doing so using a wet cooling tower, water at a rate of ∼100 kg/s or 3.2 million tonnes per year would be needed (Odabaee, et al. (2010)[3]).

While dry cooling towers are not uncommon in power generation plants, their application to geothermal power generation needs a special consideration because (i) more heat needs to be disposed of per kWe generated, and (ii) the condensing fluid in most moderate-temperature binary power plants is not steam but a hydrocarbon or a refrigerant. In his $CO_2$ based EGS research, Atrens, (2011)[2] noted: *"Lower site cooling temperature is shown to be more important than higher geothermal reservoir temperature by a factor of approximately three (on a degree basis)"*.

## 1.3 Motivation and Research Questions

As mentioned in Section 1.1, the present study is in part motivated by the published results of numerical investigations on aluminum foam heat exchangers in comparison with conventional finned type counterpart. Two of such studies at QGECE, Odabaee, et al. (2009)[4] and Odabaee, et al. (2011a)[5], show that a single tube covered with metal foam exhibiting superior performance 'by an order of magnitude' compared to a finned tube design. However, except for a study by T'Joen et al. (2010)[6], where a single row of foam-covered tubes arranged vertically was investigated, little is known about the performance of tube banks where all tubes are arranged in two-dimensional array (i.e. both vertically and horizontally in relation to the direction of airflow).

In conventional design of heat exchangers constructed out of materials other than metal foams, efficiency enhancement has been attempted by external means such as modification of the incoming flow. Some studies, e.g. Sohal and O'Brien (2001)[7], Tsutsui and Igarashi (2006)[8] showed that an improved performance of finned or simple surfaced heat exchanger elements can be achieved by adding upstream vortex generators. By the same principle, the arrangement of the tube bank in the fashion adopted in this study will cause the first vertical row of tubes to behave as the vortex generators to other tubes downstream. Due to a vertical only, one-dimensional arrangement of multiple heat exchanger tubes in their study, vortex shredding action of the first row onto the next few was not applicable and obviously T'Joen et al. (2010)[6] were not able to verify the effect. The shortcoming encountered here, however, had helped shape some initial plans of this current study. Its task list on multi-row testings as outlined in Section 1.1 partially accords T'Joen et al. (2010)'s work as providing an additional level of motivation.

The experimental portion of this present study constitutes a sub-project within the Heat

Transfer Group, one among four under the umbrella of QGECE (the other three are: Turbine and Power Cycle Studies, Fractures and Reservoirs Managements, and Power Transmission). One expectation at the end is to achieve a high ground of theoretical and practical knowledge; which may be directly applied to the design of compact, lightweight, and more efficient prototypes of novel heat exchange devices. It is anticipated that aluminum foam heat exchangers of suitable designs would enhance heat transfer appreciably while keeping the pressure drop to an accountable level. Nevertheless, the end results are largely dependent on positive answers to the following two research questions:

1. In practical situations, what level of advantage the foam based heat exchangers provide compared to conventional heat exchangers in the context specified?

2. Will the outcomes in (1) be satisfactory in overcoming practical impediments already identified in other laboratories particularly the heat transfer/pressure drop trade-off?

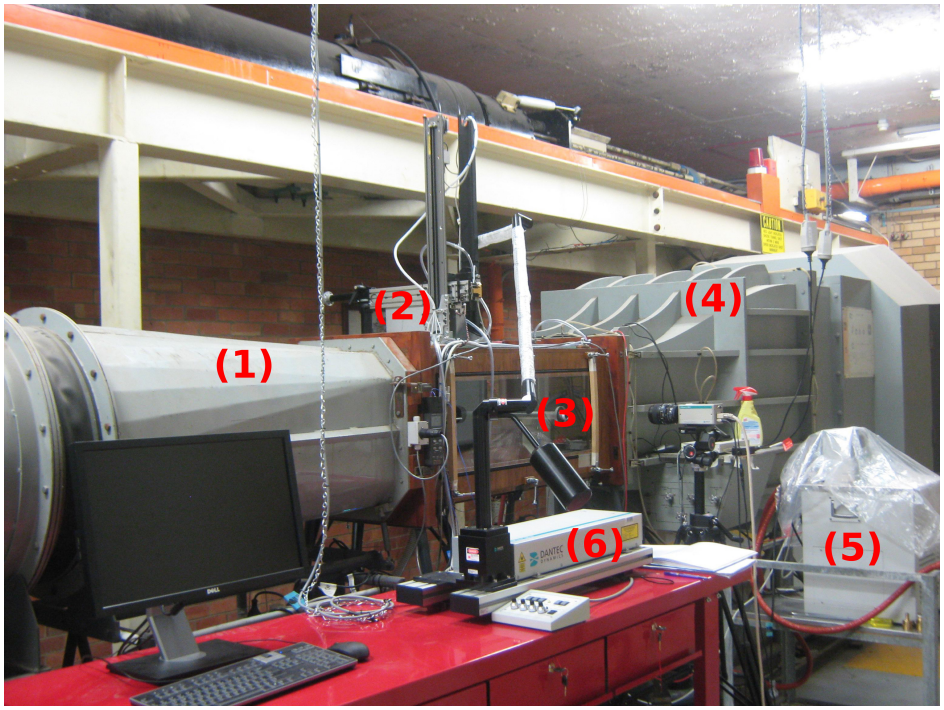


FIGURE 1.1: The wind tunnel set up for use in the experiments

## 1.4 Description of the Test Facilities

The test rig is an open circuit wind tunnel shown in Figure 1.1 and schematically in Figure 1.2. The air is drawn into the tunnel from the right-hand side through a dust filter, a honeycomb separator, and 4 sets of smoothing screen. It then passes through the settling section (a constriction plenum of 5.5:1 ratio (4)), into the test section (3). In the test section (3), the airstream flows over the hot surface of the test specimen, takes up heat, and flows

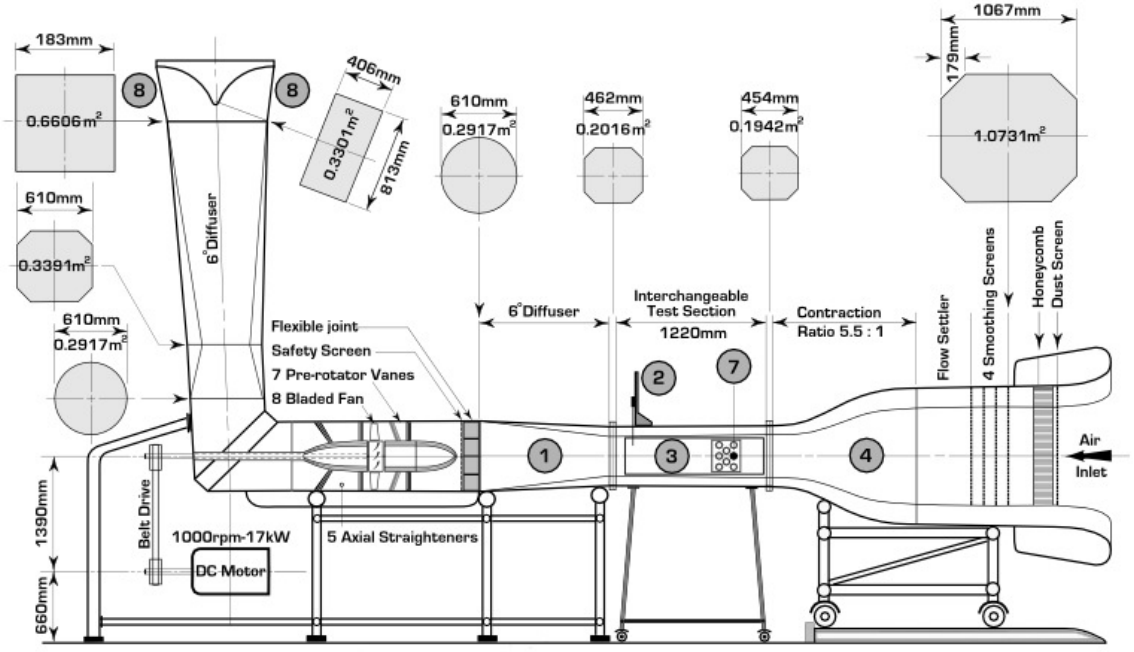


Figure 1.2: Side view schematic of the wind tunnel (not drawn to scale). The test section ③ shows the side plate ⑦ for staggered row mounting

through the downstream stabilising chamber (a 6° diffuser ①). The distance from the bell mouth air inlet (extreme right of Figure 1.2) to the test section inlet measured 3000mm, this ensures the fully developed flow field up to the maximum flow rate (10 m/s according to the manufacturer) by the time the airflow reaches the test section.

The hot air exits the tunnel through an elbow bend which diverts the airstream out of the system via the workshop ceiling ⑧. Just before the elbow, a suction blower is installed in-line and the driving shaft extends out to the prime driver which is a large 17kW DC motor. The constriction section ④ has one pressure ring at its inlet, immediately after the flow settler, and another at the exit where it joins the test section. The pressure differentials of the two rings caused by a Venturi effect are input to a differential pressure transducer which generates a signal to drive the control unit of the blower motor. The air velocity is controlled by a PID closed-loop control strategy implemented using LabVIEW software suite. Before the test, the chosen range of air velocity from 0.5 m/s to 5.0 m/s is verified by a Particle Image Velocimetry (PIV: (6) Figure 1.1) under an empty chamber condition. PIV is an accurate, non-intrusive technique which can be used to track average speed of the flow field accurately. The operation of this tool and its application to this test rig is described in a conference paper by Khashehchi, et al. (2012)[9].

The test section ③ has its cross-sectional areas measured 454mm × 454mm at the inlet and 462mm × 462mm at the exit. It is 1220mm long and divided into three compartments horizontally by two sets of adjustable Flexi-glass baffle. The middle compartment has the cross-sectional area of 454mm (W) × 210mm (H) at its inlet. During the experiments, the heat exchanger specimen is installed via two sets of side plate with pre-formed pattern of

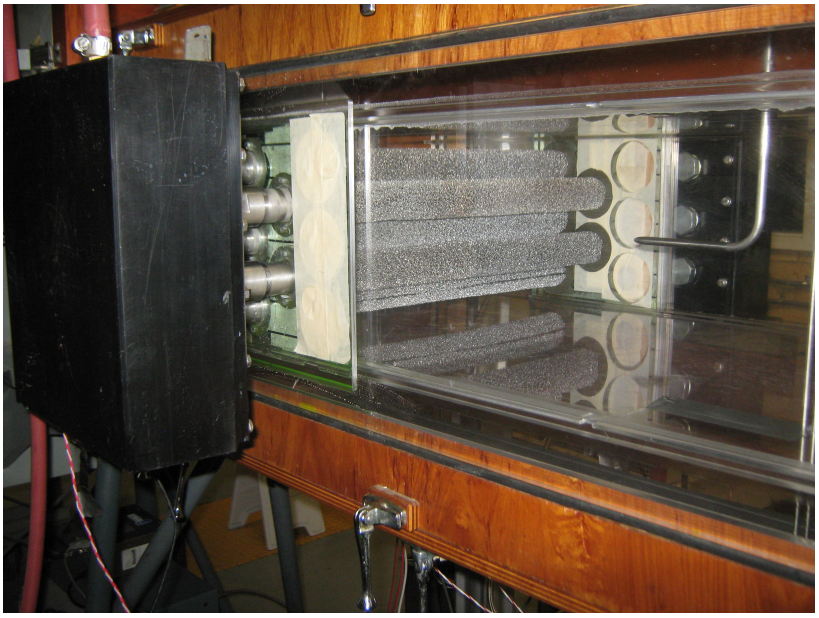

FIGURE 1.3: The test section showing the pressure drop measurement method; the pitot tube seen in the picture (right) is on the downstream; the one upstream is obscured by the specimen

intended heat exchanger configuration. A pair of pitot tube are installed at either side of the specimen whose pressure drop is to be measured (Figures 1.3 and 3.3). The upstream pitot tube, the vertical line through the center of the side plates, and the downstream pitot tube, are located at 193mm, 455mm, and 810mm, respectively from the test section inlet. The pressure difference, $\Delta P$, is measured by a differential pressure transducer with an accuracy of $\pm 1$ Pa at 150 Pa FS. Above 150 Pa, a different pressure transducer with $\pm 2$ Pa resolution is used. A pair of PT-100 RTD probes are installed in the bottom compartment near the test section inlet to measure the inlet air temperature. Exit temperature was measured by an XY traversing system ② where four PT-100 probes are mounted and can scan the designated exit area of the test section at the grid size of 10mm $\times$ 10mm, using a movement similar to that of a dot matrix printer. All PT-100 probes have $\pm 0.03$°C reading accuracy.

On the liquid side, a hot liquid mixture –made of 1 part glycol + 2 parts water by volume– is heated and maintained at 75°C in a heated tank (Figure 1.4). The tank is equipped with two sets of high power heating element providing a combined rating of 8kW. The hot liquid is circulated around a closed circuit via an insulated tubing through a pump, an accurate flow meter, the specimen core, and returns to the sump. The two heater elements inside this tank are an ON/OFF type with a crude thermostat on one set. They are switched on in turn, the dumb element first, to supply the baseline heat load quickly when needed. A coiled copper tubing immersed inside this tank forms another closed liquid loop consisting of ethylene-glycol. A Julabo F33-ME cooling/heating circulator (labelled (5) in Figure 1.1) is connected to this loop to provide an accurate temperature control by taking the control signal from a special RTD probe installed at the specimen inlet. The circulator hence functions indirectly as the liquid inlet temperature regulator by adding or removing heat (i.e. activates cooling) to the heated tank via the copper coil tubing which acts as a simple heat exchanger. The

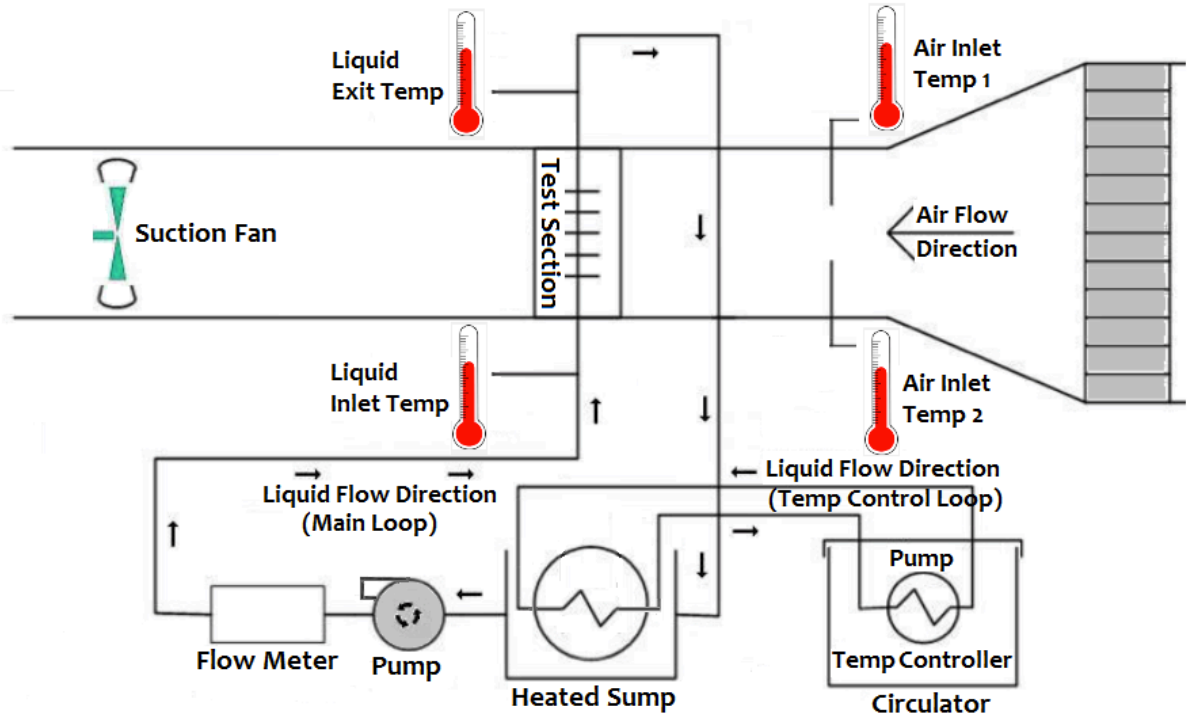


Figure 1.4: Top-view schematic of the hot liquid loop to supply heat to the heat exchanger core; adapted from J. Richards, B.Eng thesis: *Design and Performance Evaluation of Flue Gas Economisers* School of Mechanical and Mining Engineering, University of Queensland (2012)

indirect heating approach is necessary because: (i) the circulator has limited capacities for its heating power (2kW), sump volume (6.4 litres), and pump pressure (0.45bar max) and these are not enough to run multi-row experiments; (ii) the circulator liquid must be kept clean during operation to be able to maintain its maximum temperature (∼138°C). Liquid inlet and exit temperatures are measured by installing two K-type thermocouples on the inlet and exit metal fittings for single tube experiments. For tube bank experiments the two TCs are installed at the inlet and exit header units (the black block at the left hand side of Figure 1.3). The tip of each probe in all cases sits at the centre of the liquid stream.

Data logging and control of different parts of the system such as the flow rate of inlet air, its exit temperature scanning, etc. are co-ordinated by a host computer. The data file logs air inlet (measured by two RTDs, see Figure 1.4) and exit temperatures, hot liquid inlet and exit temperatures, liquid flow rate, and pressure drop across the test specimen. Before testing the foam-wrapped specimens, a plain aluminum cylinder ($d_o$ = 30mm $d_i$ = 26mm) is tested for a reference data; covering all 10 settings of airflow from 0.5 m/s to 5.0 m/s at 0.5 m/s increment. The air side Nusselt number at each flow rate is verified according to e.g. Churchill-Bernstein, and Zukauskas correlations as described in Incropera, et al. (2006) [10] to ensure trustworthiness of the test rig. Typical comparisons (for a case where $d_o$= 32mm) of measured data against results obtained by these correlations are shown in Figure 1.5.

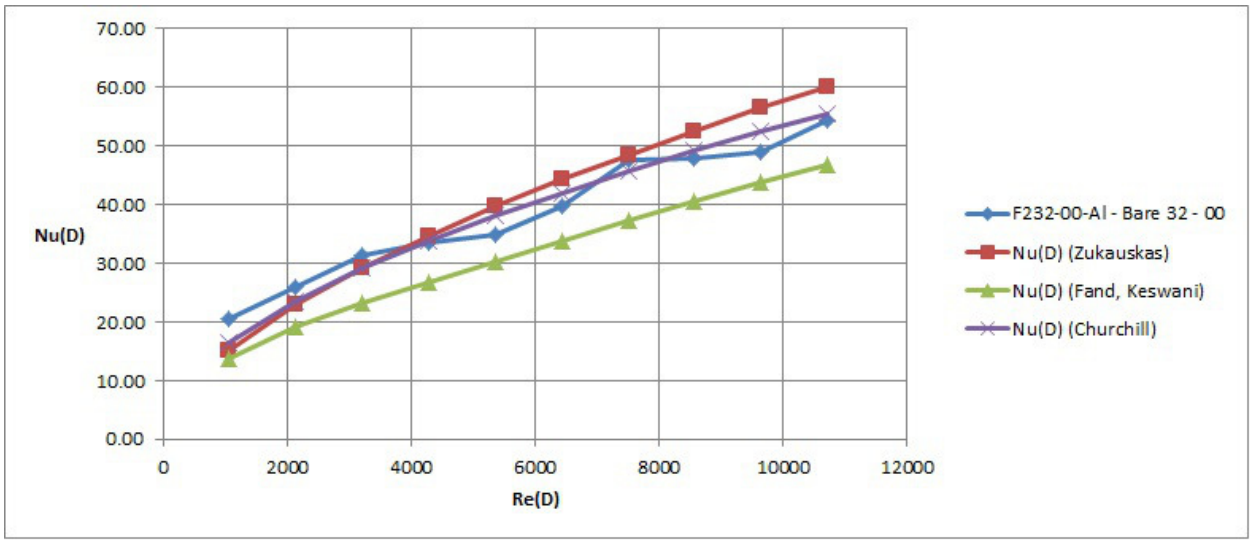


FIGURE 1.5: Reference data plotted against results of evaluating familiar correlations; specimen designation: Al-Bare = aluminum bare surface, 32 = $d_o$(mm); graphing courtesy J. Richards (2012)

## 1.5 Thesis Organization

This thesis revolves around the three dot points listed in Section 1.1. One article was published for each task to report thermo-hydraulic results of the foam based heat exchangers; in comparison with the results of conventional finned tube tested under the same conditions. Following in Chapter 2 is a review of some relevant researches on non-foam heat transfer augmentation, then the concept of augmenting heat transfer by secondary surface based on porous materials for both metal and non-metal.

Chapters 3, 4, and 5, respectively contain the re-formatted contents of the published articles for single tube, single row, and multiple row data. To be self-contained in their journal form, these articles possess a certain degree of textual duplication. Effort is made to minimize repeated contents by relocating them to the 'Introduction' chapter and references from original article are pointed to this common location as necessary. This arrangement has its pros and cons – it makes the texts more concise and provides opportunities for rewriting to clear up ambiguity if such a situation exists; but the downside is the loss of readability and its intended structure. Nevertheless, if this causes a major concern, a published version of original documents is always available from suitable on-line resources.

Chapter 6 revisits the conclusions drawn in each article and provides a combined view to justify/reject two research questions posed early on (Section 1.3). The thesis closes by proposing ideas for further works related to unresolved issues or pursuing new concepts learned throughout the entire RHD candidature.

# 2
# Literature Review

## 2.1 Preamble

This chapter surveys efficiency enhancing techniques applicable to conventional heat exchangers relying on air as a coolant where the air side forms external flow. This background knowledge is important as performance tune-ups developed for non-foam heat exchangers remain relevant for novel designs using more advanced materials which this study concentrates on. To the author's best knowledge, there are no references of experimental nature on multiple-row foam-based tubular heat exchangers available; and this present work may lead to further developments of interest to geothermal, oil and gas, and power industry.

The chapter is concluded by open literature reviews of recent development on foam-based domain focusing on high porosity metal foam.

## 2.2 Performance Enhancement of Conventional Heat Exchangers

The majority of non-foam heat exchangers falls into the type where fins are employed in myriad forms, typically on the lower density fluid side. Before the advent of porous materials, the designing, optimizing, and performance enhancing of finned-tube heat exchangers had been widely researched. Heat transfer augmentation by a mere increase of fluid-flow velocity not only impractical in some situations, but it also poses an important fundamental trade-off between heat transfer and friction-power expenditure. This fact has been well aware and can be traced back in time to the early day of thermal engineering discipline. Kays and London (1955)[11] wrote in a very beginning paragraph of page (1) in their book:

> "*... [per unit of the heat exchanger surface area] heat transfer rate varies as something less than the first power of the [flow] velocity. The friction-power expenditure is also increased with the flow velocity, but in this case the power varies by as much as the cube of the velocity and never less than the square.*"

Following the pioneers of the field in the 60's such as Kays and London (1955)[11], Briggs and Young (1963)[12], Robinson and Briggs (1966)[13], are publications from newer generation researchers – the like of Rabas, et al. (1981)[14], Kayansayan (1993)[15], and Jang, et al. (1998)[16]. At the turn of the century, the next wave of names emerged. Kim, et al. (2000)[17], Bhattacharya, et al. (2002B)[18], Matos, et al. (2004a)[19] and (2004b)[20], Ibrahim and Gomaa (2009)[21], all engaged in improving heat exchanger performances. Some of these works investigated heat transfer and pressure drop of air flowing through tube banks of conventional heat exchangers where a wide range of fin height, thickness, spacing, and root diameters are examined (Odabaee and Hooman (2012)[22]).

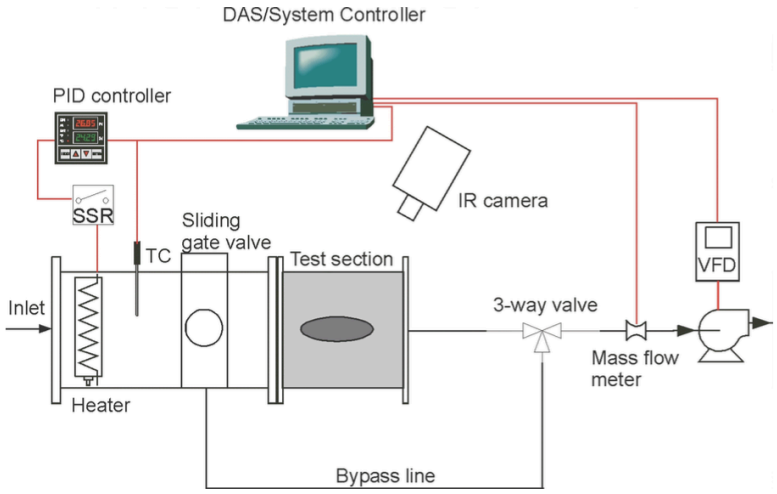


FIGURE 2.1: Schematic of the flow loop set up for use in their experiments (Sohal and O'Brien (2001)[7])

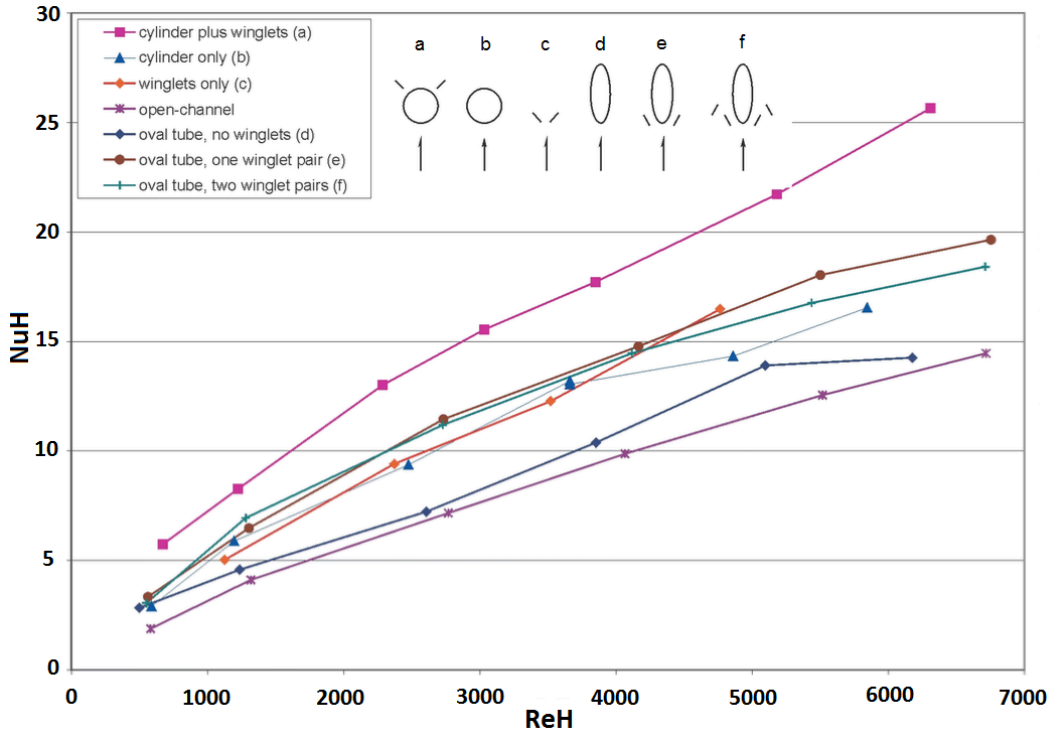


Figure 2.2: Nu - Re plot showing results of heat transfer enhancement using winglets; both Nu and Re are based on hydraulic diameter of the flow passage (Sohal and O'Brien (2001)[7])

Most notable and relevant to the interest of QGECE are the studies set up at the Idaho National Engineering and Environmental Laboratory (INEEL). A group of researchers affiliated with this laboratory created a five-year program to improve the performance of conventional air-cooled heat exchangers for binary geothermal power plants. Motivated by Jacobi and Shah (1995)[23] on the generation of longitudinal vortices, they started the program in 1999; looking at enhancing the performance of finned tubes subject to force convection. The Reynolds number under test was on the low range, ~650 to 6500 as it was dictated by a characteristic length of the test chamber. The conceptual set-up of their test rig is partially depicted in Figure 2.1. Two techniques to maximize heat transfer and minimize pressure drop were experimentally investigated, namely (i) vortex generators (winglets) were attached at strategic spots in relation to the heat exchanger elements and (ii) circular tubes were replaced by oval tubes. The INEEL research team produced four milestone reports within two years of their project inception. These are, in order, O'Brien and Sohal (2000a)[24], O'Brien and Sohal (2000b)[25], Foust, et al. (2001)[26], and O'Brien, et al. (2001)[27]. Each described variations and strategies of winglets: (i) shape (delta/square), (ii) position (downstream/upstream), (iii) number (one pair/two pairs), and (iv) angle in relation to the direction of flow (30°/45°), respectively.

Sohal and O'Brein (2001)[7] subsequently consolidated the results and presented a summary on six tube/winglet combinations as a plot of Nusselt number versus Reynolds number (Figure 2.2). They concluded that the addition of winglets increases the heat transfer coefficient by ~35% as compared to plain tubes. Corresponding increase in friction factor is in the

range 5 – 10% for Reynolds number in the range 500 – 5000. Unfortunately, the procedure for determining local heat transfer coefficient was not elaborated. O'Brien, et al. (2002)[28] extended their winglets study by setting up a separate chamber to measure pressure drop across the tube bank in addition to the chamber where heat transfer was measured. For the determination of local heat transfer coefficients where detail was missing in earlier reports, the method based on temperature correlation was fully explained.

Further detailed descriptions on this work at INEEL are provided by O'Brien, et al. (2004)[29] and O'Brien and Sohal (2005)[30]. The former focuses on oval tube with two pairs of winglets installed in a zigzag fashion upstream; while the latter emphasizes a circular tube with downstream winglets configuration. For the oval tube, they confirmed the result of 38% improvement on average heat transfer coefficient if the winglets are installed. On the penalty side, the corresponding increase in friction factor associated with the addition of a single winglet pair was very modest, less than 10% at $Re = 500$ and less than 5% at $Re = 5000$.

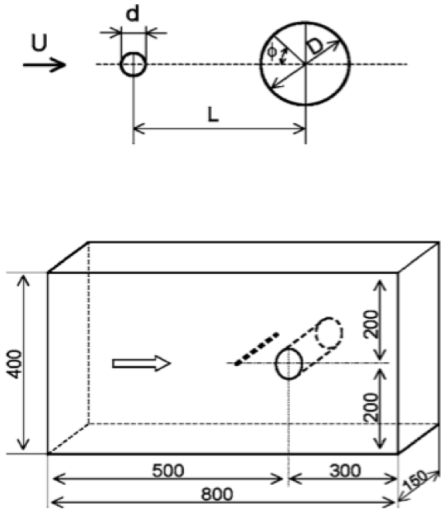


FIGURE 2.3: Schematic of the experiments performed by Tsutsui and Igarashi (2006)[8]

Tsutsui and Igarashi (2006)[8] employed a similar concept of upstream flow modification to enhance heat transfer of a plain cylinder. These authors inserted a small circular rod of different diameter in-line with a single heat exchanger cylinder arranged in a cross-flow. Their experimental schematic is depicted in Figure 2.3. The rod has the diameter ($d$) from 1mm to 12mm and it was placed in front of the cylinder with the distance ($L$) varying from 40mm to 120mm. The expected effect was that the rod would interrupt the incoming flow ($U$) of a high Reynolds number (15,000 to 62,000) and induce upstream disturbances to the flow. Because of its small size, the rod would only generate a small drag. If the rod is placed at a suitable distance, the front face of the cylinder would be exposed to its wake, thereby enhancing the average heat transfer coefficient on the cylinder. The key parameters in this study are the rod size, the distance between the rod and the cylinder, and the Reynolds number. During the experiment, the cylinder diameter ($D$) was fixed at 40mm while the

free stream velocity $U$ s varied between 4 and 24 m/s. A smoke tunnel was used to visualize the flow around the rod and the cylinder.

The authors reported the results which showed two flow patterns, depending on $d/D, L/D$, and the Reynolds number. Rods with smaller diameter tended to generate vortex shedding. In this case, the front face of the cylinder is immersed in those vortices. Bigger rods, in contrast, resulted in quasi-static vortex and heat transfer enhancement was better for all Reynolds numbers. The optimum conditions for largest heat transfer was reported at $L/D = 1.25$ and $d/D = 0.25$. The resulting overall Nusselt number at $Re$=$6.2\times10^4$ was found to be over 40% higher than that of the single cylinder without the upstream rod.

## 2.3 Prior Research on Foam Heat Exchangers

Generally, foam is a porous material with pockets of void space interconnected to form open-cell structure permeable to fluid flow. This makes foam structure to possess two important properties:- permeability and porosity. However, the term sometime refers to a structure where individual cells exist independently on their own and there is no open passage between them (see also T'Joen, et al. (2010)[6]). This study adheres to the first definition.

Foams can be manufactured from different parent materials and they share one very important characteristic – all have a high to very high specific surface area (total area per unit volume). They also have a low relative density because void space carries negligible weight. Metal such as zinc, aluminium, copper, tin, nickel are popular materials for the manufacture of metal foam whereas carbon of different forms and ceramic are typical base materials for non-metal foams. Foam media usually exhibit physical properties of their parent materials. Extended characteristics of foam materials which are of interest to specific applications are pore diameter, cell diameter, strut (or ligament) diameter, porosity, permeability, and specific surface area.

### 2.3.1 Carbon Foam Heat Exchangers

Non-metal porous materials had been available and studied more widely than their metal counterpart before the turn of the century. The early non-metal foam products were made by the pyrolysis of a polymer substrate. Walter Ford filed a method patent for this process in the early 60's to manufacture carbonaceous skeleton or reticulated vitreous carbon (RVC) (Gallego and Klett (2002)[31]). RVC is not suitable as a heat exchange material because it has a very low thermal conductivity.

There are other forms of carbon foam which possess a high thermal conductivity. Researchers from the US Air Force Materials Lab developed a process by applying a blowing technique to mesophase pitches to form a carbon foam. The foam is then stabilized prior to carbonization (Gallego and Klett (2002)[31]). At about the same time, a graphite foam with even higher thermal conductivity was discovered unexpectedly at the Oak Ridge National Laboratory (ORNL) and thermal-oriented research on foam materials started gaining a serious interest around ORNL not long afterwards (Klett, et al. (2000)[32]).

Klett, et al. (2000)[32] designed three simple heat removing devices to prove a high thermal quality of the graphite foam developed in-house at ORNL. The first heat exchanger

was made of three circular aluminum tubes $d_o = 0.64$cm. The tubes were press fit into a block of the ORNL graphite foam measured 10.1cm$^2$×2.54cm thick. The foam has 0.5 g/cm$^3$ density and 150 W/m·K of thermal conductivity. Water at 80°C was circulated through the three tubes at 11.34 litres/min. On the heat removal side, ambient air at 35°C was forced over the foam block – set inside a suitable enclosure – at 560 litres/min. During transient run, the authors reported a 3°C water temperature drop for a 30°C exit air temperature rise. This test claimed an impressive overall calculated heat transfer coefficient between 6000 and 11,000 W/m$^2$·K but with a massive pressure drop of 5.4 kPa/cm.

The second heat exchanger targeted at a replacement radiator for a 800hp racing engine. The foam block was now engineered to include through holes and fin structures around aluminum-6061 circular tubes with 0.78 diameter. During the test a much larger air volume of 39,300 litres/min was forced through the system and a much lower pressure drop of 0.03 kPa/cm was achieved. However, the overall heat transfer coefficient was reduced to 977 W/m$^2$·K.

The third described a liquid-cooled compact heat sink for electronic applications. The foam block (5×5×3.2cm$^3$) at 0.47 g/cm$^3$ density was brazed onto an aluminum plate. The heat element was mounted on the other side of this base plate and the foam side placed inside a chamber. The heat sink was tested using air as a cooling fluid. Ambient air at 140, 280, and 420 litres/min was forced through the chamber. There was no gap between the foam block and the chamber walls so all the airstream must travel through tortuous paths in the pore structure of the foam. The authors presented the pressure drop at different airflows graphically and reported the overall heat transfer coefficient to be 2500 W/m$^2$·K. According to them, this is about 80 times higher than that of the standard small car radiators whose typical figure is ∼30 W/m$^2$·K.

ORNL graphite foam was used by Strattman, et al. (2006)[33] to perform experiments on void structure, foam thickness, and foam planar orientation in relation to airflow. The air velocity considered was in the range 3 – 10 m/s so the results can be used as a benchmark for both natural and force convection in real applications. The chosen foam sample has porosity in the range 0.67-0.89 and subject to parallel airflow. The foam layer, initially 10mm for each sample, was mounted onto aluminum plate to form the test fixture. Heat was supplied to the fixture from the opposite side of the plate by an electrical heating element. The foam layer was parametrically machined away a small depth at a time and the experiments repeated until aluminum substrate was exposed. The enhancement of heat transfer was estimated by comparing the heat transfer of the exposed foam surface at each step of thickness reduction to that of the bare substrate once the foam had been completely removed.

Strattman, et al. (2006)[33] observed two results relating to graphite foam in their study: (i) that the temperature of the foam was the same as the temperature of the aluminum substrate independent of foam thickness (ii) that the heat transfer was not a strong function of the foam thickness. From (ii) they concluded that, for a parallel flow, the air penetration into the foam mass was effective to only about 3mm (or 3-5 pore layers, depending on the pore size). Therefore using foam thickness more than 3mm in similar applications would unlikely give additional advantage. Another surprised finding was the heat transfer enhancement varied inversely with the Reynolds number (decreased from about 28-10% over the Reynolds number range 150,000-500,000). Argument given was that less rigorous surface

eddies associated with low air speed allowed more amount of air to penetrate the foam mass.

Jamin and Mohamad (2007)[34] studied tubular heat exchanger partially and fully covered by a low porosity carbon foam, $\phi = 0.61$. The study targeted heat recovery in cogeneration environment where heat containing fluid usually has higher Prandtl number. As part of their investigation, the authors constructed two distinct forms of specimen. The first form consisted of foam rings of two annular lengths; with $D_i = 15.9$mm, $D_o = 22.1$mm and 26.1mm. Each foam annulus (or donut) was 5mm thick and was press-fit onto two core tubes of $d_o = 15.9$mm at 5.5mm apart. There were a total of 15 foam annuli on each tube. Similarly, for the second form, the fully covered foam tubes were made by press-fitting two sizes of foam sleeve ($D_i = 15.9$mm, $D_o = 22.1$ and 26.1mm) onto their core tube $d_o =$ 15.9mm, 152.2mm in length. The study measured heat transfer rate and pressure drop from each sample and a bare tube, all mounted vertically, in forced convection. The results were compared with those of aluminum finned tube with the specifications: $D_i = 15.9$mm, $D_0 =$ 38.1mm, $t_f = 0.38$mm, $t_p = 2.52$mm, and number of fin = 52. The largest increase in Nusselt number was achieved by aluminum fins (note the $D_o$ of finned tube), which was about three times greater than the best carbon foam case. The largest pressure drop was created by the 26.1mm full foam tube which the authors regarded its presence as a blunt object. This led to the authors' conclusion that, given the forced convection their experimental results obtained, aluminum fins were the most suitable medium for use in cross-flow heat exchangers.

In conclusion, carbon foams particularly in their graphite form have one indisputable advantage – they can be made with a relatively high thermal conductivity. However, there are drawbacks in mainstream utilization because they lack robustness of metals. In addition, in actual designs they inevitably need to be interfaced with metals (tubing, fittings, etc.) but since there is no practical bonding method between the two, ensuring low thermal resistance at the interface (see Section 2.3.2) is difficult.

### 2.3.2 Metal Foam Heat Exchangers

From heat transfer point of view in compact heat exchangers, the most obvious characteristic of porous materials justifying their use is the attractively high specific surface area. Closely related to surface area are porosity and pore diameter – which in turn dictates structural strength. Pure carbon foam is hardly fabricated to a large pore sizes (required to improve permeability) because doing so will compromise it structural strength. This issue has less concern on metal foam. For this reason, metal based foam gains a wider acceptance in industry for this area of applications.

Open literature on using metal foams as a secondary surface in enhanced and compact heat exchangers can be traced back to more than a quarter of the century. A large number of technical reports available openly has already been produced, some of which will be listed here based on their basis of relevance.

**(a) Planar Constructions**

Kaviany (1985)[35] studied heat transfer in a porous channel bounded by two isothermal parallel plates under a fully-developed laminar flow. He modified the Darcy model for transport of momentum and obtained the results, showing the correlation of the Nusselt

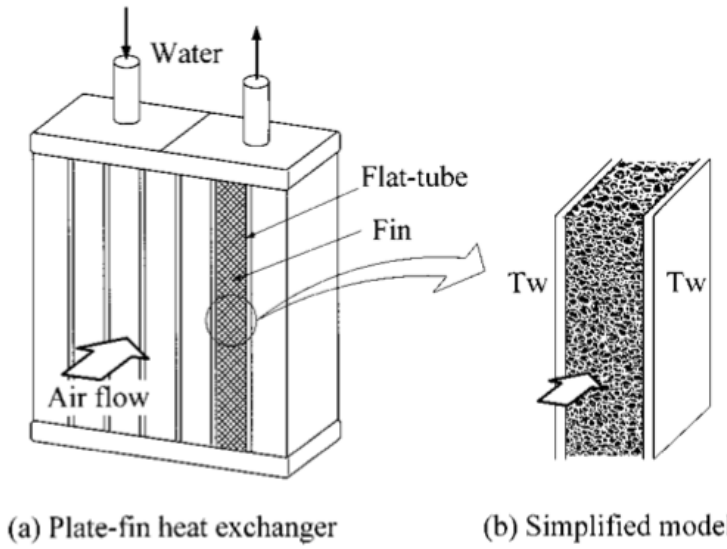


FIGURE 2.4: Experimental fixture (b) described and used by Kim, et al. (2000)[17]

number and the 'porous media shape factor' ($\Gamma$) based on channel width, porosity, and permeability. In mathematical form, this shape factor is written as $\Gamma = \sqrt{(W^2 \cdot \phi / K)}$ and, in fully-developed fields, $Nu$ increased as $\Gamma$ was increased. The author also reported that the excess pressure drop associated with the entrance region decreased when $\Gamma$ increased.

Lu, et al. (1998)[36] presented an analytical model by treating metal foam structure as cubic units consisting of heated slender cylinders to represent foam ligaments. The model used existing heat transfer data on convective cross-flow through cylinder banks as its basis to predicted heat transfer. The study investigated temperature distribution inside a foam-filled channel with constant wall temperatures. The results of overall heat transfer coefficient and pressure drop leaded to optimized design of foam structures to maximize heat transfer per unit pumping power. Two sample applications were identified as high performance heat sinks in power electronics and multi-layers heat exchangers for aeronautical industry. Due to an oversimplification of sharp-edged ligaments as slender cylinders, the authors recognized that their model may lead to overestimated results. Despite this observation, however, the trend of predictions according to the authors was in reasonable agreement with available experimental data on aluminum foams.

Kim et al. (2000)[17] performed an experimental study on a simplified model of air-cooled plate-fin heat exchangers typically found on automobiles and aircraft. Their test fixture emulated one flow passage of a conventional plate-fin heat exchanger sandwiched between two channel walls which were kept at constant temperature ($T_W$ shown by Figure 2.4). Six foam samples were tested, three with constant porosity (0.92) but varying PPI (10, 20, 40) and the other three with constant PPI (20) but different porosity (0.89, 0.94, 0.96). All six samples were aluminum 6101 foam. Compared to a conventional louvered fin, the porous fin exhibited slightly lower friction factor values at low Reynolds numbers. However, at high Reynolds number, the porous fins showed much higher friction factors compared to the louvered fin. Overall, when the volume goodness value was compared, the louvered fin

had a slightly better advantage. Among the porous samples themselves, volume goodness results indicated that porous fins with low permeability and low porosity are preferable with regard to the heat exchanger compactness. Correlations for the friction factor and modified $j$-factor (defined by the authors as $j^* = \eta_s \cdot (hPr^{2/3})/(G_c C_p) = \eta_s \cdot j$) were given to assist in the design of a plate-porous fin heat exchangers.

In a related study shortly after, Kim et al. (2001)[37] pursued the study on convective heat transfer and pressure drop characteristics of three aluminium foam samples in an asymmetrically heated channel. The samples chosen were those with a constant porosity (0.92) because this value is comparable to that of conventional fins used in air-to-air heat exchangers. The samples had pore density 10, 20, and 40 which were essentially the three described in the earlier study (Kim et al. (2000)[17]). Each sample, with the size of 90mm ($W$) × 9mm ($H$) × 188mm ($L$), was placed in a Plexiglass channel 90mm ($W$) × 9mm ($H$) cross-sectional dimension and subjected to the airflow between 1.1 and 5.4 m/s at one end; while the other end opened to the atmosphere. relationships for the practical thermal applications. The outcome was two empirical correlations describing $Nu$ and $f$ in terms of $Da$:

$$Nu = 0.0159 Re^{0.426} Pr^{1/3} Da^{-0.787} \tag{2.1}$$

According to the authors, $Re$ in the range of validity $1000 \leq Re \leq 3000$ gave an 8% maximum deviation on $Nu$, and:

$$f = \frac{1}{Re \cdot Da} + \frac{C_E}{\sqrt{D_a}} \tag{2.2}$$

Where $C_E$ is the inertia coefficient suggested in the Forchheimer-extended Darcy model for porous media. Its value varied around 0.1 for aluminum foams used in their study. The authors found that experimental results of friction factor was much higher on aluminum foams with lower permeability while the significant enhancement in $Nu$ was obtained.

Up to this point, it is evidenced that the main hurdle of porous materials for the applications in thermal exchange domain is a generally high pressure drop. This issue develops a cognizance which ties to the fact that, in most experiments, the porous specimen under study fills up the entire flow channel. To investigate the effect of flow bypass on pressure drop and hence improve the design, Kim, et al. (2003)[38] performed another experiment in which the specimen only filled half the channel height. The same sample specifications (fixed $\phi$: 0.92 and PPI: 10, 20, 40) were studied. The sample fixture were prepared by brazing a block of foam to a thin metal plate (to maximize thermal conductance). The results were analyzed in the same way and comparison was made to reference data generated by a conventional plate-fin of the same dimension. The results showed that the aluminum foam heat sinks of all PPI induced 28% less thermal resistance than the conventional plate-fin heat sink for a fixed airflow setting. In addition, the foam heat sinks have a weight merit compare to the plate-fin counterpart by roughly three quarter, making them only 25% as heavy. Among themselves, the three foams exhibited PPI dependent results. The 10 PPI foam obtained $Nu$ 16-27% higher than the 40 PPI sample due to smaller flow resistance inside the block and, hence allowing more air mass to flow through and took up more heat with it.

Bhattacharya and Mahajan (2002B)[18]) presented experimental results of heat transfer and pressure drop on what they termed 'finned metal foam heat sinks' tested under forced

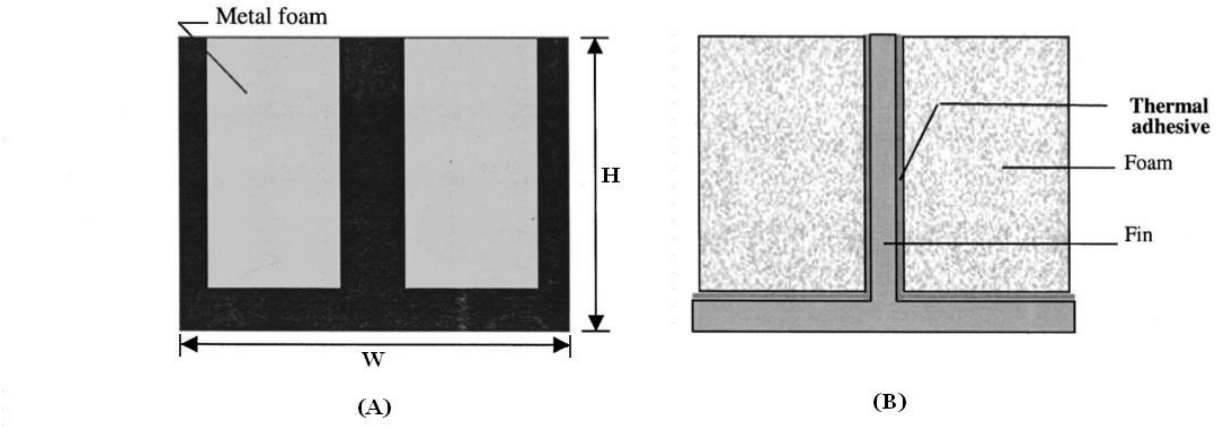


FIGURE 2.5: An experimental fixture used by Bhattacharya and Mahajan (2002B)[18] (B) based on an inception of Calmidi, et al. (2000) their research colleagues (A)

convection. The design (Figure 2.5(B)) was quoted as being suggested by Calmidi, et al. (2000: Figure 2.5(A), internal citation) where the air gap between two adjacent fins was replaced by high porosity metal foams. It was essentially similar in concept to the 'plate-porous fin' heat exchangers (Figure 2.4(b)) studied earlier by Kim et al. (2000)[17]. One distinct difference was that thermal load to be dissipated by these heat sinks also came from the bottom face of their solid base in addition to the two side walls. Two samples of aluminum foam with pore density 5 PPI and 20 PPI were employed as the enhanced surface on fin faces. Both samples had the same porosity of 0.9 and were bonded to the fin and bottom faces by thermal adhesive. The test fixtures were manufactured in-house with the number of fins from one, two, four, and six. According to the authors' nomenclature, Figure 2.5(B) constituted one fin while Figure 2.5(A) dubbed two fins as, although three fins were shown in the figure, the fins forming the channel were half the thickness of the central fin. The forced convection results showed that heat transfer was significantly augmented when fins were incorporated into the foam. The heat transfer coefficient increased with increase in the number of fins until adding more fins provided no further heat transfer benefit due to interference of thermal boundary layers. Under the flow regime chosen in the experiments, both foam samples reached heat transfer asymptote at four fins. However, being more open to airflow due to its larger pore sizes, the 5 PPI sample produced a much lower pressure drop at the same air velocity. This fact also led to higher heat transfer compared to the 20 PPI foam as the latter caused an increased flow resistance and less airflow in the foam mass was achieved.

Comparing to conventional finned heat sinks without foam commercially available for electronic cooling, Bhattacharya and Mahajan (2002B)[18]) reported an enhancement on the heat transfer coefficient $h$ by a factor of $\sim$6. However, if constraint was imposed on $\Delta P$, the overall performance gain of 1.5 to 2-fold was observed. Based on the experimental data, they concluded the study by presenting two empirical correlations for the Nusselt number $Nu$, (i) in terms of Peclet number and dimensionless ratio of hydraulic diameter to pore diameter, and (ii) a generalized $Nu$ formulation, taking into account the effects of thermal

dispersion and interfacial heat transfer between the solid and fluid phases.

In a subsequent study, Bhattacharya and Mahajan (2006)[39] conducted experiments under natural convection and reported heat transfer results in two parts. Part-I concerned simple heat sinks assembled by glueing a block of aluminum foam specimens to solid metal base using high heat conductivity adhesive. There were eight foam samples under this part with the pore density varied to include: 5, 10, 20, and 40 PPI and having porosity in the range 0.899 - 0.959. In Part-II, two aluminum foam samples, 5 and 20 PPI, with a fixed porosity at 0.9 and making up the 'finned foam heat sinks' described in their earlier study by Ref. [18] were tested and reported. The heat sinks in Part-II were constructed with one, two and four fins. All specimens were tested in both vertically (heated from the side) and horizontally (heated from the bottom); except for one sample of Part-I, the case of $\phi = 0.899$ and pore density = 5 PPI, where the test in vertical orientation could not be performed.

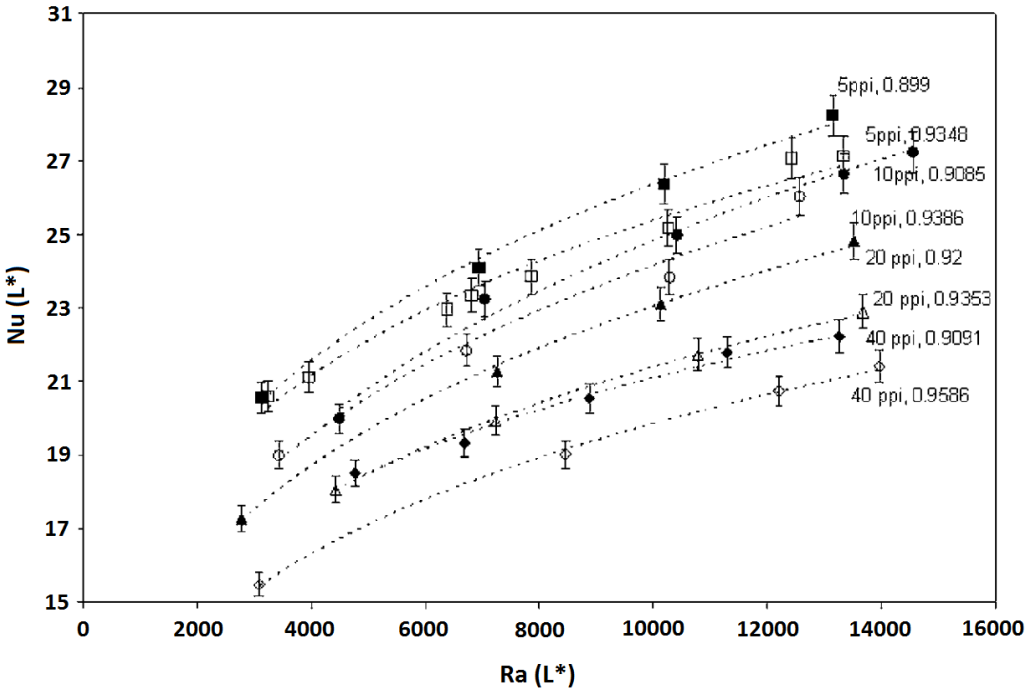


Figure 2.6: Results for natural convection of simple metal foam heat sinks in vertical orientation, Bhattacharya, et al. (2006)[39]

The results showed that, compared to a bare heated surface, the heat transfer coefficients of simple foam heat sinks of Part-I were boosted up five to six times. The trends followed the same direction for both vertical and horizontal orientations; with the graphical results of the former depicted in Figure 2.6.

However, when compared to commercially available heat sinks of similar dimensions, the enhancement was found to be marginal. Upon a closer inspection at their results the authors concluded that, for a given $\phi$, the resistance to flow decreased with an increase in pore size (i.e. less PPI) due to an increase in permeability. The end result was enhanced flow and heat transfer rate. For a given PPI, the performance was enhanced with a decrease in $\phi$ (i.e.

an increase in base metal content). This indicated that conduction through the foam (i.e. its effective thermal conductivity, $k_e$) was still a bottleneck even under buoyancy-induced convection. (*Note:* The readers should be aware that there is likely a minute error in the manuscript when the authors stated in the Abstract: *"The experimental results also show that for a given pore size, the heat transfer rate increases with porosity, suggesting the dominant role played by conduction in enhancing heat transfer."* As supported by their results shown in Figure 2.6, what the authors wanted to say was probably *"the heat transfer rate increases with decreased porosity"* as they correctly elaborated in Section 5.1 and summarized that again in their Conclusions.) Part-I was culminated by two proposed correlations of $Nu$ in terms of Darcy and Rayleigh numbers, one based on the fluid properties and the other on effective parameters of the foam.

In Part-II, Bhattacharya and Mahajan (2006)[39] reported that the 'finned metal foam' heat sinks of both PPIs (i.e. 5 and 20) were superior in thermal performance compared to the simple metal foam design of Part-I and conventional finned heat sinks available commercially. The heat transfer increased with an increase in the number of fins. However, the relative enhancement was found to slow down with each additional fin. This led to an argument by the authors that there existed an optimal number of fins beyond which the enhancement in heat transfer, due to increased surface area, was offset by the retarding effect of overlapping thermal boundary layers.

In comparison to a particular commercial heat sink of longitudinal finned design, Bhattacharya and Mahajan (2006)[39] reported an improvement in $h$ values by 12% and 16% for 2-fin and 4-fin fixture, respectively using the 5 PPI foam. For the 20 PPI specimens, these value became 9.5% and 13% a slightly less effective manifestation. In both cases, they attributed the small enhancement to a mismatch in dimensions (their specimens were 0.6 in. shorter). They also relied on the manufacturer's data for thermal resistance of the finned heat sink and were not sure if the figure was applicable to vertical or horizontal orientation. When they normalized this commercial heat sink to the same geometries as their specimens and re-compared, they found a far better enhancement by both the 5 and 20 PPI specimens over the longitudinal finned product at all range of $\Delta T$. For example the 4-fin, 5 PPI specimen in vertical orientation showed enhancement $\sim$65% at 10°C of $\Delta T$. At 50°C $\Delta T$, the enhancement figure dropped down to about 24%. For the same limits of $\Delta T$, the horizontal orientation of the same specimen produced 52% and 19% enhancement, respectively.

It should be noted that the finned metal foam heat sinks described in this study had their foam block and base plate glued together. This technique is known to cause relatively high thermal contact resistance at the interface of the two materials. De Jaeger, et al. (2012)[40] quantitatively assessed TCR by four methods of foam-substrate bonding and concluded that thermal adhesive was the worst by far. It is logical to assume that enhancement figures reported in Bhattacharya and Mahajan (2002B)[18] and (2006)[39] can be significantly improved if the foam and the base plate of specimens were bonded together by brazing.

Boomsma et al. (2003)[41] studied the effect of compressing aluminum metal foam on heat transfer and pressure drop. The motive of compressing the foam was to gain more specific area and the expectation was a higher Colburn factor when the compressed foam was applied as heat sinks for electronic cooling with a large amount of heat to be removed. The experiments performed by Boomsma et al. (2003)[41] were quite unique as (i) the foam

physical structure was intentionally modified to achieve the different physical properties outside its fabricated specifications and (ii) the specimens were tested for their heat transfer (in terms of $Nu$) and pressure drop by a liquid-cooled set-up.

The test fixture was made by brazing the foam piece of required compressed level to a solid base which acted as a heat input source, or heat spreader in their terminology, for the heat sink under test. The solid heat spreader was made from 6092 aluminum alloy while the heat sinks were made by compressing 6101 aluminum foam of 40 PPI and $\phi =$ 0.92 and 0.95 into 7 samples, 4 from 0.95 porosity base foam and 3 from 0.92 porosity. These 7 modified specimens went on tests to compare pressure drop. The authors reported that the pressure drop results were as expected i.e. the foam with lowest porosity generated the highest pressure drop and vice versa. For heat transfer comparison, the heat spreader without compressed foam attached also tested as the benchmark. The Nusselt number was reported to be the maximum on the specimens with lowest porosity and the smallest Nusselt number was found on the most porous sample (but this was still larger than the $Nu$ resulted from the bare heat spreader). This results signify that maximum heat transfer enhancement is accompanied by the largest pressure drop.

In the comparison with commercial products, Boomsma et al. (2003)[41] indicated that the compressed open-cell aluminum foam heat exchangers generated thermal resistances that were two to three times lower than the best commercially available heat exchanger tested, while requiring the same pumping power.

Mancin, et al. (2010)[42] experimentally investigated the pressure drop during air flow in six aluminum foam samples in a foam-filled channel. The results are analyzed and compare to pressure drop models available in open literature. The authors found that, among many models considered, the pressure drop model presented by Bhattacharya, et al. (2002A)[43] gave the best estimation to their data set. These authors also proposed a new, simpler, pressure drop model based on Fanning equation and validated the new model using data generated by third party laboratories.

In a subsequent follow-up of their previous studies (Refs. [42] and [44]), Mancin, et al. (2012)[45] pursued another experimental study to investigate heat transfer performance of two aluminum foam samples with the same pore density and almost identical porosity. The sample chosen has the pore density of 22 PPI and a porosity nearest to 0.93. The effect of two different foam heights, 20mm and 40mm, was assessed by installing each sample block of the same footprint (100mmW $\times$ 300mmL) in a specially built channel which forms part of the test section they used in other experiments. The total width of the chamber was 300mm so the frontal area of both samples filled up 1/3 of the test chamber to form the cross section of 100mm *times* 20mm and 100mm $\times$ 40mm, respectively. The samples were electrically heated via a base plate made by embedding a resistor wire onto a milled slot of solid aluminum 10mm thick. The two test specimens, formed by sandwiching the foam between the base plate and a top plate, were subjected to a similar regime of airflow with equivalent air mass velocity between 2.5 and 7.5 kg/m$^2$·s and three different heat settings of 250, 325, and 400W. The authors found that heat transfer was not dependent on the imposed heat flux but was affected by the flow. It was also reported that the 20mm foam block exhibited a better heat transfer performance comparing with the 40mm block. They also used the data obtained to compare the calculated results using heat transfer and pressure

drop models proposed in their two previous studies and found good general agreements.

**(b) Tubular Designs**

This section bears a direct relevance to the present study but there have been only a few publications available. The following research works dealt with single samples or an array of single row. Nevertheless, the methods shown for test apparatus and data analysis prove invaluable for the treatment of multi-row tube bundles.

Lu, et al. (2006)[46] analytically studied forced convection of a round tube fully filled with a high porosity metal foam. Uniform heat input was applied at the tube external surface along its total length and the coolant such as air or water flowed inside to remove heat via the foam structure. The Brinkman-extended Darcy momentum model and two-equation heat transfer model based on the work of Calmidi and Mahajan (2000)[47] for porous media were employed for the solutions of temperature and velocity distributions of the flow field. Subsequently, pressure drop of a single-phase flow and heat transfer were evaluated. The results showed the pressure drop as a function of permeability and that it varied exponentially with the foam PPI. Heat transfer depended on four dimensionless parameters, viz., the ratio of the tube radius to the foam pore size (geometry parameter), $\phi$, $Re$ with tube diameter as its characteristic length, and fluid–solid thermal conductivity ratio. They concluded that metal-foam filled tubes could significantly enhance the heat transfer, up to forty times that of the plain tubes of comparable dimensions.

In parallel to Lu, et al. [46], researchers from the same group Zhao, et al. (2006) [48] extended their study further on a double tube construction. They wrapped a layer of metal foam on the outer surface of the tube then wrapped the non-conductive solid wall as the outermost layer. This was essentially to form a concentric, tube-in-tube structure fully filled with the metal foam which allowed them to analyze counter flow thermal exchange. The governing model are the same as that in [46] and the analysis was set on the hotter fluid flowing inside the inner tube while the cooler fluid flowed in the annular section in the opposite direction. The outermost wall was assumed to be a perfect insulator, hence no heat exchange between the tube and the surroundings. Zhao, et al. (2006)[48] parametrically set the test conditions by varying the radius of the inner tube and filling the two fluid passages with different foams. Heat transfer performance was compared with those of two other concentric tube-in-tube designs; one with radial fins – and the other with spiral fins, fixed on the outer surface of the inner tube. They reported a significant improvement of heat transfer in the foam-filled tube comparing with both versions of the finned/foam design. It was also shown that, on both sides of the inner wall separating the two fluid streams, heat transfer performance of the metal-foam filled heat exchanger is a function of the ratio of the flow cross-sectional area and relative pore density of the metal foam filling the respective area. Unfortunately, pressure drop analysis was not discussed.

Mahjoob and Vafai (2008)[49] performed an extensive survey on existing heat transfer coefficient and pressure drop correlations of foam heat exchangers from the literature. The results were grouped into three main categories with the first describing correlations based on micro-structural properties of the metal foams. In the second category, the correlations were specific to metal foam tube heat exchangers. In the third category, correlations were specific to metal foam channel heat exchangers. Correlations listed in the second category are

those proposed by Refs. [46, 48] which, together, can predict thermo-hydraulic performance of concentric tube heat exchangers in three possible cases, i.e. the case where the inner tube of the heat exchanger is filled by a metal foam; the case where the inner tube is surrounded by a metal foam; and the case where the inner tube is filled and surrounded by metal foams. Mahjoob and Vafai 2008)[49] chose the first case to demonstrate this prediction in a counter flow setting. The two working fluids they selected were cold water flowing through the inner tube and hot exhaust gas flowing in the annular section. The porosity, permeability, pore density and mean pore diameter of the foam to fill the inner tube were 0.9272, $0.61\times10^{-7}$ $m^2$, 23 PPI, and 2.02mm, respectively. The results showed a considerable increase in the heat transfer rate (8–13 times) comparing with that of the same testing conditions but with the metal foam removed from the inner tube. For pressure drop, the authors did not explicitly give the comparison between the with-foam and without-foam conditions. They merely reported that if the foam was filling the inner tube, varying the tube diameter while maintaining the fully filled foam did not affect the pressure change significantly. Their reason being that the pressure drop is mainly affected by foam micro-structural properties and not by the tube wall. Therefore, changing its diameter would not create a considerable effect on the pressure drop.

A metal foam tube bundle based on a single row of aluminum foam heat exchangers was studied by T'Joen, et al. (2010)[6], with the aim to achieve a low pressure drop on the air side. Their heat exchangers were manufactured in-house using thin layers (4–8mm) of four different foams ($\phi$ = 0.913, 0.932, 0.937, 0.951, respectively). Two foam samples had 10 PPI density while the other two had 20 PPI. The cores were aluminum tubes with $d_o$ and $d_i$ measuring 12mm and 10mm, respectively. Thermal glue was employed as a means of contact bonding. Through wind tunnel testings the impact of various parameters on the thermo-hydraulic performance was considered, including the Reynolds number, the tube spacing, the foam thickness, bonding material, and the type of foam. The results showed that, providing a good bonding between the foam and the tubes can be achieved, metal foam covered tubes with a small tube spacing, thin foam layer, and made of foam with a high specific surface area potentially offer strong benefits at higher air velocities ($> 4$ m/s), compared to helically finned tubes. It was also reported that the air only penetrates the foam to a certain depth, resulting in a decreasing performance as the foam height increases. Finally the authors concluded that thermal glue contact bonding was found to have a devastating effects on the heat exchanger performance. They noted that more research is required to develop a cost-effective and efficient brazing process to attach metal foams to the tube cores.

Odabaee and Hooman (2012)[22] performed a numerical study on aluminum metal foam heat exchangers based on four samples of commercially available foam products with the porosity between 0.9 and 0.95. The computational domain described tubular cyclinder bundles arranged in four rows, staggered configuration. Parameters of interest included the air side Reynolds number, longitudinal and traversal pitches, foam thickness and properties. Computational results were compared with those of finned bundles of identical dimensions. The results of finned tubes under the same testing conditions were evaluated using correlations provided by Briggs and Young (1963)[12].

Among the four samples of foam, by examining velocity and temperature contours of the simulation results, Odabaee and Hooman (2012)[22] were able to relate heat transfer to

physical properties of the foam and hence understood their effects. For example, the sample with low porosity relatively possesses larger $k_f$ and heat transports better in the foam mass. When Reynolds number was low, the temperature contour across the tube bundle of this foam sample showed a high contrast such that the air exit temperature approached tube surface temperature. This means the air took up more heat, hence the explanation that lower porosity promoted higher heat transfer. This led to an important finding at low Reynolds number ($\sim$1900) the region where the exit temperature rose toward that of the tube surface occurred after the second row. In this situation, therefore, the presence of the next two rows contributed very little to further gain in heat transfer.

Comparison with the conventional finned bundle relied on the area goodness factor (defined by the Colburn's j-factor over one-third of friction factor, $f$). The authors reported that at low Reynolds number, the foam bundle exhibited the area goodness factor 2.2 - 4 times that of the finned bundle; while at the higher Reynolds number this advantage reduced to 1.4 - 1.9. On the effect of foam thickness and pitch length, it was observed that the area goodness factor decreased with the foam layer thickness and increased with the transversal pitch although the Colburn's factor changed in the opposite direction in both cases.

### 2.3.3 Comparison of Carbon and Metal Foam Heat Exchangers

Gallego and Klett (2002)[31], utilizing the test platform similar to the one designed by Klett, et al. (2000)[32], tested the efficiency of heat sinks made from ORNL graphite foam. The first part of the experiment showed the comparison of heat transfer coefficient between graphite foam and aluminum foam. Due to a high pressure drop across the graphite heat sink, the authors modified the simple block ($\sim 5 \times 5 \times 3.8$ cm$^3$) to form five unique surface geometries, namely: fins, pin-fins, blind-holes normal to the flow, blind-holes parallel to the flow, and corrugated (slotted zigzag flow path). Aluminum foam was modified into two surface types; fins and pin-fins. The unmodified surface of both materials was also included in the test, making six surface types for carbon foam and three for metal foam. During experiments, the test surface was subjected to airflow of 425 litres/min. According to the authors, the overall results showed that graphite foam produced superior heat transfer coefficient. The range was minimum 1000 W/m$^2$·K for fins and maximum 4100 W/m$^2$·K (for corrugated/zigzag path); compared to aluminum 70 W/m$^2$·K (fins) and 550 W/m$^2$·K (pin-fins). Unmodified surfaces produced 250 W/m$^2$·K (aluminum) and 2600 W/m$^2$·K (graphite foam), and they also produced the maximum pressure drop. Additional test was performed by using water as a cooling fluid on graphite foam. During the experiments water at 2.85 litres/min. was circulated through. In water, they reported the range of heat transfer coefficient between 2100 W/m$^2$·K (for fins) and 23000 W/m$^2$·K (for solid block). As expected, solid block again caused the maximum pressure drop.

# 3

# Performance Evaluation of Single Tubular Aluminum Foam Heat Exchangers

## 3.1 Abstract

Five samples of aluminum foam-wrapped tubular heat exchanger are being tested for heat transfer performance and pressure drop characteristics. The foam layer has thickness (or height) varied from 5mm to 20mm. The tests are carried out on each heat exchanger, installed horizontally in a cross-flow arrangement inside an open circuit wind tunnel, one at a time with air velocity varying between 0.5 to 5 m/s. Heat transfer rate from 75°C hot liquid, circulating through the core tube, to external air is evaluated. These results, together with temperature differential between the ambient air and the foam surface, allow evaluation of the overall thermal resistance. Pressure drops across each sample are recorded. The performance of the foam heat exchangers is assessed by comparing their thermo-hydraulic results against those of a conventional finned tube with similar dimensions and tested under the same conditions. The results show that, within the designated air velocity range, the foam heat exchanger with thicker foam layer performs better than those with thinner foam layers. However, the heat transfer advantage does not increase linearly with foam thickness – signifying the existence of an optimum thickness when an increase in pressure drop at increased air velocity is taken into account. Finally, the correlations to predict the overall thermal resistance and pressure drop are presented.

## 3.2 Introduction

Metal foams are highly porous materials consisting of mostly interconnected and randomly distributed voids called 'cells'. Typically, a cell approximate shape and form is a near-spherical polyhedron having 14 faces. Each cell face forms an open passage called 'pore' to adjacent surrounding cells in all directions. The porous structure as described therefore makes metal foam permeable, and provides very well-mixed patterns, to fluid flows in macroscopic scale. In addition, the solid backbone micro-features maintaining the existence of all cells and pores – termed 'struts' (or 'ligaments', or 'fibres') and nodes (where struts join) – have a combined effect resulting in a very high interfacial surface area between the void and its solid backbone. T'Joen, et al. [6] reported approximate figures for this area to be in a range from 500 $m^2/m^3$ to 10,000 $m^2/m^3$. This top range figure was also reported in Boomsma, et al. (2003)[41] during their work on compressed foam heat sinks.

Due to their other unique properties of high strength, high absorption to impact, low weight, excellent noise attenuation, etc. [50], metal foams offer new possibilities in emerging industries where these combined properties are sought. Nevertheless, one distinct application which can take a maximum advantage of all metal foam features and properties mentioned above is that involving high efficiency heat exchange. Three niche technological areas that fit within this broad application are; thermal processes demanding high rate of simultaneous chemical reactions [51, 52], fast rate heat removal from high power electronic components, and highly efficient heat rejection in power cycles [53] operating at low temperature differentials. A large number of studies on metal foam heat exchangers in the past decade have been centered around high performance heat exchangers of some forms [17, 41, 49, 54, 55]. Some of these studies concern fundamental investigations of the materials themselves, other are dealing with practical applications with relatively small metal foam volume. Notable examples of the latter cases are compact heat sinks for high density and high power electronic components [18, 39, 41, 54, 56]. Prior research of interest to this present study are those involving heat exchangers of tubular design, some of which have been reviewed in Section 2.3.2(b) of Chapter 2.

In forming a foam based heat exchanger, different techniques are employed to attach the foam materials to its tubular core or flat substrate. De Jaeger, et al. (2012)[40] identified four possible methods; brazing, co-casting, thermal glue bonding, and mechanical press-fitting. Their main objective was to assess TCR associated with each bonding method. They found brazing to be the best technique while press-fitting being the worst. TCR is an important factor in designing heat exchange hardware as emphasized by Fiedler, et al. (2012)[57] and minimizing it can improve heat conduction performance of composite materials significantly as elaborated in Ref [40].

The main objective of the present study is to evaluate thermo-hydraulic performances of single tubular aluminum foam heat exchangers. Focus is given to assessing their heat transfer and pressure drop characteristics resulting from different foam materials, heights, and bonding methods between the foam and the wall of solid core cylinder. This work forms a small part of a project aimed at identifying best design of a single tube, and further evaluating their performance in bundle configurations, taking economic factors into consideration. The target application of heat exchangers studied in the next stage, in their best

configured bundle form, is an air-cooled condenser in a typical low temperature turbine cycle for geothermal power plants. Geothermal energy is a potentially feasible option in Australia for a base load power generation. However, geothermal resources are located in remote locations with limited cooling water availability. To overcome this barrier and remain viable economically, it is envisaged that rejecting waste heat from geothermal power plants in this context must rely heavily on a dry cooling system.

## 3.3 Specimen Descriptions

The finned heat exchanger was manufactured in-house at the QGECE mechanical workshop. An aluminum solid bar of a length 580mm was machined to form the finned external structure. There are 89 annular fins spread across the total length of 440mm, each with the thickness of 0.6mm ($t_f$) and sits apart from one another ($t_p$) at 4.24mm. The core external diameter ($d_o$) along the tube covering with fins, i.e. the middle 440mm length, measures 30mm while the bare sections at either end have $d_o$ = 32mm. The tube has the internal diameter ($d_i$) 25.8mm. Essentially, for the most part, the tube wall where heat transfer takes place has a thickness of 2mm.

There are five samples of foam covered heat exchanger all using foam layer having 20 PPI pore density. Among them, four samples are made of the same foam type but with a different thickness; viz., 5mm, 12mm, 15mm, and 20mm. The core tube of each sample in this set is an aluminum cylinder with external diameter, $d_o$, measures 32.0mm and internal diameter, $d_i$, 28.5mm. The foam material which covers the tube in all four samples, having porosity of 0.901, is of the same alloy as the core cylinder. Except for the 15mm sample which has its foam layer pressed-fit to the core, the other three have the foam cover and the core tube bonded together by high-temperature brazing. The last heat exchanger sample has the foam thickness of 5mm bonded with thermal glue to its stainless steel core tube. The porosity of the foam layer is 0.937. The core has the same $d_o$ as those of the other four samples but with a smaller $d_i$ (28.3mm), resulting in a slightly higher wall thickness.

All foam wrapped heat exchangers, shown in Figure 3.1, are ready made commercial products. The first four were supplied by the same manufacturer. The last sample was supplied by another vendor and has the core tube and its foam layer bonded together differently. Table 3.1 summarizes physical properties of the specimens shown in Figure 3.1.

| Surface type | $D_o$ [mm] | $t$ [mm] | Materials surface/core | $k$ [W/m.K] | Bonding method |
|---|---|---|---|---|---|
| Fin, reference | 62 | 15 | Aluminum | 210 | Coherent |
| Foam - type 1 | 42 | 5 | A6101/A6061 | 5.8 | Brazing |
| Foam - type 1 | 56 | 12 | A6101/A6061 | 5.8 | Brazing |
| Foam - type 1 | 62 | 15 | A6101/A6061 | 5.8 | Press-fit |
| Foam - type 1 | 72 | 20 | A6101/A6061 | 5.8 | Brazing |
| Foam - type 2 | 42 | 5 | A1050/SS316 | 6.0 | Thermal glue |

Table 3.1: Summary of all six heat exchanger specimens

FIGURE 3.1: Specimens used in the study. Based on either foam or fin height from left to right: Foam-2 (5mm), Foam-1 (5mm), Foam-1 (12mm), Fin (15mm), Foam-1 (15mm), and Foam-1 (20mm)

## 3.4 Data Collection Procedure

Details of experimental set-up and test rig validation are described in Section 1.4. Before running the tests to collect data, all TC and RTD probes are calibrated against a FLUKE-9142 Field Metrology Well to agree within 0.001°C between the calibrator well and the probes. For each specimen under test, the air flow is set to 0.5 m/s and the liquid temperature at heat exchanger inlet is monitored until it is settled within 75±0.75°C, all relevant data as described in Section 1.4 are logged every second for 10 mins. The air flow is then increased to the next step of 0.5 m/s increment and when the liquid temperature re-settles, the process is repeated until air flow reaches 5.0 m/s.

## 3.5 Analysis

Thermal energy exchange analysis follows theoretical formulation of related parameters for forced convection around a cylinder in a cross flow. As the hot liquid mixture enters the heat exchanger core and flows to the exit, it loses heat to the cooler airstream flowing past the heat exchanger external surface. The air is forced to flow at varying velocity by the suction fan. Only the exchange of thermal energy occurring inside the test section is taken into account as the heat loss outside the test section is found negligibly small.

### 3.5.1 Total Heat Transfer

Total heat input rate to the specimen under test, $\dot{Q}$ [W], is evaluated from:

$$\dot{Q} = \dot{Q}_{liq} = \dot{m}_{liq}\bar{c}_p\Delta T \tag{3.1}$$

$\Delta T$ is the temperature differential of the hot liquid at the inlet and exit of the heat exchanger $= T_{liq,in} - T_{liq,out}$ [K].

If loss is assumed small and neglected, this is the amount taking up by the passing air:

$$\dot{Q}_{air} = h_o\eta_o A_o(T_o - T_\infty) \tag{3.2}$$

This present report adopts a concept taken by the authors such as Cavallini, et al. (2010)[58] and Moffat, et al. (2009)[56], among others, in interpreting the quantity $h_o\eta_o A_o$ together as a lumped property. In these studies, the authors attributed the ability of foam surface in augmenting heat transfer to a qualitative intrinsic property which is lumped together with the foam convective heat transfer coefficient (HTC). For example, Cavallini, et al. (2010)[58] used HTC.$\Omega^*$ to denote this combined parameter in their analysis.

### 3.5.2 Overall Thermal Resistance between two fluid streams

The effect of net radiation heat transfer between the heat exchangers and their surroundings inside the test section is insignificant and therefore not included in the calculation. With this assumption, the overall thermal resistance $R_t$ [K/W] is defined as:

$$R_t \equiv \frac{(T_s - T_\infty)}{\dot{Q}} \tag{3.3}$$

where $T_s$ is internal surface temperature of the heat exchanger [K] taken as the average of liquid inlet and exit temperatures $\frac{(T_{liq,in}+T_{liq,out})}{2}$, $T_\infty$ is the free-stream temperature of the bulk air [K], and $\dot{Q}$ [W] is as calculated by Eq. 3.1.

All heat exchangers used are new specimens and resistance due to fouling both on the liquid side and air side can be excluded. With this assumption, $R_t$ can be taken as the sum of internal surface convective resistance, conductive resistance through the tube wall, contact resistance at the interface of the tube and the foam layer, and external surface convective resistance. In equation form and the order as listed, this can be written:

$$R_t = \frac{1}{h_{liq}2\pi r_i L} + \frac{ln\frac{r_o}{r_i}}{2\pi k L} + R_c + \frac{1}{h_o\eta_o A_o} \tag{3.4}$$

where $h_{liq}$ is the convective heat transfer coefficient on the liquid side [W/m$^2$.K], $r_i$ is the tube internal radius [m], and $L$ is the length of the tube section covering with foam (or fins) which is approximately equal to the test section width [m]. On the conductive term, $r_o$ is the external radius of the tube; not including the foam and bonding adhesive [m], and $k$ is thermal conductivity of the core tube material [W/m·K]. The third term, $R_c$, is the TCR of bonding adhesive.

The last term of Eq. 3.4 needs a special consideration. To avoid impractical dealing with the foam interfacial surface area (i.e. that in contact with air), the product $h_o\eta_o A_o$ is treated in the same manner as HTC.$\Omega^*$ described in Cavallini, et al. (2010)[58]. Using this approach, $A_o$ can then be taken simply as the external surface area of the core tube under the foam

cover. It should be noted that this approach can be applied equally to planar structures or finned surfaces. In their experimental investigation of heat transfer on different aluminum foam heat sinks under natural convection in air, Bhattacharya and Mahajan (2006)[39] adopted this method in the calculation of convective heat transfer coefficient $h$ from a known total heat input rate $Q$. The equation being used was: $h = Q/A_b(T_b - T_{amb})$ where $A_b$ is the area of the base plate to which the foam block was attached, $T_b$ was its temperature, and $T_{amb}$ was the free flow air temperature.

Heat transfer performance of all specimens in this study is reported in terms of individual overall thermal resistance, $R_t$ as determined by Eq. 3.3.

## 3.6 Results and Discussion

### 3.6.1 Thermal Resistance

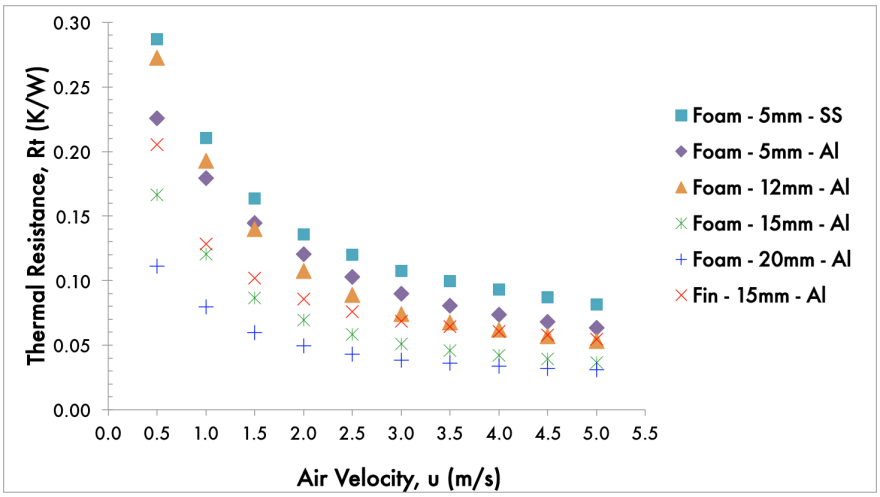


FIGURE 3.2: Overall thermal resistance of all six specimens plotted against air velocity

The plot of thermal resistance against air velocity is shown by Figure 3.2. It is apparent that the heat exchangers with smaller foam layer thickness is less efficient in rejecting heat, i.e. has more thermal resistance, at the same range of air velocity. This is as expected in all cases of the specimens. Another notable result is that the two samples with the same foam thickness (5mm) have a significant difference in their thermal resistances. The 5mm-SS (s316 stainless steel core tube, Table 3.1) performs poorer. This can be attributed to three possible reasons. Firstly, The 5mm-SS sample uses thermal glue bonding method between its foam layer and the core tube. The authors have previously examined thermal contact resistance (TCR) in a separate study. Depending on air velocity, it was found that thermal glue bonding had TCR between 10% and 19%, (corresponding to air velocity 1.5 m/s to 5.0 m/s) of the total thermal resistance if brazing method TCR is treated to be small and can be disregarded. Secondly, the 5mm-SS has a higher porosity compared to the 5mm-Al (0.937 and 0.901). Higher porosity is associated with less interfacial surface area and it is usually the case that the heat transfer is decreased. This effect is consistent with the findings of

previous works such as those of Angirasa (2002)[59], and Mancin, et al. (2011)[60]. Thirdly, sample 5mm-SS has stainless steel core tube with higher wall thickness and lower $k$ value than those of the core tube of 5mm-Al sample.

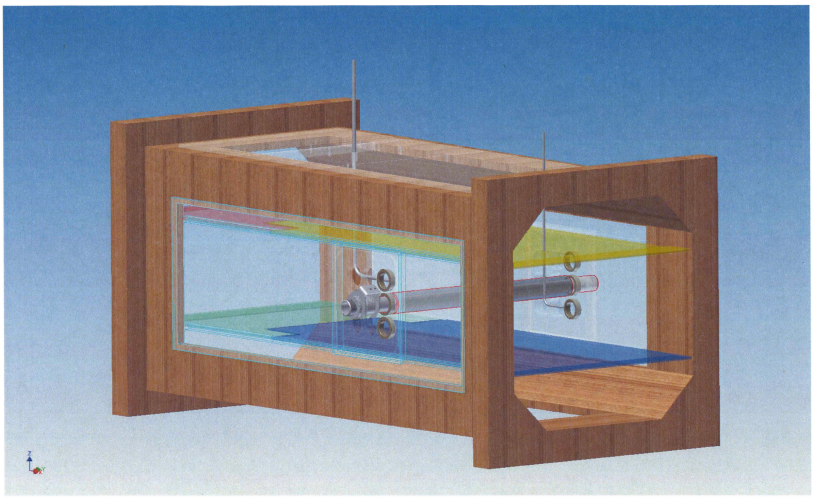

Figure 3.3: The test section showing the method of pressure drop measurement

### 3.6.2 Pressure Drop

The effect of different surface types on heat transfer can be assessed by comparing the results of Fin-15mm and Foam-15mm. In this comparison, the finned tube has no TCR between all its 89 annular fins and the core tube because the heat exchanger was made as a single piece from a solid aluminum round bar. In contrast the Foam-15mm sample has the maximum TCR because the foam layer and the core tube were press-fit together. Press-fitting gives the highest TCR according to De Jaeger, et al. (2012)[40]. Despite the double disadvantage, the Foam-15mm still performs considerably better than the same thickness Fin-15mm. If the pressure drop data being discussed in the next section is also taken into account, it can be concluded that the overall performance of foam surface is undoubtedly more favorable.

Pressure drop data are purely measured values at two imaginary planes perpendicular to the direction of the air flow. The plane upstream locates at 200mm away from the centre line of the test sample, and the one downstream locates 420mm away from the same reference. At each plane, a pitot tube was installed from the top panel to the depth horizontally aligned with the centrelines of the test section and the heat exchanger tube being tested. The difference in total pressure between the two pitot tubes is taken as the pressure drop across the sample.

Figure 3.3 shows the general setting of the two pitot tubes for pressure drop measurement. This arrangement is necessary to keep the closed-loop air velocity control functioning the way it was calibrated.

The foam materials covering all foam samples are of similar alloy ($k \sim 220 - 235$ W/m.K) and having the same PPI. If two heat exchangers are wrapped with the same thickness, the

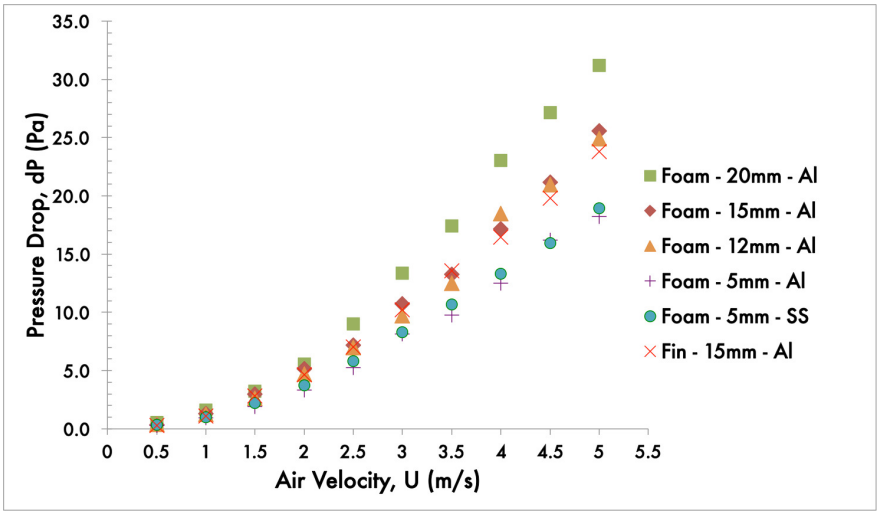


FIGURE 3.4: Pressure drop of all six specimens plotted against air velocity

expectation on pressure drop characteristics should likewise be similar. The pressure drop for all specimens under test, plotted against the air velocity, is shown by Figure 3.4.

Following the argument and expectation outlined above, pressure drop comparison of the two 5mm foam tubes is well confirmed. The pressure drop is known to be affected by tangible, macroscopic properties of the specimens [49]. Because the two 5mm foam heat exchangers have very similar physical dimensions and foam specifications, their pressure drop results are therefore predictively similar. The thin layer of thermal conductive glue being added on the external surface of 5mm-SS tube core to bond its foam matrix doesn't manifest a different effect to the results.

Over the whole range of designated air velocity, the general trend of foam thickness toward pressure drop it generates is as expected for all test samples. The sample with the highest add-on thickness generates the maximum pressure drop while those with the lowest thickness generate the minimum pressure drop. The curves diverge toward the maximum air velocity.

The effect of different modified surface structure of the same thickness or height, i.e. foam 15mm vs. finned 15mm, to pressure drop is not significant – with the finned tends to cause less pressure drop especially toward the higher air velocities. For all samples, their pressure drop up to the air velocity of 3.5 m/s are not varied greatly apart.

### 3.6.3 Effect of Surface Type on Heat Transfer and Pressure Drop

To visualize the combined effectiveness of the foam heat exchangers, thermo-hydraulic data of 15mm foam are plotted in comparison with those of the 15mm finned-tube, as shown in Figure 3.5. This is however not the plot showing heat transfer as the dependent variable on the pressure drop. It is rather an X-Y graphing of heat transfer and pressure drop at each airflow where the latter is represented along the X-axis and the former along the Y-axis. The data points shown on each curve are discrete values corresponding to the airflow of 0.5, 1.0, 1.5, 2.0, ..., up to 5.0 m/s (a total of 10 on both curves). It is done this way to avoid

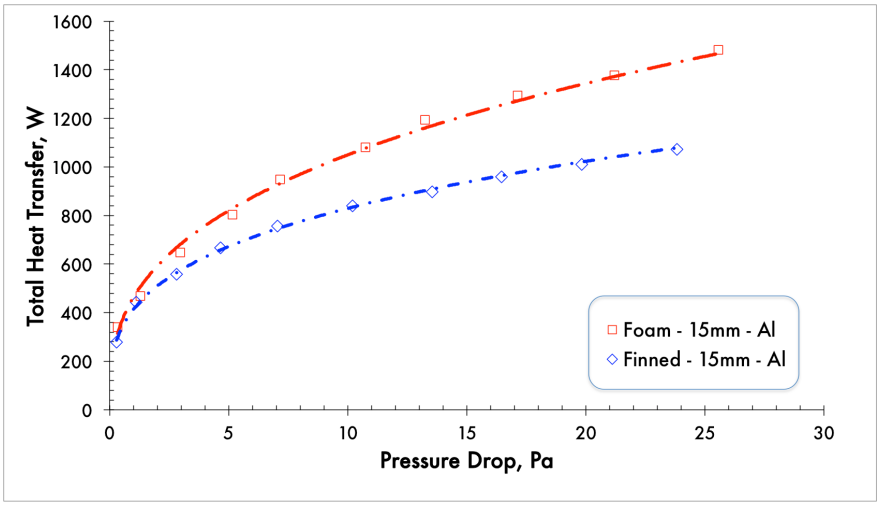


Figure 3.5: Performance comparison of aluminum foam and finned tube of the same $D_o$ and identical core dimension

charting the data on a more complicated 3-dimensional plot. In interpreting the data, one must track the order of each point and mentally related back to its original air velocity. Data labels are not used as they clutter the plot area and degrade readability.

As an example, referring to the rightmost two points – both are the condition for airflow of 5 m/s, at which point the foam tube transfers heat at the rate 1,450W and generate the pressure drop at 26Pa while the finned tube transfers heat at the rate 1,050W and generate the pressure drop at 24Pa. Data between discrete points can be interpolated proportionally.

From the earlier discussion, note that the two curves shown in this plot represent the worst case scenario of the foam tube and the best case for the finned specimen being used in the test. This is due to the foam tube having the maximum TCR and the finned tube having none. Nevertheless, it is seen here that the trends of the two curves diverge as the pressure drop increases. This shows that while the increase in rate of heat transfer $\dot{Q}$ for the finned tube slows down, $\dot{Q}$ of the foam tube continues to rise with the increase of pressure drop (i.e. corresponding to the increase of air velocity or the Reynolds number, $Re_d$ of the air flow). Put it differently, over the range of the Reynolds number under this test conditions, the foam tube exhibits a better heat transfer performance at the same pressure drop. For example, at about 25 Pa (corresponding to $Re_d = 10590$, or $U = 5$ m/s – see Figure 3.4) $\dot{Q}$(foam) $\sim$ 1450 W and $\dot{Q}$(fin) $\sim$ 1060 W, a 37% enhancement.

Following methodology presented by Moffat (1988)[61], the root-sum-square is used to combine an error due to instrument bias and a statistical error evaluation. Propagation of errors to derived variable follows the method present by Kirkup (1994)[62]. All propagated errors on $\dot{Q}$ are less than 10%.

### 3.6.4 Thermal Resistance and Pressure Drop Correlations

Following the approach used by Hooman and Merrikh (2010)[63], two correlations of the form $Y = \psi.\frac{D_o}{d_o}^{\alpha}.U^{\beta}$ are proposed to assist in the prediction of overall thermal resistance

($R_t$) and pressure drop ($\Delta P$) of the foam heat exchanger tubes. $Y$ is the target parameter being predicted which can be either $R_t$ or $\Delta P$, $\frac{D_o}{d_o}$ is foam to core tube external diameter ratio, $U$ is air velocity, and $\psi, \alpha, \beta$ are empirical coefficients specific to the two cases, i.e. $R_t$ or $\Delta P$. The Least Squares Method (LSM) and an iteration technique are used to determine the best fit correlations taking $U$ as the independent quantity, $Y$ as the dependent quantity in the ($U_i$, $Y_i$) data set where $i = 1$ to 10 ($U_1 = 0.5, U_2 = 1.0, U_3 = 1.5, ..., U_{10} = 5.0$).

From all ten ($U_i$, $Y_i$) data pairs the residual $\Delta Y_i$, defined as $Y_{i,observed} - Y_{i,calculated}$, are squared and summed to form the sum of residual square; $S = (\Delta Y_1)^2 + (\Delta Y_2)^2 + ... + (\Delta Y_{10})^2$. According to the LSM, the best values for $\psi, \alpha$, and $\beta$ are found by minimizing $S$. The LSM is a well-established procedure [63] so its treatment won't be repeated here. Full details and its theory can be consulted in statistical or data interpretation references such as [62]. The final correlations are as shown in Eqs. 3.5 and 3.6.

$$\Delta P = 0.807. \left(\frac{D_o}{d_o}\right)^{0.859} .U^{1.828} \tag{3.5}$$

$$R_t = 0.289. \left(\frac{D_o}{d_o}\right)^{-1.617} .U^{-0.595} \tag{3.6}$$

These correlations fit the general experimental data well with the pressure drop yielding a more accurate prediction. The maximum $\Delta P$ errors from the thickest foam tube to the thinest one (i.e. 20mm, 15mm, 12mm, 5mm) are 17.1%, 17.9%, 10.9%, and 10.8% respectively. These errors represent extreme outliers which occur at air velocity below 1 m/s because, at low velocity, the denominators involve in fraction calculation are small numbers. If these outliers are excluded, all errors of the four thicknesses covering all velocity range are lower than 8%. For $R_t$, the maximum errors for the same order of foam thickness are 5.6%, 10.1%, 39.4%, and 24.4%, respectively.

Correlations in thermo-fluids are usually presented in non-dimensional forms. To adhere to this practice, $\Delta P$ can be expressed as a dimensionless friction factor, $f$, by a familiar quadratic relation:

$$\Delta P = f.\rho_a.U^2 \tag{3.7}$$

where $\Delta P$ is as calculated by Eq. 3.5. By replacing the diameter ratio $\frac{D_o}{d_o}$ with a simpler notation $Dr$ and converting the velocity term to Reynolds number with $d_o$ as its characteristic length, $f$ can be written as:

$$f = 2.675 Dr^{0.859}.Re_{d_o}^{-0.172} \tag{3.8}$$

Eq. 3.8 exhibits its form and magnitude similar to $F$ in relation to $Re$ as reported by Mancin, et al. (2010)[42] in their study of air flow through full channel occupied by aluminum foams. According to this study (Ref. Eq. 15) $F \sim Re^{-0.1014}$.

For thermal resistance, since $R_t$ has the dimension of K/W, it follows that multiplying it by $k_a.d_o$ will produce dimensionless thermal resistance, $\hat{R}$. Hence, in a similar fashion, Eq. 3.6 can be expressed in its dimensionless form as:

$$\hat{R} = R_t.k_a.d_o = 0.024 Dr^{-1.617}.Re^{-0.595} \tag{3.9}$$

The thermal conductivity term used in Eq. 3.9 is taken as the 'effective thermal conductivity' $k_f$ of the foam. It was defined by the manufacturer as the conductivity of the three-dimensional array of solid ligaments or struts that form the foam structure. It is usually evaluated by a simplified relation: $k_f = k_{solid} \times \rho_f^* \times 0.33$; where $\rho_f^*$ = relative density of the foam in decimal and 0.33 is a coefficient representing the foam structure geometric or 'tortuosity' factor.

## 3.7 Conclusions

In this study five foam wrapped heat exchangers of tubular design are tested for their thermo-hydraulic performance using a finned tube of comparable dimensions as a benchmark sample. Available foam specimens allow the study of foam thickness effect on heat transfer and pressure drop. In addition, three different bonding methods applicable among six specimens in this study aid in interpreting data associated with respective specimens. The results show that, for thermal efficiency, overall thermal resistance decreases with the increase of foam layer thickness. However, this thermal advantage comes at the expense of increasing pressure drop. Depending on target applications, as a single tube, the resulting pressure drop may be acceptable as it does not differ significantly from that of current heat exchanger design. The foam wrapped heat exchanger with suitable foam thickness is seen to give heat transfer benefit while keeping the pressure drop at the same level as that causes by the finned tube. Experimental results are also helpful in developing correlations to predict relevant variables of interest. This study defines two correlations to predict pressure drop and thermal resistance using the same set of input parameters. Non-dimensional forms of these two variables are also presented.

# 4

# Performance Evaluation of Tubular Aluminum Foam Heat Exchangers in Single Row Arrays

## 4.1 Abstract

Two sets of three tubular heat exchangers, constructed by wrapping aluminum foam of different thickness around cylindrical tubes, are being tested for heat transfer performance and pressure drop characteristics. Each set of heat exchangers is mounted such that it forms an array of a single, vertical row inside a low airflow wind tunnel. The tests are carried out under cross-flowing air velocity between 0.5 and 5.0 m/s at 0.5 m/s interval. Taking kinematic viscosity of the air as $15.5 \times 10^{-6}$ and selecting external diameter of the cylinder as its characteristic length this range of airflow corresponds to the Reynolds number between 2000 and 20000. The effects of foam thickness and transversal pitch distance are discussed and thermo-hydraulic results are benchmarking against those of a conventional finned tube array. It is found that within the designated range of airflow and the same level of compactness, the heat exchanger array with thicker foam layer enhances heat transfer 1.5 to 1.8 times compared with the one having thinner foam. In an array with fixed foam thickness, heat transfer improves at narrower pitches. At a discussion of the results, two empirical correlations to predict friction factor and thermal resistance are presented.

## 4.2 Introduction

This study aims at achieving data from 4 sub-tests of single row heat exchangers in order to make 5 thermo-hydraulic performance comparisons: (i) metal foam heat exchangers and circular finned heat exchangers having similar physical dimensions and the same transversal pitch between each tube, (ii) metal foam heat exchangers and finned surface heat exchangers

with the same transversal pitch between each tube but the foam thickness is 3-fold less than the fin height, (iii) 'thick' foam and 'thin' foam heat exchangers with the same transversal pitch between each tube, the foam thickness ratio is 3:1 (iv) 'thick' foam and 'thin' foam heat exchangers with different transversal pitch between each tube but the same edge-to-edge gap of the foam surface, and (v) 'thin' foam at wide pitch and 'thin' foam itself at narrow pitch with the pitch ratio of 1.4:1.

## 4.3 Specimen Descriptions

FIGURE 4.1: Specimens used in the study: Circular Finned (center), Foam-1 (aluminum foam covered, 15mm thick, right), and Foam-2 (aluminum foam covered, 5mm thick, left)

| Surface type | $D_o$ [mm] | $t$ [mm] | $d_o$ [mm] | $d_i$ [mm] | $\phi$ [-] | PPI [1/in.] | Materials surface/core |
|---|---|---|---|---|---|---|---|
| Circular Fin | 62 | 15 | 30 | 25.8 | - | - | MS1020/1020 |
| Foam-1 | 62 | 15 | 32 | 28.5 | 0.901 | 20 | A6101/A6061 |
| Foam-2 | 42 | 5 | 32 | 28.3 | 0.937 | 20 | A1050/SS316 |

TABLE 4.1: Summary of the three heat exchanger specimens

The two aluminum foam heat exchanger samples used in the tests are supplied by two different manufacturers. The first sample, Foam-1, (a set of three tubes) has its foam layer attached to the core by means of brazing. On Foam-2, the core tube is a stainless steel and it is bonded to the foam layer by a thermally conductive adhesive. The finned heat exchangers were fabricated in-house at QGECE mechanical engineering workshop. A carbonized steel solid bar of a length 580mm was machined to form external coherent annular fins. There are 96 fins spreading across the total length of 442mm, each with the thickness ($t_f$) of 0.6mm and sits apart from one another ($t_p$) at 4.6mm.

Each tube of the three samples is shown together in Figure 4.1 and their physical features are summarized in Table 4.1. Because of its thicker foam layer, Foam-1 heat exchanger array is loosely termed "thick foam", and likewise Foam-2 is "thin foam". These terms will be adhered to in the remainder of the text.

## 4.4 Data Collection Procedure

The preparation in terms of instrumentation and setting up the wind tunnel follow the same procedure implemented in Chapter 3. Extra steps which are required to carter for data dealing with pitch length are explained as follow.

Initially, the two Flexi-glass baffles are set such that the middle compartment has its cross-sectional area of 454mm ($W$) $\times$ 151mm ($H$) at the inlet. At $H = 151$mm, 'thin' foam specimens can be mounted at 48.3mm transversal pitch ($S_T$) to achieve edge-to-edge of the foam surface = 6.3mm. In this configuration, 'thin' foam has $\hat{X}_T = 1.51$ and the three tubes form the "compact" array.

Subsequently, the gap between the two baffles are widened vertically to $H = 210$mm. Finned- and 'thick' foam specimens can then be mounted at 68.3mm transversal pitch to achieve edge-to-edge of the finned-/foam surfaces = 6.3mm. When mounted at this pitch length ($S_T = 68.3$mm), the edge-to-edge of 'thin' foam is 26.3mm apart and the resulting arrangement is the "wide-pitched" array, in contrast to the "compact" array at $S_T = 48.3$mm above. With this configuration, all three sets of specimens, 'thick' foam, 'thin' foam, and finned tubes have $\hat{X}_T = 2.13$.

In all configurations, the top and bottom gaps between each baffle and its corresponding tube is about half of the edge-to-edge gaps. With this arrangement, each array can approximate an infinite number of tubes.

For each heat exchanger array under test, the airflow is set to 0.5 m/s and the liquid temperature at heat exchanger inlet manifold is monitored until it is settled within 75$\pm$0.75°C, all relevant data are logged every second for 10.7 mins to gain a total of 640 data points. The airflow is then incremented by 0.5 m/s to the next measuring step and when the liquid inlet temperature re-settles, the process is repeated until the airflow reaches the final velocity at 5.0 m/s.

## 4.5 Data Reduction and Analysis

Due to the difficulty in obtaining reliable measurements of the foam surface areas, analyzing thermal exchange adopts thermal resistance analogy to determine the parameters of interest. In our study, the hot glycol/water mixture flows inside the tube array and forms an unmixed stream while the cross-flowing air constitutes a mixed, external flow.

### 4.5.1 Finned Tube Benchmarking

Although the main theme of this study is on foam-surfaced heat exchangers, the conventional finned tubes are also tested. The reasons for this sub-test are, firstly to use their results as

the baseline values against which the results from foam heat exchangers can be compared. Secondly, these baseline results may be verified against similar previous studies to ensure the validity and fitness of the testing rig being used. Thirdly, the procedure employed in finned tubes analysis is to be followed consistently for subsequent studies of the multi-row, foam-based, heat exchanger arrays.

### 4.5.2 Heat Transfer

Total heat transfer, $\dot{Q}_t$ [W], is evaluated from thermal input rate on the liquid side and it is used for all subsequent calculations:

$$\dot{Q}_t = \dot{Q}_h = \dot{m}_h \bar{c}_{p,h} \Delta T \tag{4.1}$$

$\Delta T$ is the temperature differential of the hot liquid at the inlet and exit of the heat exchangers $= T_{h,in} - T_{h,out}$ [K].

Assuming no surface fouling, the heat flow path due to two-fluid temperature difference has a total thermal resistance:

$$R_t = \frac{1}{h_i A_i} + \frac{ln\left[\frac{D_o}{D_i}\right]}{2\pi k L} + R_c + \frac{1}{\eta_o h_o A_o} \tag{4.2}$$

and

$$R_t = \frac{1}{UA} = \frac{1}{U_o A_o} = \frac{1}{U_i A_i} \tag{4.3}$$

The parameter $\eta_o$ in Eq. (4.2) is a number between 0 and 1 and is termed *overall surface efficiency*. It characterizes the quality of heat transfer surfaces independent of fouling factor. For finned surfaces, it can be calculated from fin efficiency $\eta_f$ and geometrical parameters specific to each fin design [10]. This study is not directly focused on finned heat exchangers and $\eta_o$ is simply taken to have a value close to 1 when calculating finned tube data. In addition, the fins and their base tubes are integral components; so contact or bonding resistance $R_c$ is assumed to be 0.

There are a number of correlations developed for the determination of $Nu$ of internal flow in circular tubes. In this study ($Re_{d,i} = 4900$), the Gnielinski-Petukhov correlation [10] is chosen. Once the Nusselt number is known, the heat transfer coefficient is readily calculated:

$$h_i = \frac{Nu_{di} k_h}{d_i} \tag{4.4}$$

With $h_i$ determined, $h_o$ (Eq. (4.2)) is known. For the convenience of comparison in experimental studies in general, heat transfer coefficient is usually represented by its respective Nusselt number (Eq. (4.4)) - whence $Nu_{Do} = h_o D_o / k_c$.

Huisseune, et al. (2010)[64] thoroughly reviewed open literature of finned tube heat exchanger bundles to compare the results of their single row tube bank. Establishing that none of the available thermo-hydraulic correlations can describe the results of their experiments,

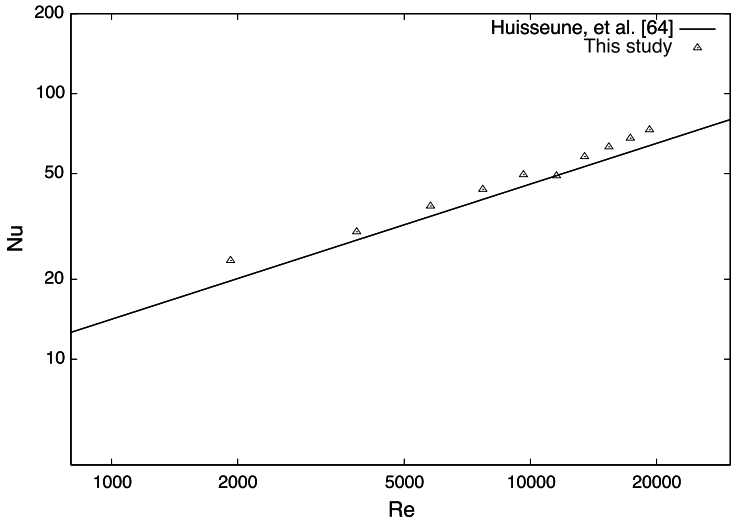


Figure 4.2: One-row finned tube array heat transfer comparison of Huisseune, et al. (2010)[64] correlation and the results of this study

| Authors | $u_\infty$ [m/s] | $Re_D$ [-] | $D_o$ [mm] | $\hat{X}$ [-] | $D_o/D_i$ [-] | $A_{W\times H}$ [mm$^2$] | No. of tube | $A_{min}$ [m$^2$] |
|---|---|---|---|---|---|---|---|---|
| Huisseune, et al. [64] | 0.7-7.4 | 1000-14100 | 13 | 1.92-3.27 | 1.91 | 485×255 | 8-10 | Varied[1] |
| This study | 0.5-5.0 | 1900-19200 | 32 | 2.13 | 1.94 | 454×210 | 3 | 0.0492 |

Table 4.2: Parameter comparison of finned tubes in this study and those used to formulate correlation cited in Figures 4.2 and 4.3 ([1] depending on the number of tube mounted in the test section)

they proposed their own. The proposed correlation relates the Nusselt number to Reynolds number and the ratio of transversal tube pitch to the tube external diameter. The results of our study agree very well with this correlation. Figure 4.2 shows the results of our discrete heat transfer data on the $Nu - Re$ plot in comparison to the curve plotted by applying our data to the Huissenune's correlation. $Re$ is based on maximum velocity as the air passes the minimum free flow cross sectional area at the tube array. Geometrical parameters of the two studies are shown in Table 4.2 where $A_{W\times H}$ is the cross sectional area of the test section at its inlet and $A_{min}$ is the minimum free flow area.

### 4.5.3 Pressure Drop

For the purpose of comparison, the pressure drop data is expressed in terms of the surface friction factor using the relationship presented by Kays, et al. (1955)[11] and modified by Huisseune, et al. (2010)[64].

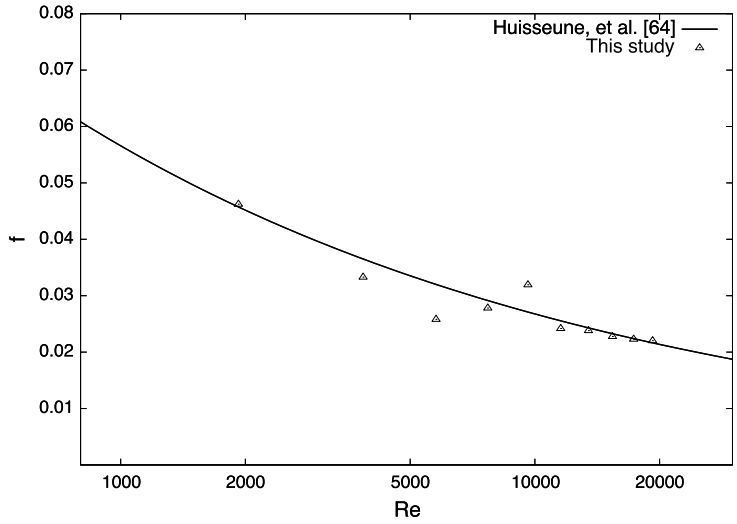


Figure 4.3: One-row finned tube array surface friction factor comparison of Huisseune, et al. (2010)[64] correlation and the results of this study

$$f = \frac{A_{min}}{A_t}\left[\frac{2\Delta P.\rho_a}{G^2}\right] \tag{4.5}$$

Comparing the calculated friction factor using Eq 4.5 to our discrete measured data again produces a very close agreement, as shown by Figure 4.3. The glitch of $f$ showing the wrong trend at $Re$ approximately 6000 - 10000 is likely because this study reports maximum $\Delta P$ at each velocity setting instead of its mean value to calculate $f$.

The satisfactory results of these comparisons are taken as an indication that the procedure, functionality of the test rig, and measurement techniques used for this study produce reliable data. Despite these similarities of thermo-hydraulic results, there are differences in some areas between the two studies. For instance, Huisseune, et al. (2010)[64] circulated the liquid through the core tubes in two passes, treated both flow streams as being "mixed", and used heat exchangers with helical fins in their measurements. Nevertheless, it is helpful to assume that the effect of these differences is within the uncertainty limits which they quoted at $\pm 11\%$ for Nusselt number and $\pm 19\%$ for surface friction factor.

## 4.6 Results and Discussion

In our analysis, the three heat exchanger tubes making up the single row array are treated as a lumped unit with a conceptual total surface responsible for dissipating $\dot{Q}_t$ between the hot liquid and the air. The effect of net radiation heat transfer between the heat exchanger array and its surroundings inside the test section is insignificant and therefore not included in the calculation.

### 4.6.1 Thermo-hydraulic Comparison of Foam and Finned Surfaces

'Thick' foam heat exchanger tubes have similar physical dimensions and are set inside the test section with the same transversal pitch as the finned tubes ($D_o = 62$mm, $D_i = 32$mm, $\hat{X}_T = 2.13$) during the tests.

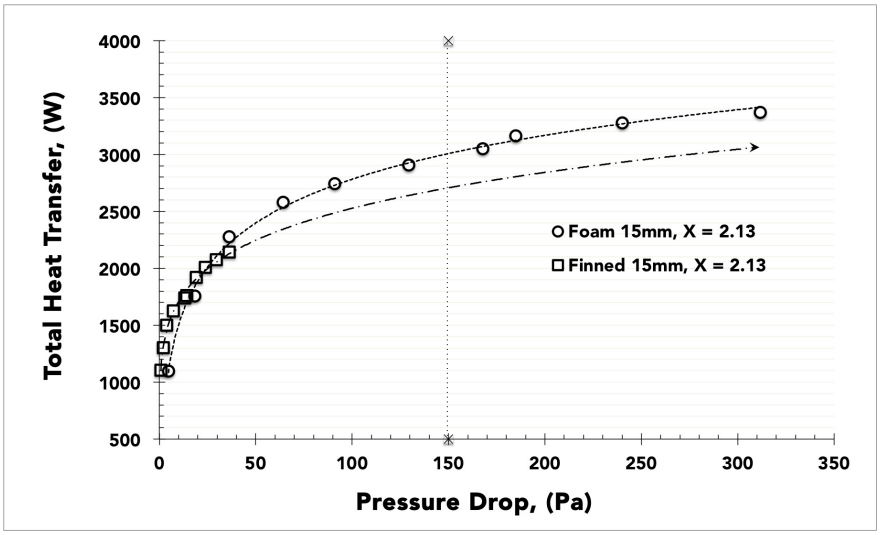


Figure 4.4: Total heat transfer and pressure drop of foam surface heat exchangers compared to those of finned heat exchangers with the same dimensions and tube pitch

Figure 4.4 shows a comparison of their thermo-hydraulic quality via a scatterplot of $\dot{Q}_t$ versus $\Delta P$. This plot has its limitation as the range of $\Delta P$ for finned heat exchangers operating within the same range of airflow is very narrow. However, if the trend line is applied and the upper forecast is extended to the comparable pressure drop attained by the foam bundle, a reasonable quantitative comparison can be made. In addition, the same trend was observed between these two samples when experiments on single tube were previously reported [65]. Comparison of single tube provides a concrete conclusion of this trend as both the foam and finned heat exchangers produce a similar range of pressure drop when subjected to airflow between 0.5 and 5.0 m/s (see detailed explanation in Section 3.6.3 to interpret this plot).

It can be speculated from Figure 4.4 that, although the foam array produces pressure drop approaching 9-fold that of the finned row at maximum air flow, it is more efficient in sinking heat to the air stream. In other words, the foam heat exchanger array has a relative merit over its finned counterpart because it provides a higher heat transfer at the same pressure drop. Looking at the curves for both heat exchangers, it is obvious that there is no significant performance gain running them beyond $\Delta P$ greater than ~150 Pa as shown by the vertical, dotted, cut-off line.

### 4.6.2 Heat Transfer of Foam Heat Exchanger Arrays

One area of difficulty in most previous studies of the subject is the lack of agreeable and standardized methods in evaluating foam surface areas. This study adopts thermal resistance

concept to report heat transfer comparisons between 'thick' and 'thin' foam heat exchangers for three experiment settings: (i) 'Thick' foam at transversal pitch ($\hat{X}_T$) = 2.13, (ii) 'Thin' foam at $\hat{X}_T = 2.13$, and (iii) 'Thin' foam at $\hat{X}_T = 1.51$.

The overall thermal resistance $R_t$ [K/W] between the hot liquid inside the tube and the external cross-flowing air is evaluated by Eq. (4.3). Figure 4.5 shows the results of the three measurements summarized above.

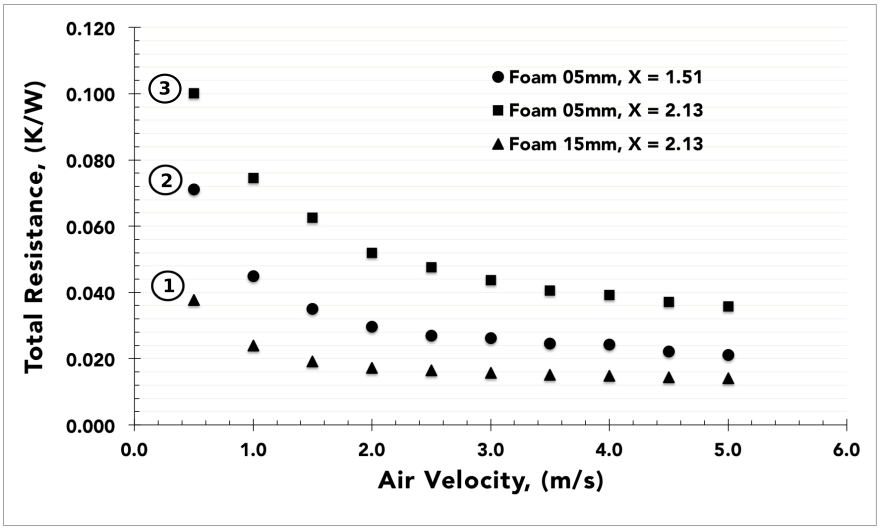


Figure 4.5: Total thermal resistance, $R_t$, of three measurements on 'thick' foam (Foam-1) and 'thin' foam (Foam-2) heat exchangers

In Figure 4.5, curves ① and ② show the effect of a different foam thickness in two compact arrays, while curves ② and ③ show the effect of a different tube pitch of the thin foam array. It is seen that the cylinder array with thinner foam layer is less efficient in rejecting heat, i.e. has more thermal resistance for the entire range of airflow. All $R_t$ curves show the trend of wider gap and sharp decreases at lower flow rates in the range 0.5 to 2.0 m/s. From 2.5 m/s to the top end of air velocity each curve converges toward one another and exhibits the parallel trend with the horizontal axis. It is apparent that there would be no further gain in heat transfer for airflow beyond 5.0 m/s. For the 'thick' foam array, the cut-off velocity is reached earlier because its $R_t$ curve levels off earlier ($\sim$ between 2.0 and 2.5 m/s). This trend has no negative effect on our target application as a typical buoyancy range controlling the natural draft inside moderate height cooling towers is far less than 5.0 m/s.

Considering the effect of foam thickness as shown by curves ① and ②, one logical reason 'thin' foam performs poorer than 'thick' foam is the amount of surface area available for thermal exchange, i.e. thinner foam layer means less interfacial surface area. This is, however, not a straight forward matter as the depth of air penetration cannot be easily determined and will be discussed further in the next section. Secondly, as shown in Table 4.1, 'thin' foam uses thermal adhesive to attach the foam layer to its core tubes. This causes the presence of the $R_c$ term in Eq. (4.2), thus increasing its $R_t$; while the brazing technique employed by 'thick' foam provides negligible $R_c$ according to De Jaeger, et al. (2012)[40]. Thirdly, 'thin' foam has higher porosity compared to 'thick' foam (0.937 versus 0.901). Higher porosity is

associated with less interfacial surface area; hence less heat transfer as already noted. The third effect is somewhat obscure but is nevertheless consistent with the results observed in many previous works such as those of Angirasa (2002)[59], and Mancin, et al. (2011)[60]. Lastly, the core tube of 'thin' foam is made of stainless steel with a much less $k$ value than that of aluminum ($\approx$ 14.1 W/m.K versus 210 W/m.K) and the tube wall is slightly thicker (1.85mm versus 1.75mm). These two factors cause $R_c$ of the 'thin' foam to be higher.

Curves ② and ③ confirm an established knowledge that heat transfer decreases with increased tube pitch. At normalized transversal pitch $\hat{X}_T = 2.13$, the gaps between each pair of tubes is much wider (26.3mm versus 6.3mm). In this setting, the maximum local velocity between tubes is less and the amount of air bypassing the foam surface is more, hence the decrease in heat transfer. However, it is interesting to observe that the two curves of thin foam array maintain a consistent difference between them without converging toward the high airflow region.

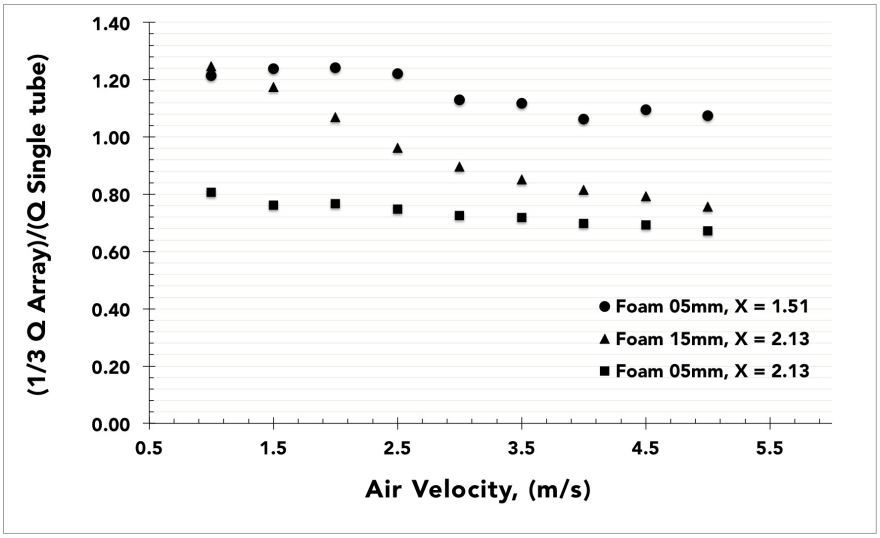


Figure 4.6: Ratio of heat transfer on one tube equivalent of a heat exchanger array to heat transfer on the same tube running in a single tube mode

To perceive the effect of grouping the heat exchanger tubes into a tube bundle, heat transfer of a one-tube equivalent of all three arrays is calculated and the result is compared with heat transfer of the same tube when it was run in single tube experiments. Figure 4.6 shows the ratio of the two heat transfers for all three foam heat exchanger configurations. In this plot, the compact thin foam array has the best advantage when run in a bundle form; and the effect of tube spacing is again as expected. With one exception of the data point at the lowest airflow of the two compact arrays, the trend of bundle effect of all three heat exchanger arrays is decreased with the increase of airflow. It is evident that the 'thick' foam shows the worst outcome with the ratio decreases from the level of compact thin foam to the wide pitch thin foam. It may be concluded that for high mass flow applications, thick foam provides less advantage than thinner foam layer in relative terms, i.e. when they both are set with the same minimum free flow area through the tube array.

### 4.6.3 Air Side Heat Transfer Resistance

All measurements in this study are performed on clean samples and fouling resistance is excluded from overall heat transfer resistance calculation. Thermal resistance of the air side is quantified by the last term of Eq. (4.2).

The variable $\eta_o$ is a conceptual foam surface efficiency describing its combined conduction and advection quality. Unlike its counterpart for finned surface, it doesn't have a clear mathematical definition due to a complicated geometry of the foam structure. In this study it is treated as an intrinsic part of the whole external surface and is reflected in the external resistance term. This approach is previously adopted by Cavallini, et al. (2010)[58] who used HTC.$\Omega^*$ to denote the combined efficiency and heat transfer coefficient as a single quantity. Regarding the foam surface area, Moffat, et al. (2009)[56] suggested that it should also be kept together with the other two and heat transfer calculation is consistently done via $R_o$.

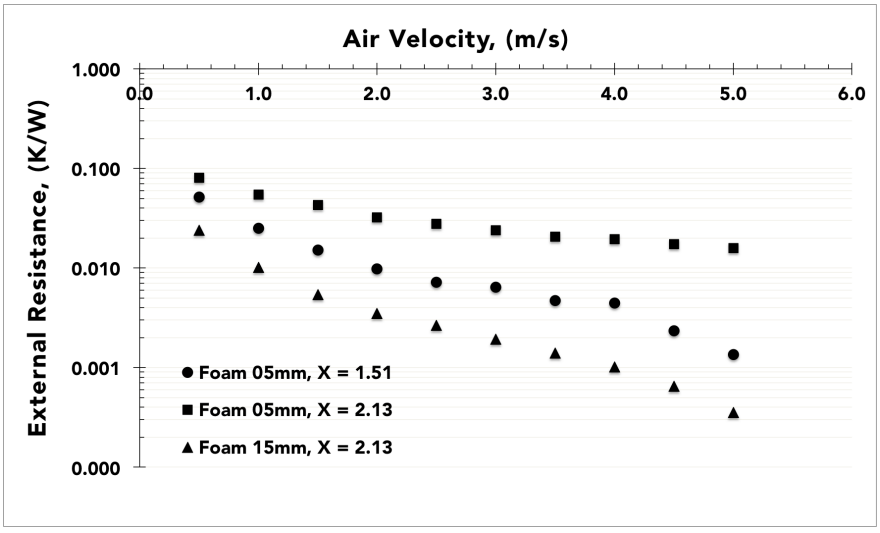


Figure 4.7: External thermal resistance of 'thick' and 'thin' foam tube arrays, – the thin foam array has two pitch settings

$R_o$ of the three foam heat exchanger configurations plotted against air velocity is shown by Figure 4.7. Each curve in this plot is calculated indirectly by subtracting the first three terms on the right hand side of Eq (4.2) from $R_t$. As noted, $R_c$ is only present on 'thin' foam due to thermal adhesive bonding. Thermal adhesive, even with a highly conductive filler, still has substantial effect on heat transfer. The authors had examined $R_c$ experimentally in a previous study [66] using one of these 'thin' foam samples. In this separate experiment, $R_c$ of the 'thin' foam is obtained by comparing its total heat transfer with that of the other 'thin' foam tube with the same dimension but with its foam layer brazed onto the core (so $R_c$ of the reference tube = 0). However, due to the difference in foam porosity and type of alloy between the two samples, the resulting $R_c$ had been overestimated. In this current study, $R_c$ of the 'thin' foam is evaluated by modeling the adhesive layer as a constant thickness annulus surrounding its tube core.

It can be observed from Figure 4.7 that, when run as a compact heat exchanger array (i.e. $\hat{X}_T = 1.51$), 'thin' foam has a relatively small value of $R_o$ which approaches $R_o$ of

'thick' foam toward the maximum airflow (note the log scale on y-axis). As a result, it can be predicted further that if TCR is removed –by brazing the foam to the core tube, for example– curve ② in Figure 4.5 will shift closer to curve ① and heat transfer of 'thin' foam array will increase. In brief, it can be concluded that in a bundle arranged with an appropriate pitch distance, a good performance is possible even with only a thin foam layer. This result and the observation of heat transfer ratio in Figure 4.6 reinforce at least two reports in open literature that air is likely penetrates a small pore depth of the foam. Straatmann, et al. (2006)[33] previously reported this in their study of parallel flow over carbon foam and T'Joen, et al. (2010)[6] showed similar results on their single row metal foam in a cross-flow experiment.

### 4.6.4 Pressure Drop

Pressure drop data are purely measured values using a pair of pitot tubes described in experimental set-up. Data points as shown in the plot of Figure 4.8 are the maximum values extracted from the 640 rows of pressure drop data files.

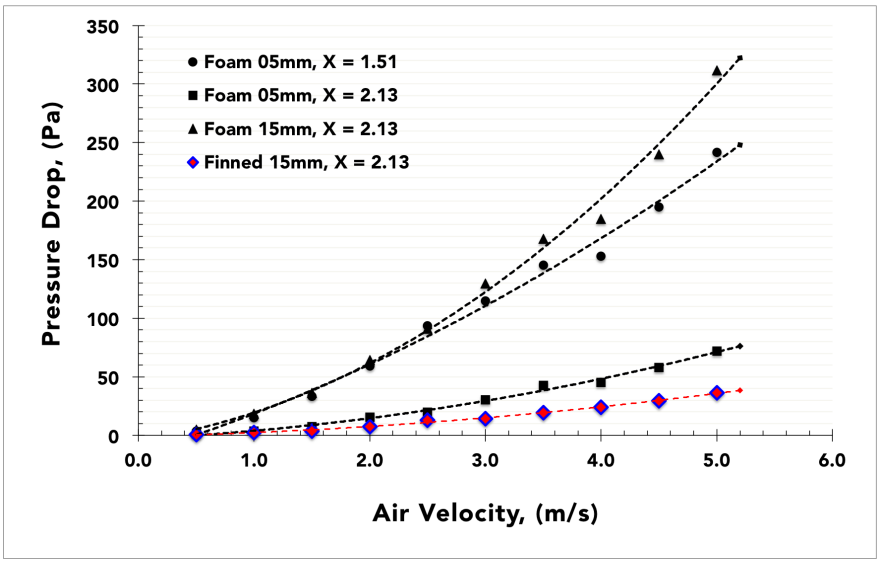


Figure 4.8: Pressure drop of all three specimens – plotted against air velocity; in comparison with the reference pressure drop generated by the finned tube array

The pressure drop, $\Delta P$, of the flow across porous media is known to be affected by tangible, macroscopic properties of the specimens [49] particularly the porosity, permeability, and surface roughness. In metal foam, it is also affected by mechanical compression applied during fabrication; as this would alter local porosity and permeability. In almost all applications, $\Delta P$ is increased with the flow rate. Shown in Figure 4.8, the pressure drop curves of the two compact arrays, thick foam at $\hat{X}_T = 2.13$ and thin foam at $\hat{X}_T = 1.51$, locate closer to each other. Those of the wide pitch thin foam and compact finned arrays sit together further down at relatively low values.

If $\Delta P$ is the only parameter considered, the disadvantage of foam surface is immediately seen in this plot. At wide pitch setting, even with only one-third of the surface layer thickness

(i.e. $D_o - D_i$) and over four times larger gaps between tubes, 'thin' foam still exhibits larger pressure drop compared with the finned array. For 'thick' foam, when the thickness layer and the gaps between tubes are the same, the foam surface causes a pressure drop over 9-fold larger than that of the finned surface at the top air velocity of 5 m/s.

At a first glance, 'thick' foam stands out for its maximum pressure drop. Of all specimens, each trend shows an increase of $\Delta P$ with the increased airflow. The results from Figure 4.8 are as expected and confirm the many previous studies found in open literature. Unlike the heat transfer, the pressure drop curves diverge toward the maximum air velocity - signifying that if the airflow is to further increase, $\Delta P$ will continue to rise.

Comparison between two foam compact arrays also produces expected results. Since the two sets have the same gap dimension between tubes, the relative blockage footprint inside the test section is the same. The fact that 'thin' foam produces lower pressure drop is due to one intuitive reason, it has a thinner foam layer. The porosity of the two is likely not the determining factor for this outcome as the difference between them is not substantial. Lastly, by increasing the pitch distance, single row heat exchanger array with constant foam thickness reduces its blockage ratio and causes $\Delta P$ to decrease.

In the preliminary study involving a single tube comparison [65], $\Delta P$ across a single tube of 'thick' foam and that of the single finned tube (both with $D_o = 62$mm) is not significantly different for the entire range of 0.5 to 5.0 m/s airflow. This is most likely due to a high proportion of air by-pass as these tubes are installed in the middle mounting hole (the middle black dot in Figure 1.2) and the two baffles are set at 210mm apart. Since a similar amount of air by-pass potentially happens when the thin foam is set in a wide pitch bundle, it is logical that its pressure drop compares fairly with the finned tube reference array.

### 4.6.5 Empirical Correlation

Technical reports and journal articles on thermal applications of metal foam have turned out in a large number in the past decade. However, specific focus on using this novel material in practical, large scale heat exchangers is still limited. As such, the literature on real life metal foam heat exchangers and their test data are not readily available. For single row heat exchanger study based on metal foams, the authors are aware of only a few publicly accessible articles to help assess the goodness of data generated in our labs. Among those few, the work of T'Joen, et al. (2010)[6] provides the most relevant and helpful treatment to this study. Unfortunately, with the differences in dimensions of specimens being used plus their different testing schemes, an accurate comparison is relatively difficult; particularly when thermo-hydraulic correlations are not provided and original data sets cannot be accessed.

In an effort to aid in future comparisons of similar studies, two empirical expressions to predict pressure drop and total heat transfer resistance are constructed. The two are based on the power relation of related independent variables to one dependent variable which is either the friction factor or the total thermal resistance. Friction factor is related to two independent variables which are the airflow and blockage ratio. The latter is defined as the ration of the pitch distance, $S_T$, to external diameter of the foam, $D_o$. Thermal resistance is modeled by three independent variables, the airflow, the blockage ratio, and the foam thickness.

Thermal resistance is dimensionless if it is multiplied by two arbitrary variables having the dimensions of length (m) and thermal conductivity (W/m·K), and this is the method adopted in this report. For the independent variables, two are already accounted for, i.e. (i) the foam thickness is represented by $D_o$ to $D_i$ ratio, and (ii) airflow is expressed in terms of the Reynolds number. The last variable that comes as a feature of the bundle, the tube spacing, is represented by the ratio of the transversal pitch distance and the external diameter of the core, i.e. $\hat{X}_T = S_T/D_i$.

By fitting the data from three configurations of single row foam heat exchangers as described, using the least square of error, the final form of the two correlations are:

$$f = \frac{85.181 \left[\frac{S_T}{D_o}\right]^{-3.863}}{Re_D^{0.186}} \tag{4.6}$$

$$\hat{R} = \frac{1.486 \times 10^{-6} . \hat{X_T}^{1.356}}{Re_D^{0.482} . \left[\frac{D_o}{D_i}\right]^{2.675}} \tag{4.7}$$

## 4.7 Conclusions

In this study, metal foam heat exchangers of tubular design are tested for their thermo-hydraulic performance using a finned tube of comparable dimensions as a benchmarking sample.

In comparing heat transfer between two foam thickness, it is observed that the performance gain in heat transfer isn't increased in a direct proportion with the increase in foam layer thickness. Taking the heat transfer ratio between the 'thick' and 'thin' foams when both are arranged in a compact configuration reveals a gain by thick foam ranging from 1.8 at the smallest airflow to 1.5 at the largest airflow. However, with good designs and sound technical strategies, the foam-wrapped heat exchangers with suitable foam thickness can give heat transfer benefit while keeping the pressure drop at the similar level as that caused by conventional finned tubes. It has been verified that one way of achieving this, if space is not a limiting factor, is to extend the pitch length such that the bundle acts as a collection of less resistive individual tubes.

# 5

# Performance of Tubular Aluminum Foam Heat Exchangers in Multiple Row Bundles

## 5.1 Abstract

Two sets of aluminum foam cylinders, 5mm and 15mm thick, are being tested in 2- and 3-row bundles for their thermo-hydraulic performance. The bundles are formed using fixed transversal and longitudinal pitch distances and subject to airflow between 0.5 and 5.0 m/s at 0.5 m/s interval under cross-flow. The effects of foam layer thickness and the number of row under staggered configuration are investigated. Thermo-hydraulic results are benchmarking against those of a conventional finned tube bundle of similar dimensions and assembled using the same pitch distances.

## 5.2 Introduction

This chapter presents thermo-hydraulic results of two-row and three-row aluminum foam heat exchanger bundles arranged in fix-pitched, staggered configuration. Comparisons of results are made between bundles with an equal number of rows for two different foam layer thicknesses; using respective data of a conventional finned cylinder bundle as the reference. It is condensed from the last report of a measurement series after that of single tubes and single row arrays, where objectives of the study and the application target are documented. Varying-pitched, in-line bundles of the same specimens were also tested but the reference data of the finned bundle for these series were unavailable so their results are excluded. Tube bundles under tests reported in this chapter are formed by mounting either five (2-row) or eight (3-row) individual cylinders horizontally inside the wind tunnel in a cross-flow fashion. Prior research works of interest are reviewed in Chapters 2, 3 and 4, respectively.

## 5.3 Specimen Descriptions

Figure 5.1: Specimens used in the study: Circular Finned (center), Foam-1 (aluminum foam covered, 15mm thick, right), and Foam-2 (aluminum foam covered, 5mm thick, left)

The same set of specimens used in single row arrays described in Chapter 4 are used again in this experiment. Eight cylinders of each specimen are required – 2-row measurements of staggered configuration need five cylinders while the full-fledged 3-row need eight. There appearance and physical specification are recapitulated by Figure 5.1 and Table 5.1.

| Surface type | $D_o$ [mm] | $t$ [mm] | $d_o$ [mm] | $d_i$ [mm] | $\phi$ [-] | PPI [1/in.] | Materials surface/core |
|---|---|---|---|---|---|---|---|
| Circular Fin | 62 | 15 | 32 | 25.8 | - | - | MS1020/1020 |
| Foam-1 | 62 | 15 | 32 | 28.5 | 0.901 | 20 | A6101/A6061 |
| Foam-2 | 42 | 5 | 32 | 28.3 | 0.937 | 20 | A1050/SS316 |

Table 5.1: Summary of the three heat exchanger specimens

## 5.4 Methodology

The tests are performed to obtain six data sets in total; these are heat transfer and pressure drop data for two- and three-row bundles for each specimens. Figure 5.2 shows the pattern of cylinder mounting plate installed either side of the test section for the pitch lengths chosen for this experiment. It is seen that in all direction the center-to-center distance of any two

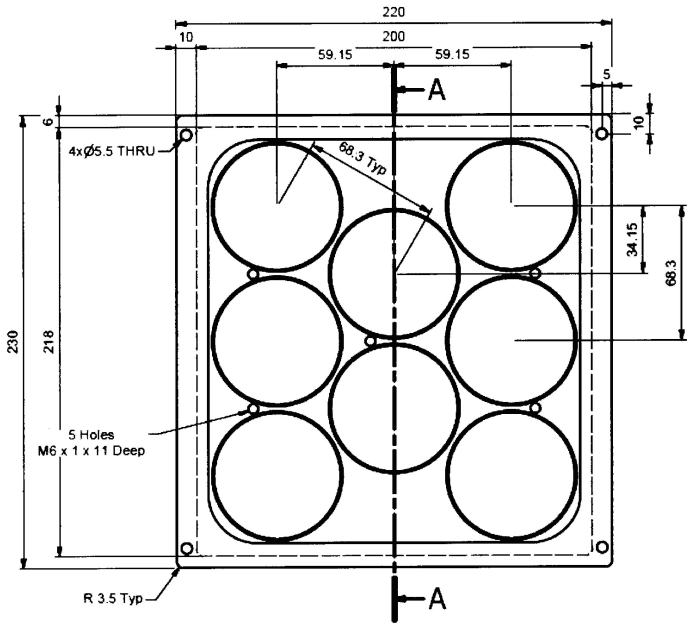


Figure 5.2: Dimensions of a mounting plate used in forming two- and three-row bundle, both transversal and longitudinal pitches are fixed at 68.3mm and 59.2mm, respectively

cylinders is 68.3mm and geometrically it follows that $S_T = 68.3$mm while $S_L = 59.2$mm. All three specimens have $d_o = 32$mm, therefore (see Table 5.1) $\hat{X}_T$ and $\hat{X}_L$ are 2.13 and 1.85, respectively. The two baffles are set such that the distance between the edge of the top cylinder and the top baffle is 1/2 the inter-tube, edge-to-edge distance; and likewise for the bottom cylinder. This dictates that, when mounted, the finned and 'thick foam' cylinder bundles have inter-tube distances at 6.3mm while those of the 'thin foam' bundle are 26.3mm. Technically, the bundle would behave like arrays of infinite number of tubes in vertical direction if half of a cylinder of suitable size is installed on either side of the middle row. However, due to practical difficulties to set the bundle up in this fashion, the results presented herein are subject to this limitation.

Data taking are again performed in the usual manner. For each heat exchanger array under test, the airflow is set to 0.5 m/s and the liquid temperature at heat exchanger inlet manifold is monitored until it is settled within 75±0.75°C, all relevant data are logged every second for 10.7 mins to gain a total of 640 data points. The airflow is then incremented by 0.5 m/s to the next measuring step and when the liquid inlet temperature re-settles, the process is repeated until the airflow reaches the final velocity at 5.0 m/s.

## 5.5 Data Reduction and Analysis

Data analysis follows the same procedure as outlined in Chapters 4 and 5, relying on the basic heat transfer relationship of Eqs. (4.1) to (4.4). The product $UA$ in Eq. (4.3) is calculated by the $\varepsilon - NTU$ method [11]. This procedure is preferable to the LMTD method as it requires only the inlet temperature of fluids exchanging heat, their flow rates, and other few thermal

properties which are usually known.

### 5.5.1 Finned Tube Benchmarking and Comparison with Literature Results

Finned tube results are included as a baseline reference and it is important they are verified for validity. Familiar $Re$ – $Nu$ plots are usually employed to compare thermal behavior of typical two-fluid heat exchangers.

Open literature offers limited source of experiment data on tubular heat exchanger bundles with small number of rows. Sparrow and Samie (1985)[68] reported their work on one- and two-row bundles of annular finned cylinders both for aligned and staggered configurations. For one row array, they studied the effect of transversal pitch on thermo-hydraulic results using 6 different settings for $\hat{X}_T$. On two-row bundle, $\hat{X}_T$ was fixed at 1.52 and $\hat{X}_L$ was parametrically varied for the same set of 6 values to investigate the effect of longitudinal pitch on heat transfer and pressure drop of the bundle. In this experiment, the cylinders were mounted vertically and, since heat was supplied using electrical heaters, heat transfer can be analysed on a per-row basis. The experiment results of two-row staggered bundle reported by Sparrow and Samie (1985)[68] are the source of literature comparison to verify finned bundle data generated from measurements in our study.

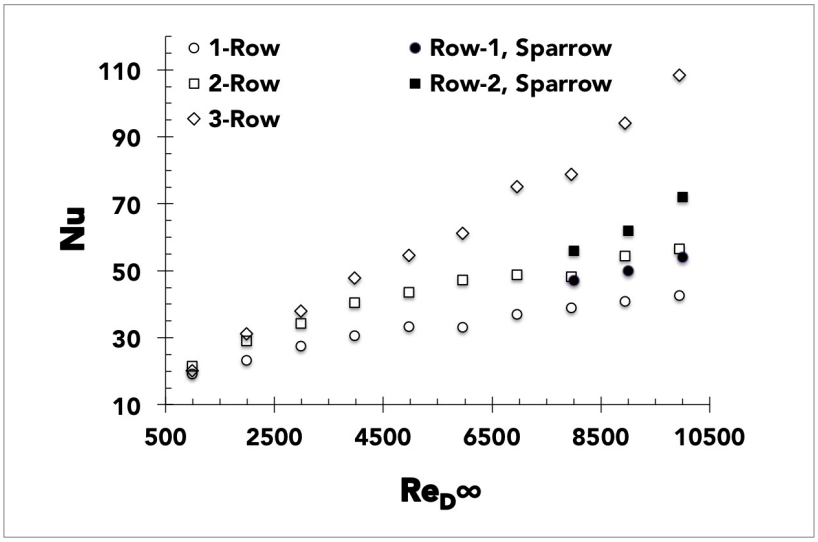


FIGURE 5.3: Heat transfer comparison between multi-row bundles of this study and Ref. [68] (black-filled data points, only data fall into our range of $Re$ are shown)

### 5.5.2 Heat Transfer

Heat transfer results from Sparrow and Samie (1985)[68] were reported on individual row for single row, as well as first row, and second row of two-row bundle. For staggered configuration, they found that $Nu$ of the first row in a two-row bundle wasn't sensitive to longitudinal pitch and its values across the range of the Reynolds number under test were essentially the

same to those of the single row. However, on the second row of two-row bundle, $Nu$ was sensitive to longitudinal pitch with performance improvement 30–45% over single row $Nu$.

### 5.5.3 Pressure Drop

Sparrow and Samie (1985)[68] presented their pressure drop data using a non-dimensional number, $Kp_\infty$, defined by $(\Delta P)/(\frac{1}{2}\rho.\vec{u}_\infty^2)$ and termed 'pressure loss coefficient'. $Kp_\infty$ definition is adopted in this part to cast our pressure drop data for comparison. Among six $\hat{X}_L$ settings of Ref. [68], the closest match to this study, $\hat{X}_L = 1.79$, is chosen to compare thermo-hydraulic results. Some other key parameters for the two studies are listed in Table 5.2.

| Original work | $\vec{u}_\infty$ [m/s] | $Re_D$ [-] | $D_o$ [mm] | $\hat{X}_T$ [-] | $\hat{X}_L$ [-] | $A_{W\times H}$ [mm$^2$] | No. of tube |
|---|---|---|---|---|---|---|---|
| Ref. [68] | 4-16 | 8,000-40,000 | 32 | 1.52 | 1.79 | 610×305 | 7—7 |
| This study | 0.5-5 | 900-10,000 | 32 | 2.13 | 1.85 | 454×210 | 3—2 |

Table 5.2: Parameter comparison of finned tube, 2-row staggered bundle s in this study and those used in Sparrow and Samie (1985)[68] ($A_{W\times H}$ is the cross sectional area of the test section at inlet)

Comparison of the two studies outlined in Table 5.2 produces mixed results. Figure 5.3 shows our heat transfer results with limited data points from Sparrow and Samie (1985)[68] superimposed using black-filled marks. The latter are $Nu$ comparison between the first and second rows data of their lower end of $Re$ but coincide with the top range of our $Re$. For our results, the '2-row' represents the combined heat transfer of the first and second row of the bundle. It is seen that $Nu$ of the 2-row is less than twice that of the one-row figure. Instead the average improvement in this regard is calculated to be 29% over the entire range of $Re$ shown in Table 5.2. However, if $\dot{Q}_t$ (in Watts) is compared instead of $Nu$ and adjustment is made to infer the presence of the third tube in the second row, $\dot{Q}_t$ of 2-row bundle manifests as double that of a single row array. Briefly, in either case, the larger heat transfer of the second over the first row (or over the single row) as reported by Sparrow and Samie (1985)[68] is not observed. Nevertheless it can be seen that $Nu$ on 3-row bundle at the top range of $Re$ is larger than triple the $Nu$ of 1-row array. It is likely that, for our pitch combination, turbulence behind the first two row produces the maximum effect on the third row at that particular condition.

For pressure loss, the comparison in Figure 5.4 shows a nearly complete agreement; although with a lower range of $Kp_\infty$ reported by Sparrow and Samie (1985)[68]. The two curves in Figure 5.4(B) are the best-fit trend lines representing pressure loss coefficients of 1-row finned tube array of our study and twice of this figure, respectively. In summary, 2-row, finned bundles in staggered configuration would typically have $Kp_\infty$ slightly larger than twice $Kp_\infty$ of a single row array regardless of longitudinal pitch setting. $S_L/D_f$ in 5.4(A) has the same definition as $\hat{X}_L$ in Table 5.2.

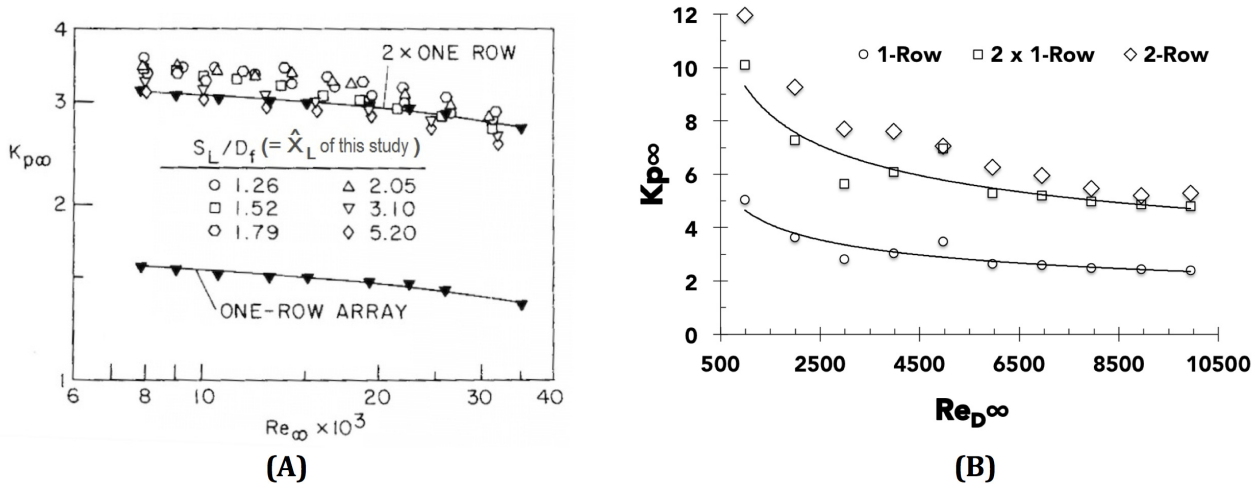


FIGURE 5.4: Summary of pressure drop results expressed in terms of pressure loss coefficient, $Kp_\infty$, as studied in Ref. [66] (A); in comparison with that of the current study (B)

## 5.6 Results and Discussion

In our analysis, appropriate number of heat exchanger tubes making up bundles under test are treated as a lumped unit with a conceptual total surface responsible for dissipating $\dot{Q}_t$ between the hot liquid and the air. The effect of net radiation heat transfer between the heat exchanger bundle and its surroundings inside the test section is insignificant and therefore not included in the calculation.

### 5.6.1 Thermo-hydraulic Comparison of Foam and Finned Surfaces

Figure 5.5 unveils thermo-hydraulic results via a scatter plot of total heat transfer versus pressure drop of the three samples under test, each with two data sets corresponding to the number of row in respective bundles. The readers should be reminded that this is not a functional plot of $\dot{Q}_t$ on $\Delta P$; it is rather a graphical rendition of two associative variables. Both of them are dependent on airflow which is excluded from the plot for readability reason (see detailed explanation in Section 3.6.3). Figure 5.5 allows qualitative comparisons on selected samples when the condition of airflow is known. For instance, at a first glance, the 3-row 'thick foam' and 3-row finned samples exhibit an impression that they provide a similar effectiveness as their data points nearly coincide up to ∼120 Pa on $\Delta P$ axis. Obviously, this plot has its limitation as the range of $\Delta P$ for four samples out of six are narrow. However, if the trend line is applied and the upper end extended to the comparable $\Delta P$ attained by the highest pressure drop sample (as shown by the bottom curve for 2-row 'thin' foam), other reasonable quantitative comparisons may be made.

On 2-row tube banks with 15mm external diameter, the 'thick' foam bundle produces much larger benefit comparing with the finned bundle. At a similar pressure drop of ∼80 Pa, its heat transfer is improved by 35% over that of the finned bundle while requiring only 40% of air velocity (i.e. 2 m/s *vs* 5 m/s). 'Thin' foam bundle performs poorly in an absolute

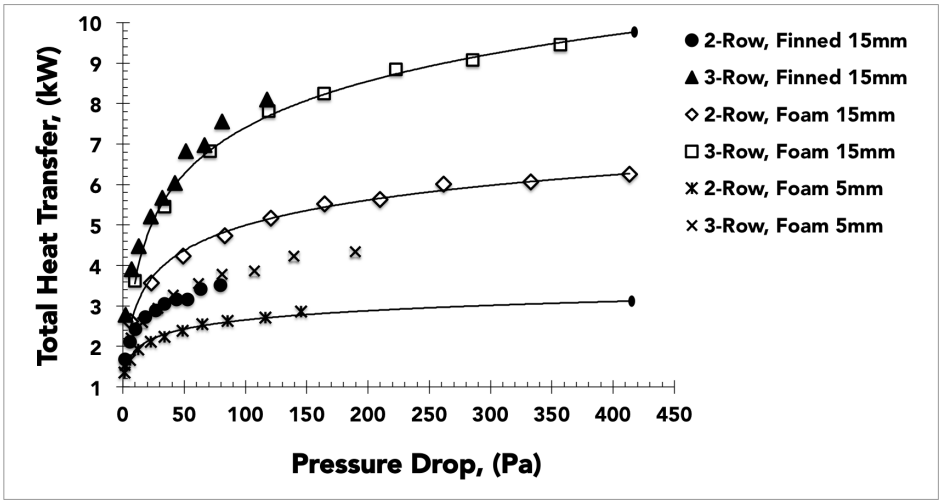


Figure 5.5: Scatter plot of total heat transfer and pressure drop for three heat exchanger samples, set at two- and three-row on each sample with the same pitch lengths $\hat{X}_T = 2.13$ and $\hat{X}_L = 1.85$. Reference data from finned bundle have their markers filled in black.

sense as shown in the figure, but may still be comparable to finned bundle if cylinder size and compactness are taken into account. Taking the same data point of 80 Pa on a 2-row configuration, for instance. At this operating point, finned bundle disposes of 33% more heat but the foam bundle possesses 33% thickness of surface enhancement layer and requires only 80% of air velocity (i.e. 4 m/s *vs* 5 m/s). There are three other factors affecting the performance of the 'thin' foam, (i) compactness, (ii) TCR, and (iii) conductive thermal resistance of the tube wall and thermal adhesive layer. At current fixed pitches, $\hat{X}_T = 2.13$ and $\hat{X}_L = 1.85$, the inter-tube gap on the finned bundle is 6.3mm while that of the foam bundle is 26.3mm. In our single row study [67], total thermal resistance of 'thin' foam array decreases by 67% (corresponding to heat transfer enhancement of 55%) when the inter-tube gap is reduced from 26.3mm to 6.3mm.

TCR has a devastating effect on heat transfer according to T'Joen, et al. (2010)[6] where its contribution to total thermal resistance varies between 6% and 55%. During our single tube study in Chapter 3. it is found that total heat transfer on 'thin' foam cylinder improves between 14% and 29% over the range of airflow from 0.5 m/s to 5.0 m/s if TCR is not present. Finally, 'thin' foam has its core tube made of stainless steel and its negative effect on conductive thermal resistance through the tube wall is previously discussed.

As noted in Chapter 4 for single row setting of the same samples, there is no significant performance gain operating the arrays at $\Delta P$ greater than ~150 Pa. The same results are realized for multi-row bundles seen in Figure 5.5. It is obvious that running multi-row foam covered cylinders with similar dimensions to the finned counterpart below this 'cut-off' $\Delta P$ produces double benefits, (i) heat transfer is either sharply enhanced or on-par at the worst case, and (ii) it does so at much reduced air velocities (2-3 m/s); which suits our target application in natural draft cooling towers.

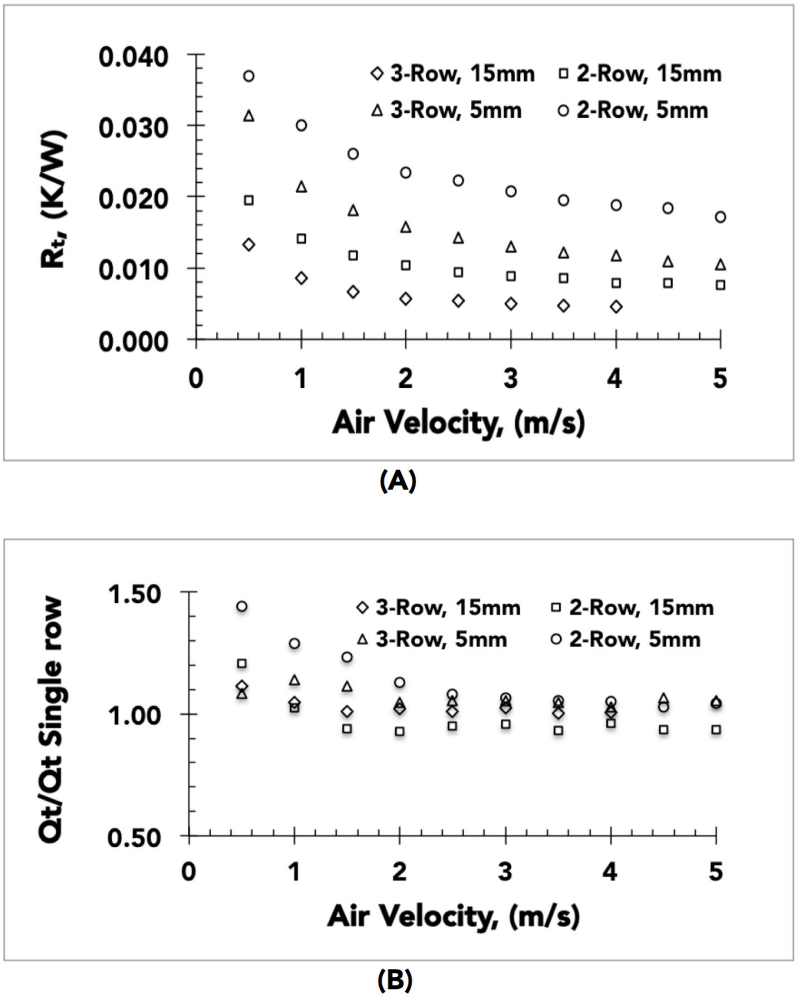


FIGURE 5.6: (A) Overall thermal resistance, $R_t$, of 2- and 3-row 'thick' and 'thin' foam heat exchangers, and (B) total heat transfer ratio of multi-row bundles for 1-row equivalent and their single row result

### 5.6.2 Heat Transfer of Foam Heat Exchanger Bundles

One area of difficulty in most previous studies of the subject is the lack of agreeable and standardized methods in evaluating foam surface areas. Since efficiency enhancement occurs at the foam structure, a suitable approach for quantitative comparison of the foam layer performance is needed. This study adopts thermal resistance concept in reporting heat transfer comparisons between foam heat exchanger bundles. The overall thermal resistance $R_t$ [K/W] between the hot liquid inside the tube and the external cross-flowing air is evaluated by Eq. (4.3); and the results of 'thick' and 'thin' foam multi-row bundles are shown in Figure 5.6(A).

Figure 5.6(A) is self-explanatory and the results are as expected. It is seen that the 'thin' foam bundles are less efficient in rejecting heat, i.e. have higher thermal resistance for the entire range of airflow. The results for 'thin' foam shown here take into account other negative factors discussed in the last section. Two data points are missing from the 3-row

'thick' foam bundle. The reason for this is that at 4.0 m/s airflow, the hot liquid circuit reaches its thermal capacity and the liquid inlet temperature cannot be maintained at 75°C if air velocity further increases. All $R_t$ curves show the trend of fast decreases at lower airflow in the range 0.5 to 2.0 m/s and level off from 2.5 m/s toward higher velocities. With the exception of 2-row 'thin' foam bundle, there would be no significant further gain in heat transfer beyond 5.0 m/s of airflow.

In open literature, eg. [10] and [68], it is readily shown that multi-row bundles of smooth or finned cylinders produce inter-row turbulence in the wake which can promote heat transfer on the rows downstream. Longitudinal pitch is one known parameter controlling heat transfer augmentation on the second row cylinders and beyond. In our foam bundles, this tendency is observed and can be verified by comparing $1/2^*\dot{Q}_t$ of 2-row bundles or $1/3^*\dot{Q}_t$ of 3-row bundles to their respective $\dot{Q}_t$ on the corresponding single row array. The results of such comparisons for a fixed $\hat{X}_L$ in this test are as shown in Figure 5.6(B). In this plot, both 2- and 3-row 'thin' foam bundles show better enhancement in heat transfer on their second and third rows than the 'thick' foam bundles. One possible explanation for this outcome is that, at the same $\hat{X}_T$ and $\hat{X}_L$ settings, bundles with wider inter-tube gaps can take a better advantage of turbulence generated by preceding rows . For the 'thin' foam itself, it is unclear why the 2-row bundle exhibits a better enhancement ratio than the 3-row counterpart when the second row consists of only two cylinders. However, in all case, the higher performance is achieved at the lower end of airflow regime which again better suits the requirement of our target application.

### 5.6.3 Pressure Drop

Pressure drop data are purely measured values using a pair of pitot tubes described in experimental set-up. Data points shown by the four curves in Figure 5.7 are the dimensionless form of pressure drop defined as $\Delta P_{max}/\rho.\vec{u}_\infty^2$ and termed friction factor, $f$.

Friction factor of 'thick' foam and finned bundles tend to decrease toward the high Reynolds number while those of the 'thin' foam bundles appear to be constant across the whole range of the Reynolds number. This is the same trend found in pressure drop of single row data if compact and wide-pitch arrays are compared. Friction factor shown in Figure 5.7 of all samples are as expected.

If $\Delta P$ is the only parameter considered, the disadvantage of foam surface is immediately seen in this plot. At wide pitch setting i.e. the 'thin' foam sample, even with only one-third of the surface layer thickness $(D_o - D_i)$ and over four times larger gaps between tubes, 'thin' foam bundles still exhibit larger pressure drop compared to the finned bundles. For 'thick' foam, when the thickness layer and the inter-tube gaps are the same, friction factor of the foam surface are between 3 to 6 times larger than that of the finned surface for the same number of row in the bundle. However, for practical application, the comparison on pressure drop alone may not be sufficient and can be misleading. If cost is not a limiting factor, by taking into an account the heat transfer enhancement, the foam bundle of suitable thickness may provide a better relative benefit as discussed earlier in Section 5.6.1.

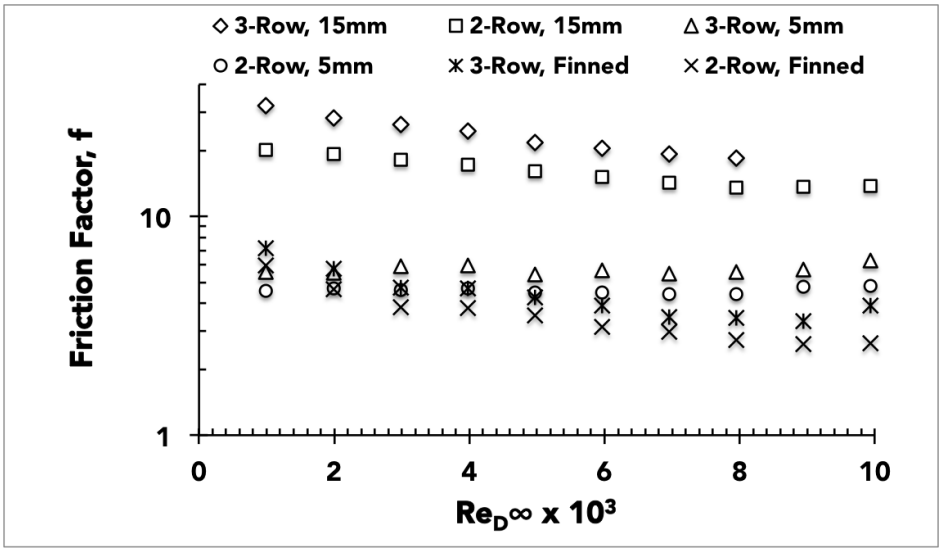


FIGURE 5.7: $\Delta P_{max}/\rho.\vec{u}_{\infty}^{2}, (f)$, of 'thick' and 'thin' foam bundles – plotted against the Reynolds number; in comparison with the reference '$f$' generated by finned tube bundles

## 5.7 Conclusions

In this report, 5mm and 15mm aluminum foam cylinders are tested in 2- and 3-row staggered bundle for their thermo-hydraulic performance. Annular finned tube bundle of 15mm fin height of the same number of row is employed as a benchmarking sample.

In comparing heat transfer between four data sets of the foam bundles, it is observed that the second and third rows in the bundle have their heat transfer enhanced over the first row; most likely due to turbulence generated by preceding row(s). Pressure drop is still a major drawback in metal foam heat exchanger bundles but it can be justified provided relative gain in heat transfer is taken into account and physical parameters are chosen to suit desirable operating conditions. Pressure drop is reported in terms of friction factor and, depending on the number of row, the foam bundle is found to have friction factor 3 to 6 times larger than that of the finned bundle with similar dimensions. However, with good designs and sound technical strategies, the foam-wrapped bundles with suitable foam thickness can give tangible heat transfer benefit while keeping the pressure drop at the same level as that caused by conventional finned bundles. It has been earlier verified that one way of achieving this, if space is not a limiting factor, is to extend the pitch length such that the bundle acts as a collection of less resistive individual cylinders.

# 6

# Reflection on Research Questions, Conclusion, and Further work

**Recap:**
Three stages of data collection are performed in the tubular metal foam heat exchanger test series, namely: single tubes, single row arrays, and multiple row bundles. Although the main theme of the project portrays condensers as the target application, setting up the facilities to generate low-pressure, low-temperature steam was not within an easy reach in terms of resources and venue. Besides, controlling steam properties over changing environments to obtain consistent data involves high risk. It is the reason that the decision was made early on at the beginning of the measurement campaign to treat the specimens as generic heat exchangers and the tests are carried out entirely in single phase flow. Despite this deviation from the main purpose, the data obtained made it possible to address two research questions set out at the beginning of this study.

There are five specimens in the first stage, those with the foam thickness of 20mm, 15mm, 12mm, and two types of 5mm. In the second and third stages, specimens are limited to two foam thicknesses consisting of 15mm ('thick foam') and 5mm ('thin foam'). The last test series covers two row and three row tube bundles organized in staggered configuration. For each data set of the foam cylinders undergoing test, the finned tubes having fin height 15mm are tested in parallel with the same number of tubes to collect baseline reference data for thermo-hydraulic comparison.

**Single Tubes**
The main point of discussion on the results of one cylinder experiments comes from Figures 3.2 and 3.5. From the first figure it is clear that the thickness of foam layer around the core tube directly influences heat transfer, the larger the thickness the higher heat transfer rate. This influence, however, doesn't go linearly and thicker foam does not necessarily provide

maximum relative advantage over the thinner foam. In fact, for all data collected in single tube tests, the best overall performance is provided by the 15mm as it heat transfer converges to that offers by the 20mm foam as $Re$ increases to the range of intended application (corresponding to air flow rate ∼2.0 - 3.0 m/s). Following this plot, thermo-hydraulic results of 15mm foam is compared to the 15mm finned cylinder via a heat transfer/pressure drop scatter plot; portrayed in the second figure. Although airflow data is not included, it is seen that the trend for total heat transfer continues to increase in both surface types but foam surface provide a faster rate for heat transfer as the $Re$ increases.

In the situation where blockage ratio on the flow passage is low such as this single tube test, the pressure drop effect as a result of increased flow rate isn't pronounced. If the flow increases further, the foam surface tube will continue to offer a better benefit in terms of heat transfer than the finned tube at the same pressure drop. However, this scenario isn't particularly useful in practice since a lot of flow (hence the power needed to produce that flow) is required for a relatively small return in total heat transfer. In theory, the knowledge of how single cylinders behave is important for analyzing tube bundles which are usually employed in actual applications.

**Single Row Arrays**

Other than the test for reference data from the finned tube array, single row data are collected from three tests: thick foam compact pitch, thin foam compact pitch, and thin foam wide-pitch, all consist of three heat exchanger tubes. The results for these tests show that both the foam thickness and the transversal pitch have an effect on heat transfer and pressure drop. Thermo-hydraulic responses of the foam array to changes in foam thickness and pitch length are in agreement with conventional tube arrays reported in open literature. i.e. (i) thicker foam layer gains higher heat transfer and pressure drop, (ii) at constant thickness, shorter pitch gains higher heat transfer and pressure drop.

Figure 4.6 shows the combined effect of 'bundling' and pitch length on heat transfer. A logical interpretation of this plot is that, when forming an array, total heat transfer result of thin foam cylinders as a group increases as a function of airflow at the same rate as a single cylinder does. The magnitude of this increase however is dependent on the pitch. It is seen that, per tube basis, a compact array with suitable pitch length can boost up heat transfer by 20% compared to a single tube. In contrast, the thick foam array behaves differently. Only the effect of one fixed pitch is seen here where the heat transfer per tube increases at a slower rate with airflow than a single cylinder.

On fin versus foam comparison, Figure 4.4 shows the same trend as seen previously for the case if single tube experiments. At the maximum airflow setting of 5 m/s, the finned array causes the pressure drop ∼40 Pa and delivers 2.1kW of heat transfer. At this same pressure drop the foam array delivers 2.3kW or 9.5% improvement; but it only needs 1.5 m/s of airflow to achieve it. If this amount of heat transfer is the design point, the cooling tower will only need a natural draft to operate. If the foam array is the one employed and more heat transfer is required, the obvious option is to increase the airflow. At 3.0 m/s it can exchange 2.9kW and causes 130 Pa of pressure drop. Heat transfer data is not readily available for finned array at this amount of pressure drop but its curve can be reasonable extrapolated and the heat transfer can be estimated to ∼2.5kW at an indeterminate but prohibitively high airflow to operate.

Flow data cannot be easily appreciated in a simple 2D plot such as Figure 4.4 but with only 10 discrete data points to track it is not difficult to identify velocity figure associated with each of them. It is also seen in this plot that from a logical point of view, there is no real relative merit to gain after the flow rate of 3.0 m/s since the pressure drop will increase dramatically at small increase of heat transfer.

**Multiple Row Bundles**

Carrying on the heat transfer-pressure drop scatter plot to multiple row bundles while its discussion is still fresh in mind, attention should be now turned to Figure 5.5 where the same concept of thermo-hydraulic comparison applies. Multi-row experiments are performed on thin foam bundles for: (i) staggered and aligned configuration, (ii) compact and wide-pitch for each configuration in (i). For a concise comparison, only their staggered row data are presented along side those of the finned- and thick foam of the same arrangement. In this Figure, the finned bundles' reference data points are solid filled.

Consider the finned and thick foam bundles by first taking the 3-row data points. It is seen that the increases of heat transfer and pressure drop on both surface types follow one another along the same path. However, at the pressure drop about 120 Pa where both bundles can dissipate ∼8kW of heat, the finned bundle has already attained its maximum airflow the foam bundle only requires 2 m/s (*Note:* it should be reminded from Chapter 5 that the maximum airflow on thick foam, 3-row bundle stops at 4 m/s as the heater unit reaches its capacity at that point. Beyond that the inlet temperature of the liquid can no longer be maintained within 75±0.75°C, the requirement for steady state assumption. It follows that the 3-row foam bundle only has 8 total data points available to work with). Another point of interest here is that at the same pressure drop of 120 Pa, the single row foam array is running at ∼3.4 m/s, 1.4 m/s more, and yet can only dump 2.8 - 2.9kW of heat (Figure 4.4).

For the 2-row case, along the same line of reasoning, the benefit provides by the foam surface over the fins is more pronounced. In addition, these positive outcomes happens at the desire range of air flow of typical natural draft regimes.

The thin foam array and bundles showed unappealing results. However, these specimens possess physical limitations which were identified at the conclusion of single cylinder measurements. Their poor performance in 2- and 3-row bundles are therefore expected.

## The Research Questions Revisit:

(1) In practical situations, what level of advantage the foam based heat exchangers provide compared to conventional heat exchangers in the context specified?

*Answer:* The level of advantage is significant, as has been shown. All of the results discussed are based on unoptimized specimens and there are ample room and technical possibilities to improve.

(2) Will the outcomes in (1) be satisfactory in overcoming practical impediments already identified in other laboratories particularly the heat transfer/pressure drop trade-off?

*Answer:* The short answer in a technical sense is definitely 'yes, the outcomes prove satisfactory'. The best argument, backed by experimental results, is that for all tests the

maximum benefit of employing foam surface occurs at lower end of airflow in the range 2.0 - 3.0 m/s which is desirable as it matches the operation of natural draft cooling tower nicely.

## General Conclusion:

Hot sedimentary aquifers (HSA) and hot fractured rocks (HFR) geothermal resources have a promising potential for base load power production in Australia. Tapping these resources for electricity generation need considerations on innovative thermal management to overcome water shortage for cooling. Air-cooled metal foam heat exchanger is one possible answer for this endeavor. However, as with any other new, emerging technologies, it will take time to transfer a proved concept from laboratories out to the fields.

## Further Works:

### Pressure Drop Reduction Strategies

Over a year elapsed into the candidature before a full trust in the preliminary experimental results was anchored. The heat transfer benefit of tubular foam heat exchangers particularly for the $D_o = 15$mm proved to be real and the development of refined prototypes to tackle pressure drop was seriously engaged. Although the comparison with their finned counterpart in all tests already showed an edge of benefit as they are, improving the designs to achieve pressure drop reduction would further increase the foam heat exchangers performance.

Under the support of the UQ Graduate School through their GSITA scheme and the host institution, ETH in Zürich, a small project was created to explore alternative designs of tubular foam heat exchanger. Figure 6.1 shows one of such designs, referred to as 'hybrid'. They were appropriately constructed with one side consists of conventional fins and the other with foam. Tests have been carried out since early 2013 with promising outcomes. Heat transfer tests were performed in a small wind tunnel while resistance to flow was measured in the form of drag force using a water tunnel (Figure 6.1(D)). The flow regime in the water tunnel during drag force measurements was adjusted such that the range of Reynolds number matched that in the wind tunnel where heat transfer was measured.

Preliminary result on heat transfer of a single hybrid heat exchanger shows a maximum improvement of 39% over that of the full-foam cylinder while the drag force is smaller over the same range of Reynolds number. On both tests, the hybrid heat exchanger was mounted such that the fin side faced the incoming flow.

### Fouling Concern

Being tortuous in structure, the foam is evidently prone to clogging. Study on fouling and mitigation techniques can be crucial in practicality and acceptance of the concept.

### Prototype Fabrication

Method used in-house so far to fabricate the test specimens relies on thermal adhesive. It will be beneficial, for material engineering discipline for example, to explore economical methods of fabricating foam and solid substrate together as single pieces. This would eliminate the effect of TCR and further improve system performance significantly.

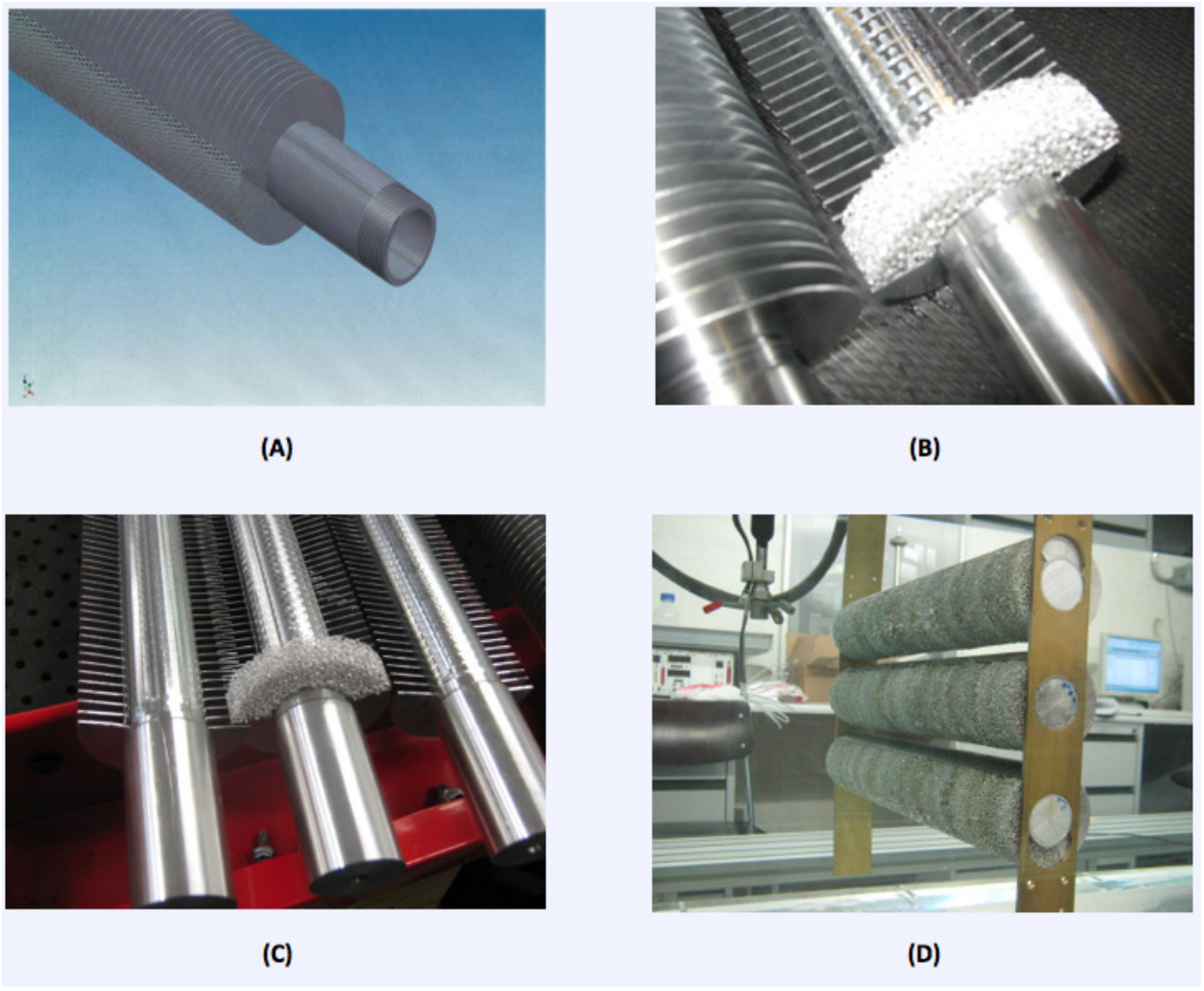


FIGURE 6.1: Hybrid tubular specimens (A) machinist's impression, (B) prototype, (C) construction, and (D) drag evaluation

# Bibliography


[1] GeoscienceAustralia and ABARE. *Australian energy resource assessment*. Report, Australian Government, Canberra, Australia (2010).

[2] A. D. Atrens. *Carbon-Dioxide-Based Engineered Geothermal Systems*. Ph.D. thesis, Mechanical and Mining Engineering, University of Queensland, Brisbane, Australia (2011).

[3] M. Odabaee, K. Hooman, and H. Gurgenci. *Entropy-energy analysis of metal foam heat exchangers as air-cooled heat exchangers*. In *Proceedings of the 3rd International Conference on Porous Media and its Applications in Science and Engineering*, ICPM (Montecatini, Italy, 2010).

[4] M. Odabaee, K. Hooman, and H. Gurgenci. *Comparing the tube fin heat exchangers to metal foam heat exchangers for geothermal applications*. In A. Budd, ed., *Australian Geothermal Energy Conference*, 69699 (GeoScience Australia, Brisbane, Australia, 2009).

[5] M. Odabaee, K. Hooman, and H. Gurgenci. *Metal foam heat exchangers for heat transfer augmentation from a cylinder in cross-flow*. Transport in Porous Media **86**, 911 (2011).

[6] C. T'Joen, P. De Jaeger, H. Huisseune, S. V. Herzeele, N. Vorst, and M. De Paepe. *Thermo-hydraulic study of a single row heat exchanger consisting of metal foam covered round tubes*. International Journal of Heat and Mass Transfer **53**, 3262 (2010).

[7] M. S. Sohal and J. E. O'Brien. *Improving air-cooled condenser performance using winlets and oval tubes in a geothermal power plant*. Geothermal Resources Council Transactions **25** (2001).

[8] T. Tsutsui and T. Igarashi. *Heat transfer enhancement of a circular cylinder*. Journal of Heat Transfer **128**(3), 226 (2006).

[9] M. Khashehchi, K. Hooman, T. Rosgen, and A. Ooi. *Turbulence characteristics in the wake flow behind a heated cylinder with different surface roughness*. In *15th International Symposium on Flow Visualization* (Minsk, Belarus, 2012).

[10] F. Incropera, D. DeWitt, T. Bergman, and A. Lavine. *Fundamentals of Heat and Mass Transfer* (Wiley, 2006), sixth ed.

[11] W. Kays and A. London. *Compact Heat Exchangers: A Summary of Basic Heat Transfer and Flow Friction Design Data* (National Press, Palo Alto, California, USA, 1955). Third Ed: McGraw-Hill, NY, Reprinted (1984); Krieger Publishing Co., FL, Reprinted (1998).

[12] D. Briggs and E. Young. *Convection heat transfer and pressure drop of air flowing across triangular pitch banks of finned tubes.* Chemical Engineering Progress Symposium Series **59**(41), 1 (1963).

[13] K. Robinson and D. Briggs. *Pressure drop of air flowing across triangular pitch banks of finned tubes.* Chemical Engineering Progress Symposium Series **62**(64), 177 (1966).

[14] T. Rabas, P. Eckels, and R. Sabatino. *The effect of fin density on the heat transfer and pressure drop performance of low-finned tube banks.* Chemical Engineering Communications **10**(1-3), 127 (1981).
http://www.tandfonline.com/doi/pdf/10.1080/00986448108910930.

[15] N. Kayansayan. *Thermal characteristics of fin-and-tube heat exchanger cooled by natural convection.* Experimental Thermal and Fluid Science **7**(3), 177 (1993).

[16] J. Y. Jang, J. T. Lai, and L. C. Liu. *The thermal-hydraulic characteristics of staggered circular finned-tube heat exchangers under dry and dehumidifying conditions.* International Journal of Heat and Mass Transfer **41**(21), 3321 (1998).

[17] S. Kim, J. Paek, and B. Kang. *Flow and heat transfer correlations for porous fin in a plate-fin heat exchanger.* ASME. J. Heat Transfer **122**(3), 572 (2000).

[18] A. Bhattacharya and R. Mahajan. *Finned metal foam heat sinks for electronics cooling in forced convection.* Journal of Electronic Packaging - Trans of the ASME **124**, 155 (2002).

[19] R. Matos, T. Laursen, J. Vargas, and A. Bejan. *Three-dimensional optimization of staggered finned circular and elliptic tubes in forced convection.* International Journal of Thermal Sciences **43**(5), 477 (2004).

[20] R. Matos, J. Vargas, T. Laursen, and A. Bejan. *Optimally staggered finned circular and elliptic tubes in forced convection.* International Journal of Heat and Mass Transfer **47**(6–7), 1347 (2004).

[21] T. A. Ibrahim and A. Gomaa. *Thermal performance criteria of elliptic tube bundle in crossflow.* International Journal of Thermal Sciences **48**(11), 2148 (2009).

[22] M. Odabaee and K. Hooman. *Metal foam heat exchangers for heat transfer augmentation from a tube bank.* Applied Thermal Engineering **36**(0), 456 (2012).
http://www.sciencedirect.com/science/article/pii/S1359431111006156.

[23] A. Jacobi and R. Shah. *Heat transfer surface enhancement through the use of longitudinal vortices: A review of recent progress.* Experimental Thermal and Fluid Science **11**(3), 295 (1995).

[24] J. E. O'Brien and M. S. Sohal. *Local heat transfer for finned-tube heat exchangers using oval tubes.* In *Proceedings of NHTC'00 - 34th National Heat Transfer Conference* (Pittsburgh, PA, USA, 2000). http://www5vip.inl.gov/technicalpublications/Documents/2809223.pdf.

[25] J. E. O'Brien and M. S. Sohal. *Heat transfer enhancement for finned-tube heat exchangers with winglets.* In *Proceedings of 2000 ASME International Mechanical Engineering Congress and Exposition* (Orlando, FL, USA, 2000).

[26] T. D. Foust, J. E. O'Brien, and M. S. Sohal. *Numerical and experimental methods for heat transfer enhancement for finned-tube heat exchangers with oval tubes.* In *35th National Heat Transfer Conference* (Anaheim, CA, USA, 2001).

[27] J. E. O'Brien, M. S. Sohal, and P. C. Wallstedt. *Local heat transfer and pressure drop for finned-tube heat exchangers using oval tubes and vortex generators.* In *ASME International Mechanical Engineering Congress and Exposition* (New York, NY, USA, 2001).

[28] J. E. O'Brien, M. S. Sohal, T. D. Foust, and P. C. Wallstedt. *Heat transfer enhancement for finned-tube heat exchangers with vortex generators: Experimental and numerical results.* In *12th International Heat Transfer Conference* (Grenoble, France, 2002). http://www5vip.inl.gov/technicalpublications/Documents/2808463.pdf.

[29] J. E. O'Brien, M. S. Sohal, and P. C. Wallstedt. *Local heat transfer and pressure drop for finned-tube heat exchangers using oval tubes and vortex generators.* Journal of Heat Transfer-Transaction of the ASME **126**, 826 (2004).

[30] J. E. O'Brien and M. S. Sohal. *Heat transfer enhancement for finned-tube heat exchangers with winglets.* Journal of Heat Transfer-Transaction of the ASME **127**, 171 (2005).

[31] N. Gallego and J. Klett. *Carbon foams for thermal management.* In *International Seminar on Advanced Applications for Carbon Materials* (Jeju Island, Korea, 2002). http://web.ornl.gov/~webworks/cppr/y2001/pres/114927.pdf.

[32] J. Klett, R. Ott, and A. McMillan. *Heat exchangers for heavy vehicles utilizing high thermal conductivity graphite foam.* In *SAE Technical Paper Series 2000-01-2207* (Government and Industry Meeting, Washington, D.C., USA, 2000).

[33] A. Straatman, N. Gallego, B. Thompson, and H. Hangan. *Thermal characterization of porous carbon foam - convection in parallel flow.* International Journal of Heat and Mass Transfer **49**, 1991 (2006).

[34] Y. Jamin and A. Mohamad. *Enhanced heat transfer using porous carbon foam in cross flow – part i: Forced convection.* Journal of Heat Transfer-Transaction of the ASME **129**, 735 (2007).

[35] M. Kaviany. *Laminar flow through a porous channel bounded by isothermal parallel plates.* International Journal of Heat and Mass Transfer **28**(4), 851 (1985).

[36] T. Lu, H. Stone, and M. Ashby. *Heat transfer in open-cell metal foams.* Acta Materialia **46**(10), 3619 (1998).

[37] S. Y. Kim, B. H. Kang, and J.-H. Kim. *Forced convection from aluminum foam materials in an asymmetrically heated channel.* International Journal of Heat and Mass Transfer **44**, 1451 (2001).

[38] S. Y. Kim, J. W. Paek, and B. H. Kang. *Thermal performance of aluminum-foam heat sinks by forced air cooling.* Components and Packaging Technologies, IEEE Transactions on **26**(1), 262 (2003).

[39] A. Bhattacharya and R. Mahajan. *Metal foam and finned metal foam heat sinks for electronics cooling in buoyancy-induced convection.* ASME Journal of Electronic Packaging **123**(3), 259 (2006).

[40] P. De Jaeger, C. T'Joen, H. Huisseune, B. Ameel, S. De Schampheleirea, and M. De Paepe. *Assessing the influence of four bonding methods on the thermal contact resistance of open-cell aluminum foam.* International Journal of Heat and Mass Transfer **55**, 6200 (2012).

[41] K. Boomsma, D. Poulikakos, and F. Zwick. *Metal foams as compact high performance heat exchangers.* Journal of Mechanics of Materials **35**, 1161 (2003).

[42] S. Mancin, C. Zilio, A. Cavallini, and L. Rossetto. *Pressure drop during air flow in aluminum foams.* International Journal of Heat and Mass Transfer **53**, 3121 (2010).

[43] A. Bhattacharya, V. Calmidi, and R. Mahajan. *Thermophysical properties of high porosity metal foams.* International Journal of Heat and Mass Transfer **45**(5), 1017 (2002).

[44] S. Mancin, C. Zilio, A. Cavallini, and L. Rossetto. *Heat transfer during air flow in aluminum foams.* International Journal of Heat and Mass Transfer **53**(21–22), 4976 (2010).

[45] S. Mancin, C. Zilio, L. Rossetto, and A. Cavallini. *Foam height effects on heat transfer performance of 20 ppi aluminum foams.* Applied Thermal Engineering **49**(0), 55 (2012). Thermal and Environmental Issues in Energy Systems (ASME/ATE/UIT).

[46] W. Lu, C. Zhao, and S. Tassou. *Thermal analysis on metal-foam filled heat exchangers. part i: Metal-foam filled pipes.* International Journal of Heat and Mass Transfer **49**, 2751 (2006).

[47] V. Calmidi and R. Mahajan. *Forced convection in high porosity.* Journal of Heat Transfer-Transaction of the ASME **122**, 557 (2000).

[48] C. Zhao, W. Lu, and S. Tassou. *Thermal analysis on metal-foam filled heat exchangers. part ii: Tube heat exchangers.* International Journal of Heat and Mass Transfer **49**, 2762 (2006).

[49] S. Mahjoob and K. Vafai. *A synthesis of fluid and thermal transport models for metal foam heat exchangers.* International Journal of Heat and Mass Transfer **51**, 3701 (2008).

[50] M. Ashby. *Metal Foams: A Design Guide* (Butterworth-Heinemann, Boston, MA, USA, 2000).

[51] B. Boyd and K. Hooman. *Air-cooled micro-porous heat exchangers for thermal management of fuel cells.* International Communications in Heat and Mass Transfer **39**, 363 (2012).

[52] M. Weclas and J. Cypris. *Characterization of the distribution-nozzle operation for mixture homogenization by a late-diesel-injection strategy.* In *Proceedings of the Institute of Mechanical Engineers, Part D:*, vol. 226, pp. 529–546 (2012).

[53] A. Ejlali, A. Ejlali, K. Hooman, and H. Gurgenci. *Application of high porosity metal foams as air cooled heat exchangers to high heat load removal systems.* International Communications in Heat and Mass Transfer **36**, 674 (2009).

[54] W. Hsieh, J. Wu, W. Shih, and W. Chiu. *Experimental investigation of heat-transfer characteristics of aluminum-foam heat sinks.* International Journal of Heat and Mass Transfer **47**, 5149 (2004).

[55] L. Tadrist, M. Miscevic, O. Rahli, and F. Topin. *About the use of fibrous materials in compact heat exchangers.* Journal of Experimental Thermal and Fluid Science **28**(2-3), 193 (2004).
Also @$4^{th}$ International Conference on Compact Heat Exchangers and Enhancement Technology for the Process Industries, Grenoble, France, 2002.

[56] R. Moffat, J. Eaton, and A. Onstad. *A method for determining the heat transfer properties of foam-fins.* Journal of Heat Transfer-Transaction of the ASME **131**, 011603 (2009).

[57] T. Fiedler, I. Belova, and G. Murch. *Critical analysis of the experimental determination of the thermal resistance of metal foams.* International Journal of Heat and Mass Transfer **55**, 4415 (2012).

[58] A. Cavallini, S. Mancin, L. Rossetto, and C. Zilio. *Air flow in aluminum foam: Heat transfer and pressure drops measurements.* Journal of Experimental Heat Transfer **23**, 94 (2010).

[59] D. Angirasa. *Experimental investigation of forced convection heat transfer augmentation with metallic fibrous materials.* International Journal of Heat and Mass Transfer **45**, 919 (2002).

[60] S. Mancin, C. Zilio, L. Rossetto, and A. Cavallini. *Heat transfer performance of aluminum foams.* Journal of Heat Transfer-Transaction of the ASME **133**, 060904 (2011).

[61] R. J. Moffat. *Describing the uncertainties in experimental results.* Experimental Thermal and Fluid Science **1**(1), 3 (1988).

[62] L. Kirkup. *Experimental Methods : An Introduction to the Analysis and Presentation of Data* (John Wiley & Sons, Brisbane, Australia, 1994).

[63] K. Hooman and A. Merrikh. *Theoretical analysis of natural convection in an enclosure filled with disconnected conducting square solid blocks.* Transport in Porous Media **85**, 641 (2010).

[64] H. Huisseune, C. T'Joen, P. Brodeoux, S. Debaets, and M. De-Paepe. *Thermal hydraulic study of a single row heat exchanger with helically finned tubes.* Journal of Heat Transfer-Transaction of the ASME **132**(6), 061801 (2010).

[65] A. Chumpia and K. Hooman. *Performance evaluation of single tubular aluminium foam heat exchangers.* Applied Thermal Engineering **66**(1–2), 266 (2014). http://www.sciencedirect.com/science/article/pii/S1359431114000775.

[66] A. Chumpia and K. Hooman. *Quantification of contact resistance of metal foam heat exchangers for improved, air-cooled condensers in geothermal power application.* In *18th Australasia Fluid Mechanics Conference* (Australasia Fluid Mechanics Society, AMC-UTAS, Launceston, Tasmania, Australia, 2012).

[67] A. Chumpia and K. Hooman. *Performance evaluation of tubular aluminum foam heat exchangers in single row arrays.* Applied Thermal Engineering **83**(0), 121 (2015).

[68] E. Sparrow and F. Samie. *Heat transfer and pressure drop results for one-and two-row arrays of finned tubes.* International Journal of Heat and Mass Transfer **28**, 2247 (1985).